HEAVILY FLUORINATED ELECTRONIC POLYMERS

by

JEEWOO LIM

A.B. Chemistry
Princeton University, 2006

Submitted to the Department of Chemistry
in Partial Fulfillment of the Requirements for the Degree of

DOCTOR OF PHILOSOPHY IN CHEMISTRY

at the

MASSACHUSETTS INSTITUTE OF TECHNOLOGY

SEPTEMBER 2011

Signature of Author: _____
Department of Chemistry, September 6, 2011

Certified By: _____
Timothy M. Swager
John D. MacArthur Professor of Chemistry
Thesis Supervisor

Accepted By: _____
Robert W. Field
Haslam and Dewey Professor of Chemistry
Chairman, Departmental Committee on Graduate Students

This doctoral thesis has been examined by a Committee of the Department of Chemistry as follows:

Professor Gregory C. Fu: _____
Chairman

Professor Timothy M. Swager: _____
Thesis Advisor

Professor Alice Y. Ting: _____
Committee Member

Dedicated to My Grandfather

Heavily Fluorinated Electronic Polymers

By

JEEWOO LIM

Submitted to the Department of Chemistry on September 7th of 2011
in Partial Fulfillment of the requirements for the Degree of
Doctor of Philosophy in Chemistry

ABSTRACT

Building blocks, containing majority fluorine content by weight, for PPEs and PPVs have been synthesized. Some of the monomers were shown to give exclusively fluorous-phase soluble polymers, the syntheses of which were achieved by fluorous biphasic polymerization conditions. Perfluoroalkylated PPEs were found to have excellent fluorescence quantum yields and photophysical and chemical stability, and were used to demonstrate their capability in sensing electron-rich aromatic systems via fluorescence quenching. Perfluoroalkylated PPVs were shown to have poor solubility in both fluorous and non-fluorous solvents. Furthermore, the polymer displayed extremely high stability.

Utilizing the fluorous solubility of perfluoroalkylated PPE, fluorescent fluorocarbon-in-water emulsions were achieved. When perfluoroalkylated carboxylate was used as the surfactant, emulsions with surfaces that could be modified via amide-bond forming reactions were obtained. When tagged with biotin, these emulsions showed large degrees of aggregation in the presence of streptavidin.

The final chapter of this thesis describes an amide-bond forming reaction to attach gold nanoparticles selectively to the termini of single-walled carbon nanotubes utilizing surfactants to protect the sidewalls of nanotubes.

Thesis Supervisor: Timothy M. Swager
Title: Professor of Chemistry

Table of Contents

List of Figures

List of Tables

List of Schemes

CHAPTER 1

Introduction to Heavily Fluorinated Materials

1.1 Introduction to Fluoroorganic Materials

1.1.1 Element Fluorine

The name of the element fluorine derives from the mineral fluorite (calcium fluoride), which was first formally named and described in the context of metallurgy in 1530. The Latin root, *fluo*, of the mineral's name means "stream" or "current", which is derived from the usage of the mineral as an additive to lower melting points of various metal ores during their processing. In 1811, nearly three centuries after the discovery and industrial application of fluorite, the name "fluorine" was suggested. In 1886, synthesis of elemental fluorine was first described by Henri Moissan, an achievement for which he was awarded the Nobel Prize for Chemistry in 1906.[1] His electrochemical method of fluorine synthesis is the only industrial method of fluorine production to this day.[2]

Since its first synthesis, fluorine and fluorine-containing organic and inorganic compounds have been noted for their unique, sometimes unusual, properties. Fluorine gas, F_2, is highly reactive due to its low bond dissociation energy (~38 kcal/mol).[3] Hydrofluoric acid, unlike other hydrohalic acids, is a weak acid and does not fully ionize in dilute solutions.[4] Some transition-metal tetra- and higher fluorides are molecular and often volatile. Zirconium tetrafluoride is an ionic liquid,[5] while germanium tetrafluoride is a gas.[6] Uranium hexafluoride is a volatile solid under ambient conditions, a property which is utilized in uranium enrichment processes.[7] Perfluorocarbons, derivatives of hydrocarbons where all hydrogen atoms have been replaced with fluorine atoms, have boiling points nearly identical to their hydrogenated counterparts despite having molecular weights nearly four times higher. Furthermore, while branched isomers of hydrocarbons display lower boiling point compared to their linear isomers, chain isomerism has a negligible effect on the boiling points of perfluoroalkanes. Interestingly,

perfluoroalkanes have boiling points only 25-30 K higher than those of noble gases of similar molecular weights.[8]

X	H	F	Cl
BDE C-X (kcal/mol)	98	116	77
Electronegativity	2.2	4.0	3.2
Van der Waals radius (A)	1.20	1.47	1.75
Atom polarizability ($10^{-24}cm^{-3}$)	0.667	0.557	2.18

Table 1-1. Properties of fluorine atom.

A combination of microscopic properties of fluorine forms the basis of such unique physical and chemical behavior of fluorine and fluorine-containing molecules. These are summarized in Table 1-1, along with those of hydrogen and chlorine. While fluorine is the most electronegative element on the periodic table, fluorine has a relatively small van der Waals radius of 1.47Å,[9] a combination of which gives fluorine a very low atom polarizability (0.557×10^{-24} cm^{-3}), significantly lower than that of a chlorine atom (2.18×10^{-24} cm^{-3}) and even lower than that of a hydrogen atom (0.667×10^{-24} cm^{-3}).[10] These properties not only lead to a strong ionic bond in metal fluorides, but also to a strong covalent bond between fluorine and carbon, with a typical bond dissociation energy of 116 kcal/mol for sp^3-sp^3 C-F bonds.[3] While both organic and inorganic fluorides display unique material properties, inorganic fluorides are outside the scope of this thesis, which will focus on highly fluorinated organic compounds.

1.1.2 Fluoroorganic Compounds

The small size of fluorine and the strength of a C-F bond make it possible for hydrogen atoms in a compound to be partially, and sometimes even fully, substituted with fluorine atoms without significant costs in stability or alteration of structure. Although C-F bonds have much

greater dipole moments compared to C-H bonds, filled non-bonding orbitals on fluorine effectively shield the carbon atom on which it is bonded, resulting in the observed thermal and chemical inertness of fluoroorganic compounds. These properties distinguish fluoroorganic compounds from other halogenated organic compounds and are the basis of a large family of compounds with unique, sometimes even strange, properties.

Fluoroorganic compounds have met a wide variety of applications in areas ranging from biochemistry to material science. Fluorine is incorporated regularly into pharmaceutical agents, with about 20% of drugs commercialized since 1957 containing fluorine.[11] Fluorine-containing natural products, unlike the ones containing other halogens, are extremely rare, and significant amounts of effort have been dedicated to developing fluorinated pharmaceutical compounds. From the perspective of organic materials chemistry, however, fluorinated compounds, especially perfluoroalkyl-containing functional materials, have not yet received much attention. Part of this comes from the commercial availability of only a handful of starting materials containing perfluoroalkyl groups, and also from the practical difficulties in handling heavily fluorinated molecules in a laboratory setting. Furthermore, the presence of a perfluoroalkyl group in a molecule affects its reactivity in a manner that is sometimes completely reversed from that of its non-fluorinated counterpart, and only a small fraction of known organic transformations are applicable when a perfluoroalkyl group is attached directly to a reacting center.

Fluoroorganic compounds in material science can be divided into two large categories depending on the nature of the contribution of fluorine to the overall physical properties of the parent molecule. The first category consists of fluoroaryl compounds in which fluorine's electron-withdrawing nature and small size is utilized for the control of the electronics of the parent aromatic moiety without significant alteration of steric effects. The second category,

which will be the groundwork for this thesis, consists of fluoroalkyl compounds in which fluorine's size and low polarizability give rise to unique physical properties. In the following sections, representative work from both categories are discussed, followed by an introduction to fluoroalkylated materials and their largest area of application, the fluorous phase.

1.1.3 Fluorinated Materials 1: Fluoroaryl Compounds

The electron-withdrawing nature of fluorine renders hexafluorobenzene to have a quadrupole moment complementary to that of benzene.[12] This raises the melting point of a 1:1 molar mixture of benzene and hexafluorobenzene to 23.7°C, which is significantly higher than those of individual components, benzene (5.4°C) and hexafluorobenzene (5.0°C).[13] At the molecular level, hexafluorobenzene and benzene stack in a face-to-face fashion due to their

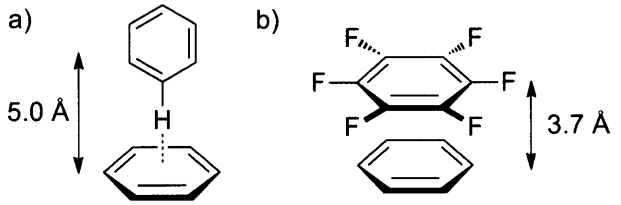

Figure 1-1. (a) Herringbone stacking in benzene. (b) Face-to-face stacking of benzene and hexafluorobenzene.

complementary quadrupoles, whereas each component by itself stacks in an edge-to-face fashion (Figure 1-1).[14] The stabilization energy of the π-stacking interaction between benzene and hexafluorobenzene relative to each component is calculated to be −4.3 kcal/mole,[15] which is similar to that of a hydrogen bond in water. The strong π-π interactions between aromatic and fluoroaromatic systems have been utilized by Grubbs and coworkers to exert topological control

over photodimerization and photopolymerization reactions of 1,3-diyines and olefins in the condensed state (Figure 1-2).[16]

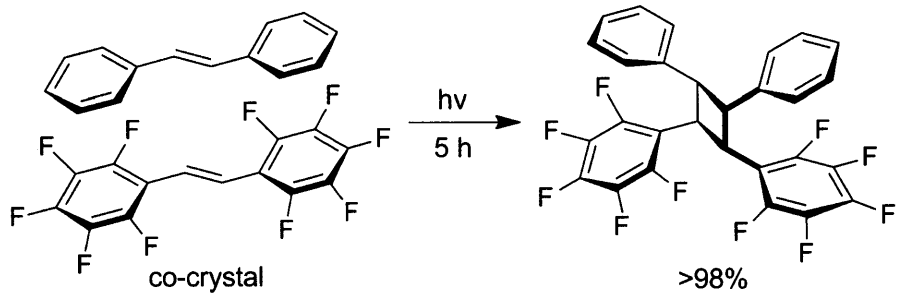

Figure 1-2. Photodimerization of stilbene and octafluorostilbene co-crystals. Topochemical control is obtained through benzene-pentafluorobenzene interaction.

Extended aromatic systems containing fluoroaryl groups are used in organic electronics to make electron-deficient (N-type) organic semiconducting material. T. Don Tilley and coworkers reported a synthesis of 9,10-diaryloctafluoroanthracene (Figure 1-3).[17] The 9,10-

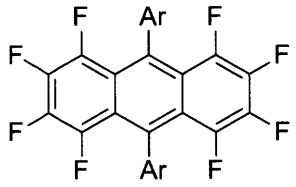

Figure 1-3. 9,10-diaryloctafluoroanthracene.

-bis(thienyl) derivative displayed donor-acceptor character. These materials displayed low LUMO levels, consistent with the electron-withdrawing nature of fluorine atoms.

1.1.4 Fluorinated Materials 2: Fluoroalkyl Compounds

In 1938, Roy Plunkett at Kinetic Chemicals in New Jersey, USA, accidentally discovered polymers of tetrafluoroethylene while attempting to make novel chlorofluorocarbon (CFC)

refrigerants. The resulting polymer, a fully fluorinated analogue of polyethylene (Figure 1-4), was patented in 1941.[18] From very early on, the polymer was noted for its extraordinary thermal

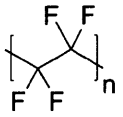

Figure 1-4. Structure of poly(tetrafluoroethylene) (Teflon™).

and chemical stability, and was used as coating materials for uranium hexafluoride containers in uranium enrichment plants. At the molecular level, the polymer was observed to have a longer persistence length and much more "sluggish" kinetics than polyethylene.[19]

While the lack of suitable solvents which could dissolve the polymer at temperature ranges suitable for its laboratory study was a severe limiting factor for experimental probe into the molecular dynamics of the new material,[20] several theoretical studies have led to an

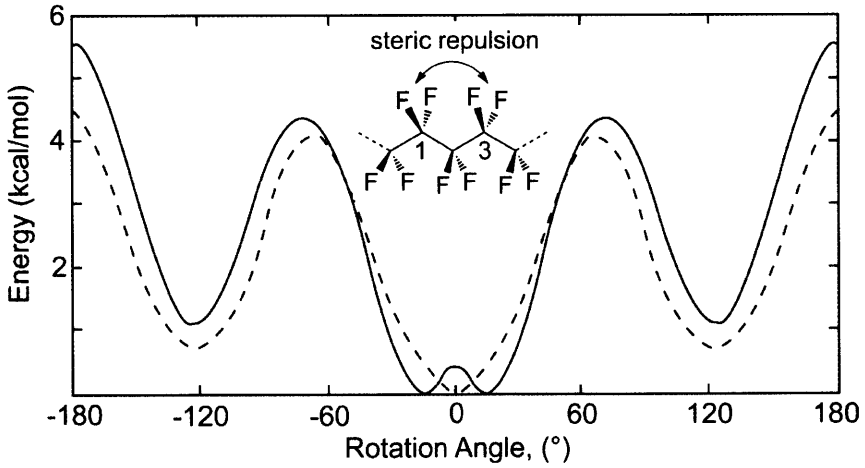

Figure 1-5. Conformational energy diagram of a fluorocarbon chain (solid) and a hydrocarbon chain (dotted). Inset shows the steric repulsion between fluorine atoms on 1,3-positions, causing an offset of energy minimum from 0°.

interesting description of the polymer. The conformational energy curve of a fluorocarbon showed that the minima of *trans* conformation were off-set by ~15° with respect to 0°, the *trans* energy minimum for alkane (Figure 1-5).[21] Furthermore, the *eclipsed* maximum is increased in fluorocarbons by ~1-1.5 kcal/mol. The off-set of energy minima and the increased barrier to rotation are attributed to the electrostatic interaction between fluorine atoms attached to carbons on 1,3-positions relative to one another (Figure 1-5, inset). This is attributed to the observed rigidity and of perfluoroalkyl chains. A more recent theoretical study reveals that fluorocarbons are not only rigid, but also have a significantly larger molecular volume and surface area compared to corresponding hydrocarbons (Figure 1-6).[22] It therefore requires significant cavitation to accommodate a fluorocarbon in a non-fluorinated medium, giving large entropic costs of mixing between heavily fluorinated and non-fluorinated materials regardless of their polarity.

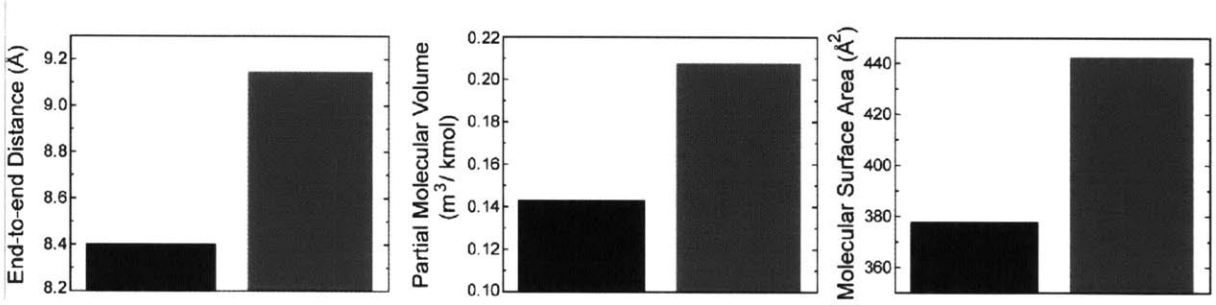

Figure 1-6. Comparison of theoretical values[22] of octane (black) and perfluoro(octane) (grey). The end-to-end distance is an average value.

The rigidity of perfluoroalkyl groups and their tendency to segregate from non-fluorinated media have been utilized in applications involving molecular alignment. Liquid crystals without cyclic structures in their mesogenic cores have been achieved in the form of semifluorinated alkanes, $F(CF_2)_n(CH_2)_mH$.[23] Also, perfluoroalkyl groups have been used as

pendants on aromatic cores to stabilize hexagonal columnar mesophase of liquid crystalline molecules.[24] Recently, water-soluble micelles from surfactants with C_{60} anion as the polar headgroup and perfluoroalkyl chains as the hydrophobic tails have been achieved.[25] While lipid micelles that utilize hydrocarbons as hydrophobic tails are known to collapse upon removal from solution, these fluorocarbon-containing micelles displayed remarkable stability, maintaining their structure on a solid substrate under vacuum.

1.2 Applications

1.2.1 Fluorous Biphase Chemistry

Among many applications involving heavily fluorinated organic materials, perhaps the most extensively studied and widely used is the "fluorous" solvent system. Most perfluorinated solvents are immiscible with non-fluorinated organic solvents at room temperature. The resulting "third" phase, immiscible with aqueous and organic phases, is known as the "fluorous phase" and is defined as the "fluorocarbon-rich phase of a biphase system."[26] Above certain critical temperature (known as the consolute temperature), which is heavily dependent on the nature and the ratio of the components, many combinations of fluorous and non-fluorous solvents become monophasic. The switch between biphasic and monophasic states is reversible and can be controlled simply by varying the temperature. Empirical criteria for solubility of a substrate in the fluorous phase include greater than 60% fluorine content by weight,[27] and a molecular structure in which perfluoroalkyl chains "sheath" the "anti-fluorous" core of the molecule.[28] Materials meeting such criteria are often soluble exclusively in the fluorous phase at room temperature.

Such a solubility profile has been utilized since the early 1990s to recover expensive catalysts following a reaction and to stabilize reactive intermediates (Figure 1-7[29]). In 1994, I.T.

Horvath and J. Rabai reported a catalytic hydroformylation[26b] process in which perfluoroalkylated phosphane ligands were used to recycle the expensive rhodium catalyst following a reaction from a toluene-perfluoro(methylcyclohexane) biphasic system. The concept was also utilized in hydroboration. Since then, a variety of ligands[30] for specific biphase catalyses have been reported, including Stille coupling,[31] Pd(0)-catalyzed allylic substitution,[32] enantioselective C-C bond formation with fluorous BINOL,[33] along with those for reactions in supercritical CO_2.[34]

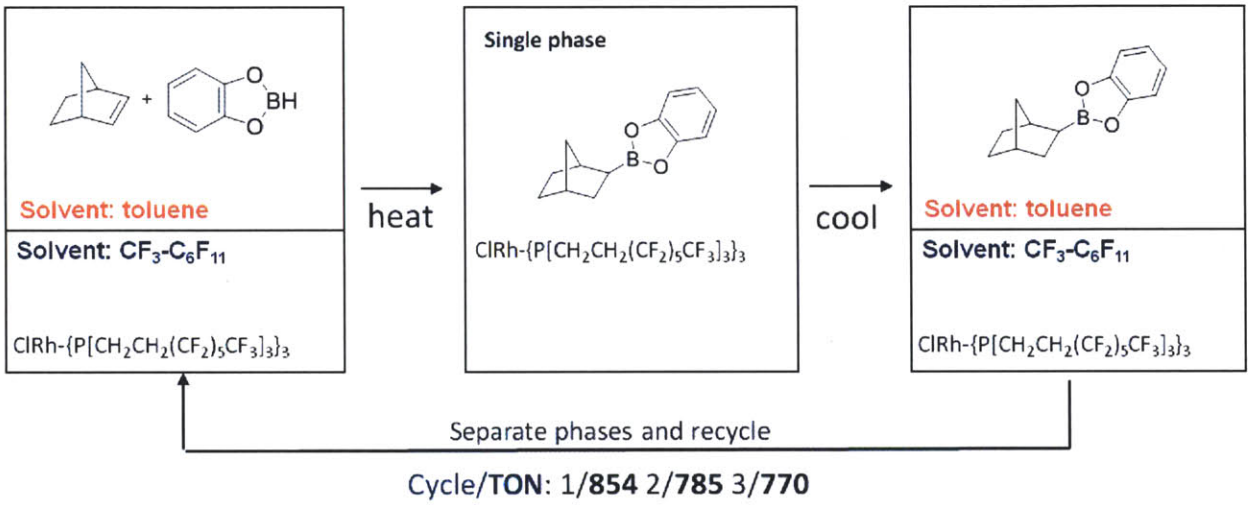

Figure 1-7. Example of fluorous biphase chemistry utilized in hydroboration.

1.2.2 Orthogonal Processing

The mutually exclusive solubility of fluorous materials in fluorous solvents has led to investigations to utilize fluorous solvents to solution-process organic electronic devices. Conventional photolithographic device fabrication involves a "lift-off" step where the photoresist is removed using aggressive organic solvents. This step has limited processing of organic electronic materials via photolithography since the active materials are also washed off the device during this step. Recently, Christopher Ober and coworkers reported that neither an

inorganic electroluminescent device based on $[Ru(bpy)_3]_2^+(PF_6^-)_2$ nor an organic P3HT (*poly*(3-hexylthiophene)) thin-film transistors showed any loss in performance when exposed to HFEs (hydrofluoroethers), a class of fluorous solvents.[35] The devices were highly unstable to non-fluorous organic solvents such as acetonitrile and xylenes, and the observed benignity of HFEs was attributed to their inability to dissolve $[Ru(bpy)_3]_2^+(PF_6^-)_2$ or P3HT. Soon thereafter, a resorcinarene-based photoresist with moderate solubility in HFEs was reported. This photoresist could be cleanly removed with HFEs during the "lift-off" step without affecting patterned active materials, enabling patterning of $[Ru(bpy)_3]_2^+(PF_6^-)_2$ and P3HT using conventional photolithographic techniques.[36] Ober also reported semifluoroalkyl polyfluorenes that were soluble in fluorous solvents and demonstrated that the material's fluorous solubility could be utilized in the fabrication of patterned electroluminescent devices.

1.2.3 Facile Formation of Microarrays for Biosample Screening

Nearly simultaneous to the investigations of fluorous biphase catalyses were the investigations of facile separation of reaction products by "tagging" them with perfluoroalkyl groups then extracting with a suitable fluorous solvent.[37] The method met a general use in combinatorial chemistry, since it did not require the use of "beads." It was also observed that a single perfluoroalkyl chain of eight carbons or longer is often enough for a facile separation of substrates using fluorous solid-phase extraction.[38] The observation was soon applied to microarrays for small biomolecule screening in which molecules such as sugars were tagged with C_8F_{17} ponytails and subsequently deposited onto commercially available Teflon-epoxy coated glass microscope slides.[39] The resulting microarrays were reported to withstand repeated washes with detergent-containing buffer solutions.

1.3 Limitations and Challenges

The unique properties of fluorocarbon-based materials have led to their applications in various areas. There are, however, limitations that leave much room for further investigation. First is the lack of tangible guidelines, beyond the highly empirical "60% rule", for designing molecules which would be soluble in the fluorous phase. It is still unknown how the structure of perfluoroalkyl chains (branched or linear) or their arrangement on a molecule alters the fluorous compatibility of the parent compound. Also, the effect of increasing conformational flexibility of a fluorous chain (by incorporation of heteroatoms) on the overall solubility has yet to be studied. Furthermore, although there have been efforts to qualitatively rate fluorous solvents in terms of both fluorophilicity and polarity (assuming the two scales are orthogonal),[40] a quantitative index, analogous to the polarity index, has not been established for fluorophilicity.

The second limitation is both the limited scope of available perfluoroalkylated materials and the relative dearth of known chemical transformations applicable to fluorocarbon chemistry. Nucleophiles are known to attack perfluoroalkyl bromides and iodides on the halogen, with the perfluoroalkyl anion acting as the leaving group.[41] Some apparent S_N2 reactions of perfluoroalkyl halides have a radical mechanism, and only "nucleophiles" which can internally stabilize radicals can be directly perfluoroalkylated using this method.[42] Also, perfluoroalkylated alkenes and alkynes are known to undergo addition reactions under very mild conditions, causing undesirable byproducts.[43] Also, the only general and scalable methodology of perfluoroalkylating aromatic halides known to date is a non-catalytic coupling reaction with a limited substrate scope.[44]

Solutions to these issues would make possible the application of fluorocarbon chemistry to endeavors requiring higher precision and finer control of molecular structures. One approach

towards the solutions would be a theoretical approach to better model systems containing perfluoroalkyl chains. Another approach would be to design and synthesize novel molecular architecture involving perfluoroalkyl chains and to study their behavior. The work described in this thesis, which is focuses on the syntheses, properties, and applications of heavily fluorinated fluorescent conjugated polymers, would take the latter approach. In the process, the unique properties of perfluoroalkyl chains are exploited to create materials with novel characteristics.

References

1. Tressaud, A., Henri Moissan: Winner of the Nobel prize for chemistry 1906. *Angew. Chem. Int. Ed.* **2006,** *45* (41), 6792-6796.

2. Villalba, G.; Ayres, R. U.; Schroder, H., Accounting for fluorine - Production, use, and loss. *J. Ind. Eco.l* **2007,** *11* (1), 85-101.

3. Greenwood, N. N.; Earnshaw, A., *Chemistry of the elements*. 2nd ed.; Butterworth-Heinemann: Oxford ; Boston, 1997; p 52-58 p.

4. Ayotte, P.; Hebert, M.; Marchand, P., Why is hydrofluoric acid a weak acid? *J. Chem. Phys.* **2005,** *123* (18).

5. Brown, P. L.; Mompean, F. J.; Perrone, J.; Illemassène, M.; OECD Nuclear Energy Agency., *Chemical thermodynamics of zirconium*. Elsevier: Amsterdam ; London, 2005; p 144p.

6. Yaws, C. L.; Braker, W., *Matheson gas data book*. 7th ed.; Matheson Tri-Gas; McGraw-Hill: Parsippany, NJ New York, 2001; p 651.

7. Johnson, G. K., Enthalpy of Formation of Uranium Hexafluoride. *J. Chem. Thermodyn.* **1979,** *11* (5), 483-490.

8. Banks, R. E.; Smart, B. E.; Tatlow, J. C., *Organofluorine chemistry : principles and commercial applications*. Plenum: New York, 1994; pp12-15.

9. Bondi, A., Van Der Walls Volumes and Radii of Metals in Covalent Compounds. *J. Phys. Chem.* **1966,** *70* (9), 3006-3007.

10. Miller, T. M., Atomic and Molecular Polarizabilities. In *CRC Handbook of Chemistry and Physics*, 81st ed.; Lide, D. R., Ed. CRC Press: Boca Raton, 2000.

11. Muller, K.; Faeh, C.; Diederich, F., Fluorine in pharmaceuticals: Looking beyond intuition. *Science* **2007,** *317* (5846), 1881-1886.

12. Vrbancich, J.; Ritchie, G. L. D., Quadrupole-Moments of Benzene, Hexafluorobenzene and Other Non-Dipolar Aromatic-Molecules. *J. Chem. Soc. Farad. Trans. 2* **1980,** *76*, 648-659.

13. Patrick, C. R.; Prosser, G. S., Molecular Complex of Benzene and Hexafluorobenzene. *Nature* **1960,** *187* (4742), 1021-1021.

14. Williams, J. H.; Cockcroft, J. K.; Fitch, A. N., Structure of the Lowest Temperature Phase of the Solid Benzene Hexafluorobenzene Adduct. *Angew. Chem. Int. Ed. Engl.* **1992,** *31* (12), 1655-1657.

15. HernandezTrujillo, J.; Colmenares, F.; Cuevas, G.; Costas, M., MP2 ab initio calculations of the hexafluorobenzene-benzene and -monofluorobenzene complexes. *Chem Phys Lett* **1997,** *265* (3-5), 503-507.

16. (a) Coates, G. W.; Dunn, A. R.; Henling, L. M.; Ziller, J. W.; Lobkovsky, E. B.; Grubbs, R. H., Phenyl-perfluorophenyl stacking interactions: Topochemical[2+2] photodimerization and photopolymerization of olefinic compounds. *J. Am. Chem. Soc.* **1998,** *120* (15), 3641-3649; (b) Coates, G. W.; Dunn, A. R.; Henling, L. M.; Dougherty, D. A.; Grubbs, R. H., Phenyl-perfluorophenyl stacking interactions: A new strategy for supermolecule construction. *Angew. Chem. Int. Ed. Engl.* **1997,** *36* (3), 248-251.

17. Tilley, T. D.; Tannaci, J. F.; Noji, M.; Mcbee, J. L., 9,10-disubstituted octafluoroanthracene derivatives via palladium-catalyzed cross-coupling. *J. Org. Chem.* **2008,** *73* (20), 7895-7900.

18. Plunkett, R. J. Tetrafluoroethylene polymers. 1941.

19. Billmeyer, F. W., *Textbook of polymer science*. Interscience Publishers: New York,, 1962; p 601 p.

20. Bates, T. W.; Stockmayer, W. H., Conformational Energies of Perfluoroalkanes. II. Dipole Moments of $H(CF_2)_nH$. *Macromolecules* **1968,** *1* (1), 12-17.

21. Bates, T. W.; Stockmayer, W. H., Conformational Energies of Perfluoroalkanes. III. Properties of Polytetrafluoroethylene. *Macromolecules* **1968,** *1* (1), 17-24.

22. Dalvi, V. H.; Rossky, P. J., Molecular origins of fluorocarbon hydrophobicity. *Proc. Natl. Acad. Sci. U S A* **2010,** *107* (31), 13603-13607.

23. (a) Wilson, L. M.; Griffin, A. C., Liquid-Crystalline Fluorocarbon Hydrocarbon Microblock Polymers. *Macromolecules* **1993,** *26* (23), 6312-6314; (b) Russell, T. P.; Rabolt, J. F.; Twieg, R. J.; Siemens, R. L.; Farmer, B. L., Structural Characterization of Semifluorinated Normal-Alkanes .2. Solid Solid Transition Behavior. *Macromolecules* **1986,** *19* (4), 1135-1143.

24. Percec, V.; Schlueter, D.; Kwon, Y. K.; Blackwell, J.; Moller, M.; Slangen, P. J., Dramatic stabilization of a hexagonal columnar mesophase generated from supramolecular and macromolecular columns by the semifluorination of the alkyl groups of their tapered building blocks. *Macromolecules* **1995,** *28* (26), 8807-8818.

25. (a) Homma, T.; Harano, K.; Isobe, H.; Nakamura, E., Preparation and Properties of Vesicles Made of Nonpolar/Polar/Nonpolar Fullerene Amphiphiles. *J Am Chem Soc* **2011,** *133* (16), 6364-6370; (b) Homma, T.; Harano, K.; Isobe, H.; Nakamura, E., Nanometer-Sized Fluorous Fullerene Vesicles in Water and on Solid Surfaces. *Angew. Chem. Int. Ed.* **2010**, 1709-1712.

26. (a) Horvath, I. T., Fluorous biphase chemistry. *Acc. Chem. Res.* **1998,** *31* (10), 641-650; (b) Horvath, I. T.; Rabai, J., Facile Catalyst Separation without Water - Fluorous Biphase Hydroformylation of Olefins. *Science* **1994,** *266* (5182), 72-75.

27. Kiss, L. E.; I, K.; Rabai, J., An improved design of fluorophilic molecules: prediction of the ln P fluorous partition coefficient, fluorophilicity, using 3D QSAR descriptors and neural networks. *J. Fluorine Chem.* **2001,** *108* (1), 95-109.

28. (a) de Wolf, E.; Richter, B.; Deelman, B. J.; van Koten, G., Highly fluorous derivatives of 1,2-bis(diphenylphosphino)ethane. *J. Org. Chem.* **2000,** *65* (17), 5424-5427; (b) Richter, B.; de Wolf, E.; van Koten, G.; Deelman, B. J., Synthesis and properties of a novel family of fluorous triphenylphosphine derivatives. *J. Org. Chem.* **2000,** *65* (13), 3885-3893.

29. Juliette, J. J. J.; Horvath, I. T.; Gladysz, J. A., Transition metal catalysis in fluorous media: Practical application of a new immobilization principle to rhodium-catalyzed hydroboration. *Angew. Chem. Int. Ed. Engl.* **1997,** *36* (15), 1610-1612.

30. (a) Mathivet, T.; Monflier, E.; Castanet, Y.; Mortreux, A.; Couturier, J. L., Unexpected synthesis of a new highly fluorocarbon soluble phosphite for biphasic catalysis. *Tet. Lett.* **1999,** *40* (20), 3885-3888; (b) Mathivet, T.; Monflier, E.; Castanet, Y.; Mortreux, A.; Couturier, J. L., Easy two-step synthesis of new tris(perfluoroalkylphenyl)phosphites. *Tet. Lett.* **1998,** *39* (51), 9411-9414.

31. Schneider, S.; Bannwarth, W., Repetitive application of perfluoro-tagged Pd complexes for Stille couplings in a fluorous biphasic system. *Angew. Chem. In.t Ed.* **2000,** *39* (22), 4142-4145.

32. Kling, R.; Sinou, D.; Pozzi, G.; Choplin, A.; Quignard, F.; Busch, S.; Kainz, S.; Koch, D.; Leitner, W., Palladium(O)-catalyzed substitution of allylic substrates in perfluorinated solvents. *Tet. Lett.* **1998,** *39* (51), 9439-9442.

33. Tian, Y.; Chan, K. S., An asymmetric catalytic carbon-carbon bond formation in a fluorous biphasic system based on perfluoroalkyl-BINOL. *Tet. Lett.* **2000,** *41* (45), 8813-8816.

34. (a) Francio, G.; Wittmann, K.; Leitner, W., Highly efficient enantioselective catalysis in supercritical carbon dioxide using the perfluoroalkyl-substituted ligand (R,S)-3-(HF6)-F-2-BINAPHOS. *J. Organomet. Chem.* **2001,** *621* (1-2), 130-142; (b) Cooper, A. I.; Londono, J. D.; Wignall, G.; McClain, J. B.; Samulski, E. T.; Lin, J. S.; Dobrynin, A.; Rubinstein, M.; Burke, A. L. C.; Frechet, J. M. J.; DeSimone, J. M., Extraction of a hydrophilic compound from water into liquid CO2 using dendritic surfactants. *Nature* **1997,** *389* (6649), 368-371.

35. Malliaras, G. G.; Zakhidov, A. A.; Lee, J. K.; Fong, H. H.; DeFranco, J. A.; Chatzichristidi, M.; Taylor, P. G.; Ober, C. K., Hydrofluoroethers as orthogonal solvents for the chemical processing of organic electronic materials. *Adv. Mater.* **2008,** *20* (18), 3481-3484.

36. Ober, C. K.; Lee, J. K.; Chatzichristidi, M.; Zakhidov, A. A.; Taylor, P. G.; DeFranco, J. A.; Hwang, H. S.; Fong, H. H.; Holmes, A. B.; Malliaras, G. G., Acid-sensitive semiperfluoroalkyl resorcinarene: An imaging material for organic electronics. *J. Am. Chem. Soc.* **2008,** *130* (35), 11564-11565.

37. Studer, A.; Hadida, S.; Ferritto, R.; Kim, S. Y.; Jeger, P.; Wipf, P.; Curran, D. P., Fluorous synthesis: a fluorous-phase strategy for improving separation efficiency in organic synthesis. *Science* **1997,** *275* (5301), 823-826.

38. (a) Zhang, W., Fluorous Linker-Facilitated Chemical Synthesis. *Chem. Rev.* **2009,** *109* (2), 749-795; (b) Zhang, W., Fluorous synthesis of heterocyclic systems. *Chem. Rev.* **2004,** *104* (5), 2531-2556.

39. Pohl, N. L.; Ko, K. S.; Jaipuri, F. A., Fluorous-based carbohydrate microarrays. *J. Am. Chem. Soc.* **2005,** *127* (38), 13162-13163.

40. Yu, M. S.; Curran, D. P.; Nagashima, T., Increasing fluorous partition coefficients by solvent tuning. *Org. Lett.* **2005,** *7* (17), 3677-3680.

41. Howell, J. L.; Muzzi, B. J.; Rider, N. L.; Aly, E. M.; Abouelmagd, M. K., On the Preparation of 1h-Perfluoroalkanes and a Mechanism for the Reduction of Perfluoroalkyl Iodides. *J. Fluorine. Chem.* **1995,** *72* (1), 61-68.

42. (a) Chen, Q. Y.; Chen, M. J., Perfluoroalkylation of 2-Mercaptobenzothiazole and Its Analogs with Perfluoroalkyl Iodides by an Srn1 Reaction. *J. Fluorine. Chem.* **1991,** *51* (1), 21-32; (b) Boiko, V. N.; Shchupak, G. M., Ion-Radical Perfluoroalkylation .11. Perfluoroalkylation of Thiols by Perfluoroalkyl Iodides in the Absence of Initiators. *J. Fluorine. Chem.* **1994,** *69* (3), 207-212.

43. Baum, K.; Bedford, C. D.; Hunadi, R. J., Synthesis of Fluorinated Acetylenes. *J. Org. Chem.* **1982,** *47* (12), 2251-2257.

44. Mcloughl.Vc; Thrower, J., A Route to Fluoroalkyl-Substituted Aromatic Compounds Involving Fluoroalkylcopper Intermediates. *Tetrahedron* **1969,** *25* (24), 5921-5940.

CHAPTER 2

Synthesis of Rigid Poly(*para*-Phenyleneethynylene) with Perfluoroalkyl Chains

Adapted from
Lim, J.; Swager, T.M. *Angew. Chem. Int. Ed.* **2010**, *49*, 7486-7488

Introduction

Organic conjugated polymers (CPs)[1] display electrochemical and photophysical properties which could be controlled by chemical modification of the polymers' molecular structures. The ability to fine-tune the properties of CPs has led to the application of these materials in areas such as sensing,[1b] polymer light-emitting diodes (PLEDs),[2] organic field-effect transistors (OFETs),[3] and photovoltaic devices.[4] Among numerous conjugated polymers, *poly*(*p*-phenyleneethynylene)s (PPEs, Figure 2-1)[5] are known for their highly emissive nature, excellent

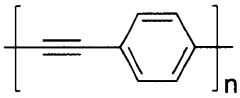

Figure 2-1. Core structure of PPE.

exciton migration lengths,[6] and robust polymerization methods[5] largely unaffected by the nature of monomers. Polymers in this family have been utilized in a variety of applications, including sensing of chemical[7] and biological[8] analytes.

While many PPEs with electron-donating substiuents have been reported, there is relative dearth of PPEs with electron-withdrawing groups. Electron-rich and electron-poor PPEs are electronically well-suited for detection of electron-poor[7c] and rich[9] analytes, respectively, and therefore a greater diversity in electron-poor PPEs would lead to an expansion of the scope of detectable analytes. Furthermore, given that the currently available platforms for PPE-based sensing are focused around solutions, thin films, and microsphere ("bead") supports,[8d, 8g] it could be anticipated that PPEs with novel physical properties which could be exploited to produce novel platforms for potential sensing would be of interest.

Perfluoroalkyl groups have several properties that make them attractive pendants on functional materials.[10] Thermal and chemical stability of the perfluoroalkyl groups could

translate directly to material stability. Also, the extremely hydrophobic nature of perfluoroalkyl groups could lead to materials with very low surface energy in solid state. From the perspective of light-emitting compounds, the rigidity of perfluoroalkyl chains may reduce vibrational energy loss, resulting in enhanced quantum yields. Also, the high electronegativities of perfluoroalkyl groups[11] would increase the electron affinity of π-systems to which they are directly attached. Another advantage of perfluoroalkylated materials is that they can display orthogonal solubility profiles, dissolving in fluorous solvents with limited solubility in non-fluorous organic solvents, allowing for facile purification via liquid-to-liquid extraction and/or fluorous solid phase extraction.[12]

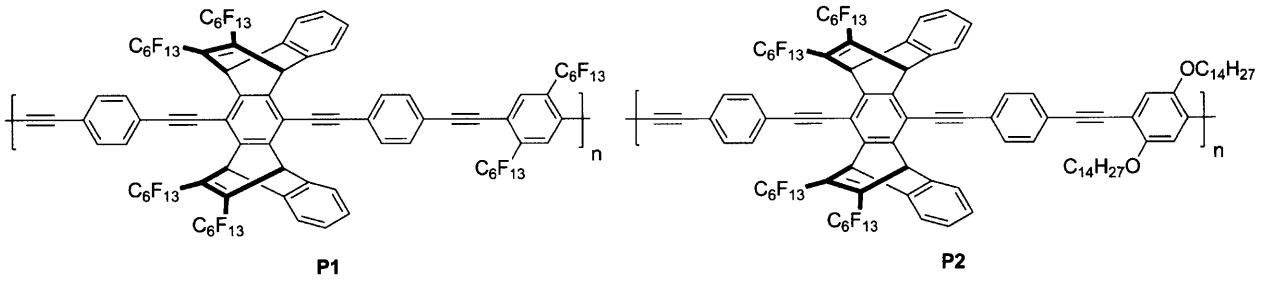

Figure 2-2. Chemical structures of **P1** and **P2**.

PPEs containing perfluoroalkyl groups have merit both in that they would allow for facile purification and processing and in that their unique physical properties would open up possibilities for novel methods of sensing. This chapter describes the syntheses and properties of two PPEs (**P1** and **P2**, Figure 2-2) from a heavily fluorinated monomer with specific design principles. One of the polymers, **P1**, contains ~60% fluorine content by weight in the form of perfluoroalkyl chains conjugated to the π-system of the polymer backbone. The polymer shows moderate to good solubility in the fluorous phase while showing no solubility in non-

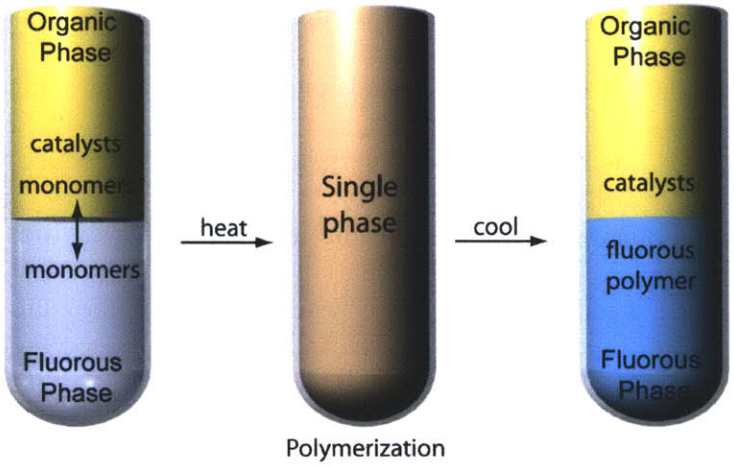

Figure 2-3. Fluorous biphase synthesis of fluorescent fluorous polymers.

fluorous solvents, and can be synthesized via fluorous biphase polymerization for facile isolation and purification of the polymer (Figure 2-3). Furthermore, the polymer displays remarkable photophysical properties such as a very high quantum yield and a small Stokes shift.

Results and Discussion

1st Generation Monomer Synthesis.

Our group has previously shown that [2.2.2] bicyclic ring structures incorporated to the main chain of fluorescent polymers prevent aggregation, via π-π stacking, of polymer chains, and

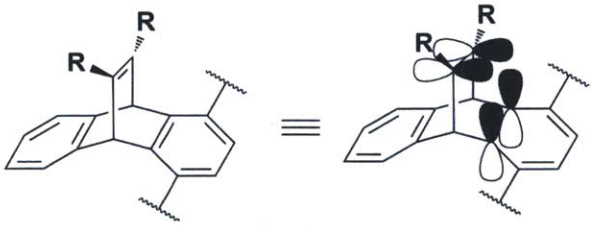

Figure 2-4. Homoconjugative interaction between the bridging alkene and benzene in a [2.2.2] bicyclic architecture.

introduce nanoscale porosity in solid state, facilitating analyte permeation into the polymer matrix. Our group has also shown that [2.2.2] bicyclic systems featuring alkenes with electron-withdrawing groups raise the ionization potential of the parent conjugated polymer through homoconjugative interactions (Figure 2-4).[9, 13] Based on these findings, a monomer with bis(perfluoroalkyl)alkenes on the [2.2.2] bicyclic ring architecture was targeted, the design principles of which are shown in Figure 2-5. The most direct approach to installing bis(perfluoroalkyl)alkene moiety involves a two-fold Diels-Alder cycloaddition reaction between perfluoroalkyne and a pentacene derivative.

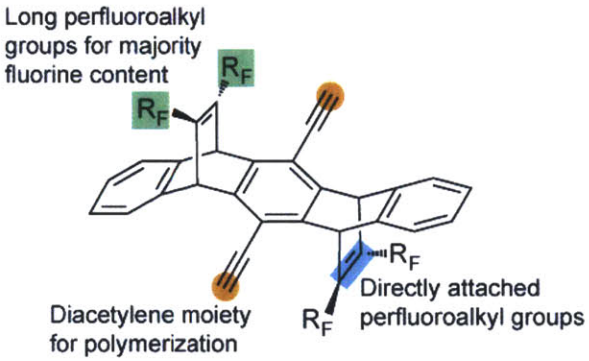

Figure 2-5. Design principles of the target PPE monomer with a non-compliant structure for potential sensory applications.

Scheme 2-1 shows the synthesis of a symmetrical perfluoroalkyne, perfluoro(7-tetradecyne) (**1**), and Scheme 2-2 shows the Diels-Alder reaction of the pentacene derivative **3**[9] with **1** and a previously reported[14] perfluoroalkyne, perfluoro(2-undecyne) (**2**). The pentacene derivative **3** has been reported to undergo two-fold Diels-Alder cycloaddition reactions with hexafluorobutyne to give the *anti* isomer as the major products (1:2 *syn*/*anti*).[9] When **3** was treated with an excess of perfluoro(2-undecyne) (**2**) in xylenes in a sealed tube at 135°C for 3 days, the corresponding di-adduct **4** was obtained in 88% yield. The longer reaction time

Scheme 2-1. Synthesis of perfluoro(7-tetradecyne) (**1**).

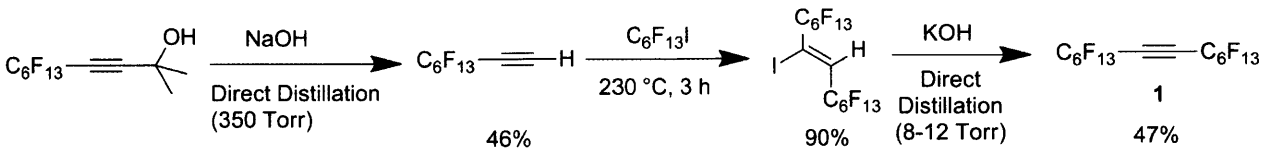

compared to that of hexafluorobutyne was attributed to the increased steric demand in **2**. The selectivity, however, was in sharp contrast to that of the hexafluorobutyne addition, giving a 1.9:1 *syn/anti* ratio.

When **3** was treated with an excess of perfluoro(7-tetradecyne) (**1**) in xylenes, no reaction took place even after 4 days at 145°C. The lack of reactivity was attributed to the poor solubility of **1** in xylenes even at elevated temperatures. When the reaction mixture was homogenized with a high-sheer mixer at 80°C before raising the temperature to 145°C, the desired two-fold Diels-

Scheme 2-2. Diels-Alder reactions of **3** with perfluoroalkynes **1** and **2**.

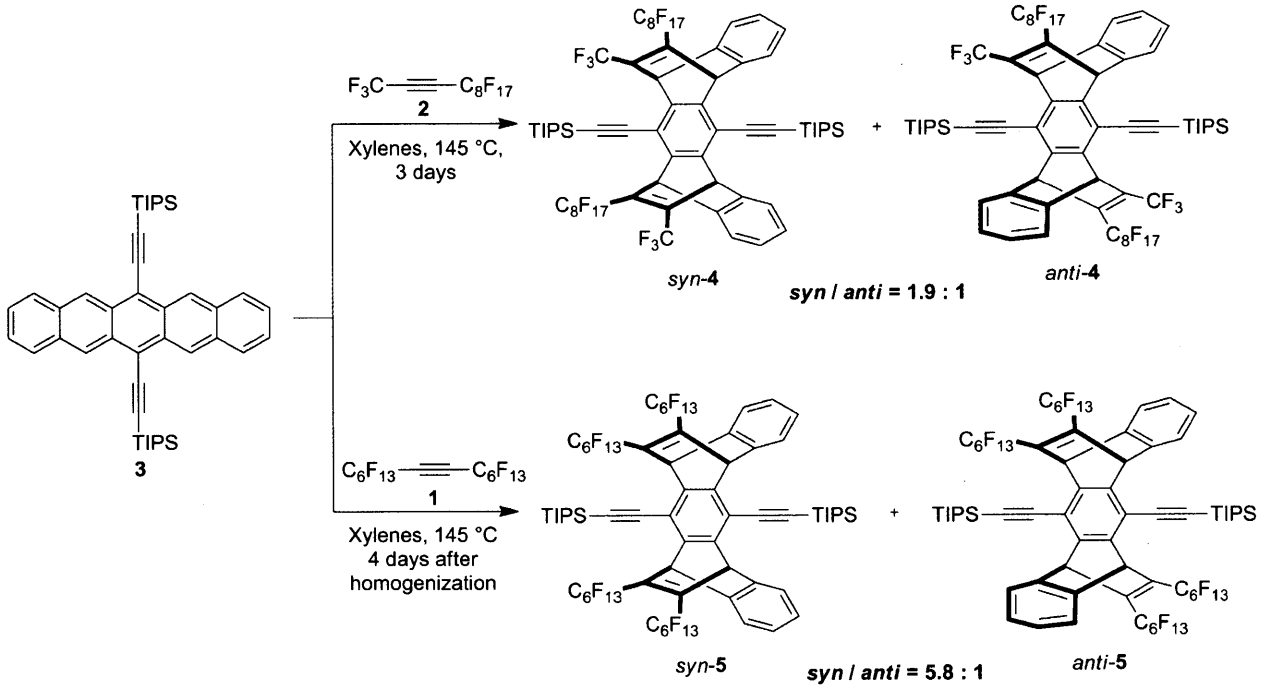

Alder reaction took place to give the corresponding diadduct **5** in 86% yield. The *syn*-selectivity was even more dramatic in this reaction, which gave a 5.8:1 *syn/anti* ratio.

The observed reversal in selectivity to favor a sterically more demanding product may be caused by a formation of emulsion of fluorous alkynes in xylenes, with the Diels-Alder reactions taking place at the interface. Emulsions, even those stabilized with surfactants, are dynamic in nature, with molecules constantly dissolving out of and into the emulsion particles,[15] and the lower *syn*-selectivity of the reaction of **2** could be associated to its higher solubility in xylenes, consistent with the observation that perfluoro(7-tetradecyne) (**1**) requires physical emulsification in order for the two-fold Diels-Alder reaction to take place, while **2** does not.

Scheme 2-3. Deprotection and structures of isomers.

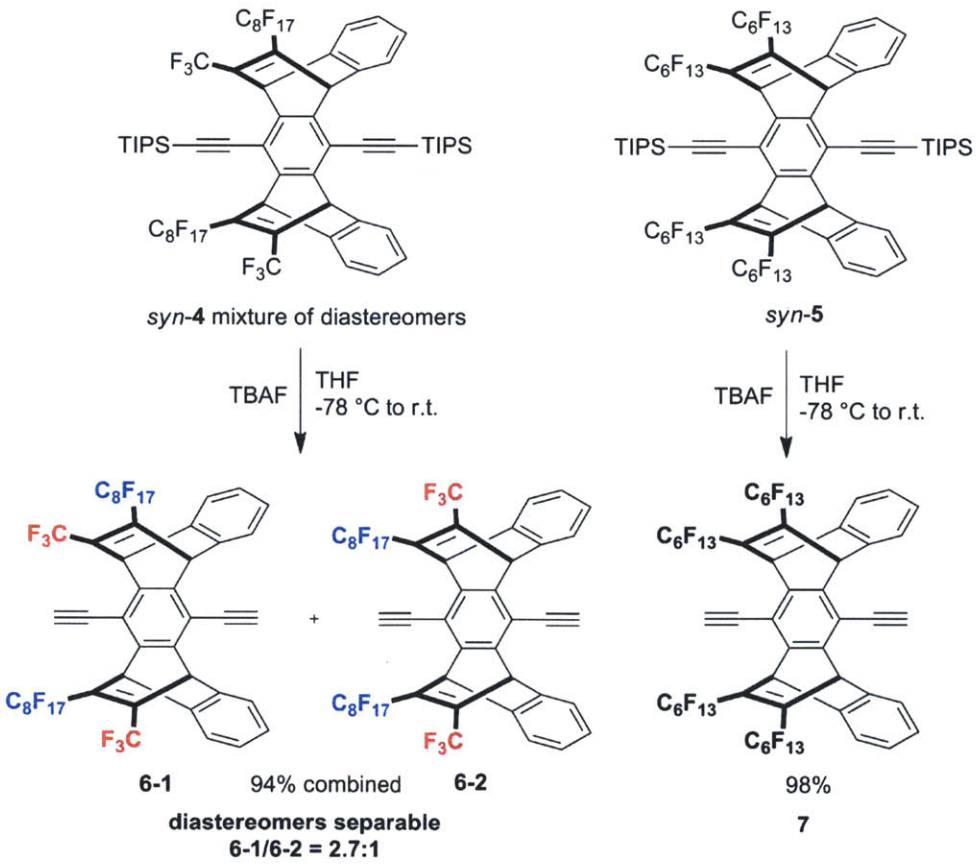

For both diadducts, **4** and **5**, the *anti*-isomers were sparingly soluble in most organic solvents while the s*yn*-isomers showed moderate-to-good solubilities. In both cases, *syn*-isomers could be isolated using a combination of recrystallization and chromatography. The *syn*-**4** isolated as a mixture of diastereomers which differed in the relative orientation of the perfluoroalkyl groups. The diasteromers were not separable at this stage. Due to the lack of solubility of the *anti*-isomers, the synthesis was carried forward using only the *syn*-isomers.

Removal of the TIPS moieties gave the corresponding diacetylenes **6** and **7**. The two diastereomers of **6** could be separated by recrystallization and chromatography to give **6-1** and **6-2**, the structure of which could be assigned via ^{1}H NMR spectroscopy (Scheme 2-3). Sonogashira-Hagihara cross-coupling polymerization between **7** and 1,4-bis(perfluorohexyl)-2,5-diiodobenzene (**8**; synthesis described in Scheme 2-4) under various temperatures and catalyst

Scheme 2-4. Synthesis of co-monomer **8**.

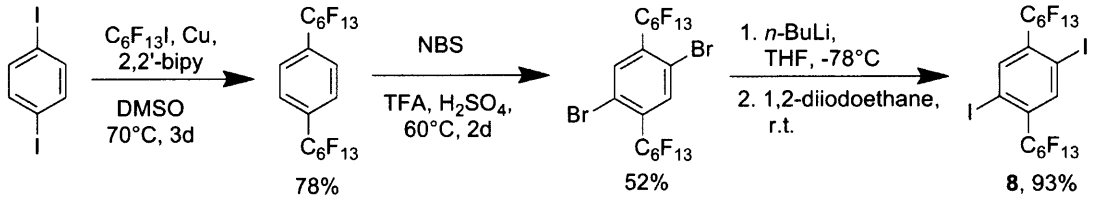

loading in toluene/diisopropylamine solvent system only gave mixtures dimeric and trimeric products. Similar results were obtained when **6-1** was subjected to identical polymerization conditions. In both cases, the oligomers were soluble in perfluorocarbon solvents, such as perfluoro(methylcyclohexane), FC-72 (perfluorohexanes), and FC-77 (perfluorooctane), as well as in non-fluorous solvents such as THF and hexanes.

In order to determine whether there were any differences in degrees of polymerization of each monomer, dynamic light scattering (DLS) on the polymer solutions were carried out. DLS

has been used previously to determine lengths of polymers, and PPEs have been reported to have persistence lengths of ~15 nm.[16] The DLS studies conducted in perfluoro(methylcyclohexane) indicated that polymers from **6-1** had length distributions (10.4 nm) higher than those from **7** (4.2 nm). Since both values were below the persistence lengths of PPEs, the result indicated that the polymerization from the **6-1** was giving materials with slightly higher degrees of polymerization. This suggested that steric effects around the reacting acetylene groups, rather than solubility, may be playing a role in preventing formation of longer polymers.

In order to address the steric issue, a new monomer, **10**, was synthesized as shown in Scheme 2-5. Monomer **7** was chosen over **6-1** and **6-2** as the starting material due to its higher fluorine content and a higher *syn*-selectivity in synthesis. Attempts to remove the TMS groups from **9** at room temperature gave bright yellow solids after chromatography. Although the NMR spectra of this product were clean, the emission spectrum from the resulting polymer suggested that there was a trace amount of highly emissive byproduct. Although NMR spectra of the product were clean, the emission spectrum suggested that the trace byproduct is from an inverse Diels-Alder reaction. The deprotection reaction of **9** with TBAF at -78°C gave the monomer **10** as a byproduct-free, off-white powder. The single-crystal X-ray structure of monomer **10** is shown in Figure 2-6.

Scheme 2-5. Synthesis of monomer **10** from **7**.

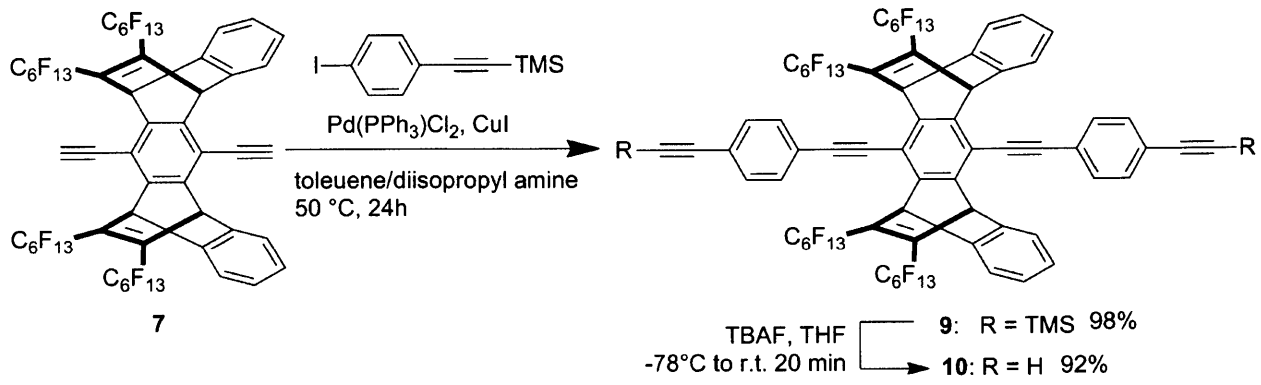

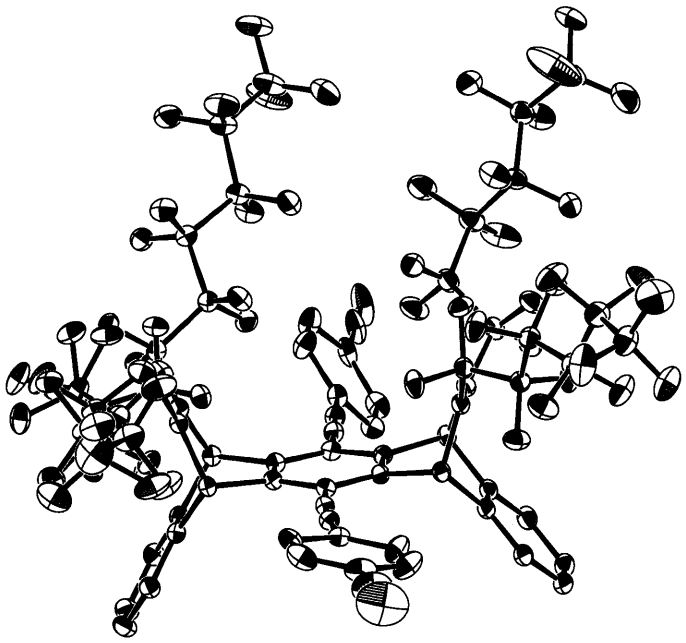

Figure 2-6. Single-crystal X-ray structure of monomer **10**. Thermal ellipsoids represent 50% probability. Hydrogen atoms are removed for clarity.

When monomer **10** was subjected to Sonogashira-Hagihara cross-coupling polymerization with diiodide **8** in toluene/diisopropyl amine solvent system, higher polymers were obtained. This polymer, however, was still soluble in non-polar solvents such as hexanes, and it was expected that fluorous solvent conditions for Sonogashira-Hagihara cross coupling reaction would yield polymers with higher molecular weights, which may subsequently render the material selectively soluble in fluorous solvents.

Fluorous Biphase Systems for Sonogashira-Hagihara Polymerization

Our initial approach was to replace toluene in toluene/diisopropyl amine system with perfluoro(methylcyclohexane). Interestingly, mixtures of perfluoro(methylcyclohexane) and diisopropyl amine became monophasic at an unexpectedly low temperature range of 40-45°C, and only separated out slowly upon cooling to room temperature. It had been previously reported

Table 2-1. Consolute temperature (T_c) of toluene/perfluoro(methylcyclohexane) mixtures.[17]

Volume Fraction of Toluene	Mole Fraction	T_c (°C)
0.900	0.943	63.7
0.800	0.880	83.1
0.700	0.810	87.7
0.600	0.733	88.9
0.500	0.647	88.6
0.400	0.550	87.2
0.300	0.440	82.0
0.200	0.314	68.7
0.100	0.169	42.8

that toluene/perfluoro(methylcyclohexane) biphasic mixtures become monophasic at moderate temperature ranges (T_c, consolute temperature) which vary depending on the ratio of the two solvents (Table 2-1), and separate out cleanly upon cooling.[17] When toluene in this system was substituted with a 1:1 mixture of toluene/diisopropyl amine as the non-fluorous component, the resulting biphasic mixtures had significantly (35-40°C) lower consolute temperatures than those of toluene/perfluoro(methylcyclohexane) mixtures. When the fluorous component of this biphasic mixture was replaced with a more polar fluorous solvent, perfluoro(*N*-propyl morpholine) (FC-770), consolute temperatures at 30-70% volume fraction of the fluorous component were all above 90°C, a temperature range impractical for PPE synthesis. Based on these observations, 1:1:1 v/v/v mixture of toluene/diisopropyl amine/perfluoro (methylcyclohexane) system was chosen for the fluorous biphase polymerization.

Polymer Synthesis

The fluorous biphase Sonogashira-Hagihara cross coupling polymerization between **10** and **8** gave, upon cooling, a biphasic mixture in which bright blue fluorescence was localized in

Scheme 2-6. Synthesis of **P1** and **P2**. The photographs show reaction mixtures at the end of the reaction irradiated with a hand-held long-wave UV lamp.

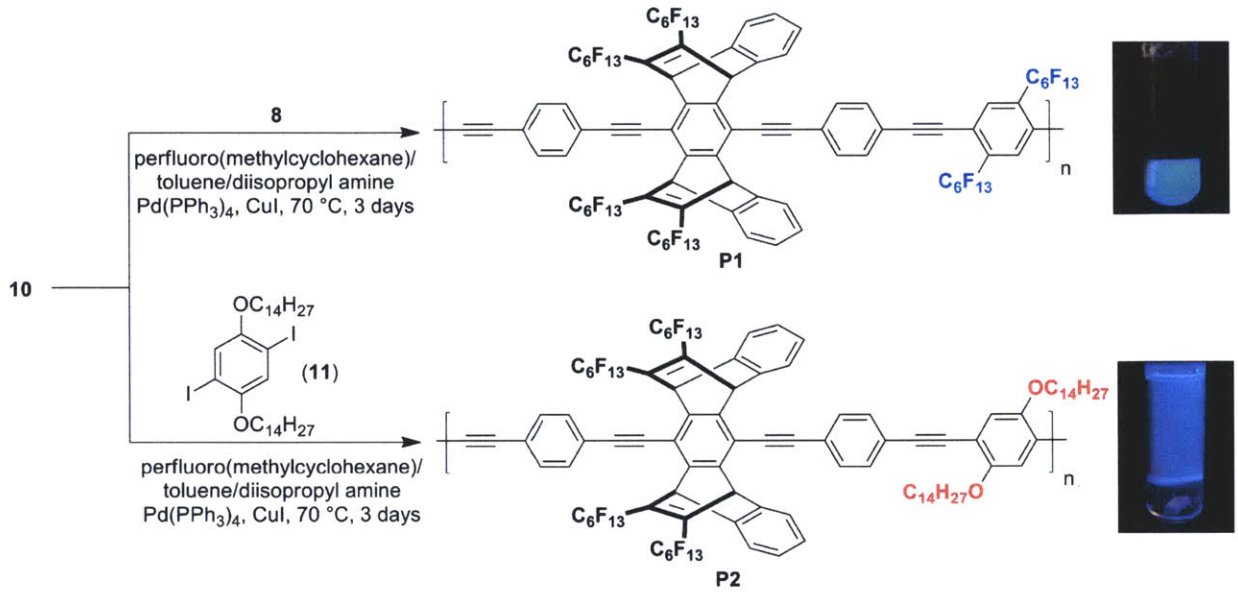

the lower, fluorous layer (Scheme 2-6). The removal of the organic layer, followed by washing the fluorous layer successively with methanol, acetone, and ethyl acetate, gave **P1** in 87% yield. Figure 2-7 shows the molar absorptivity (per phenylethynylene unit) of **P1** and oligomers (discussed earlier) obtained from the polymerization of **7** and **8**. There is a three-fold increase in the molar absorptivity, accompanied by a red-shift and sharpening of the absorption spectrum, indicating that **P1** has a significantly greater degree of polymerization than the oligomer. DLS analysis of the fluorous layer gave a value of 16.4 nm, a typical persistence length of a PPE-type polymer with a high molecular weight.[16] The polymer obtained in this manner was optically pure and was used without further purification for photophysical measurements.

When monomer **10** was treated with a non-fluorinated co-monomer **11** under identical conditions, a complete reversal of solubility was observed, with the fluorescence of the product biphasic mixture localized in the upper, non-fluorous, phase (Scheme 2-6). Removal of the

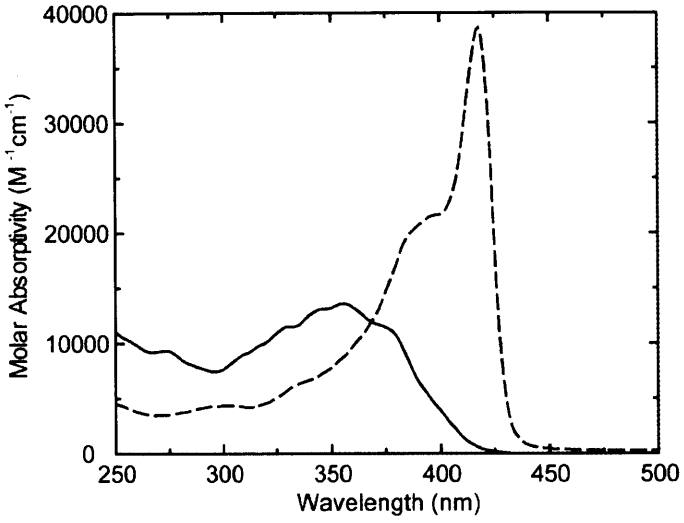

Figure 2-7. Molar absorptivity of **P1** (dashed) and oligomer from polymerization between **7** and **8** (solid).

fluorous layer, followed by precipitation of the organic layer into ethanol and washing the solids with acetone, gave **P2** in 78% yield.

Photophysical Properties

The normalized absorption and emission spectra of **P1** and **P2** are shown in Figure 2-8. Fluorous soluble **P1** displays band edge and emission maximum that are both blue-shifted in relation to the more electron-rich **P2**. A small Stokes shift (5-6 nm) and sharp absorption and emission spectra of **P1** suggest that the structure of the polymer in solution is highly rigid. Both polymers are highly fluorescent. Fluorous-soluble **P1** has a quantum yield of 0.95 in perfluorodecalin and the organic-soluble **P2** has a quantum yield of 0.84 in toluene. Furthermore, both polymers exhibit high quantum yields in thin film (0.32 for **P1** and 0.42 for **P2**).

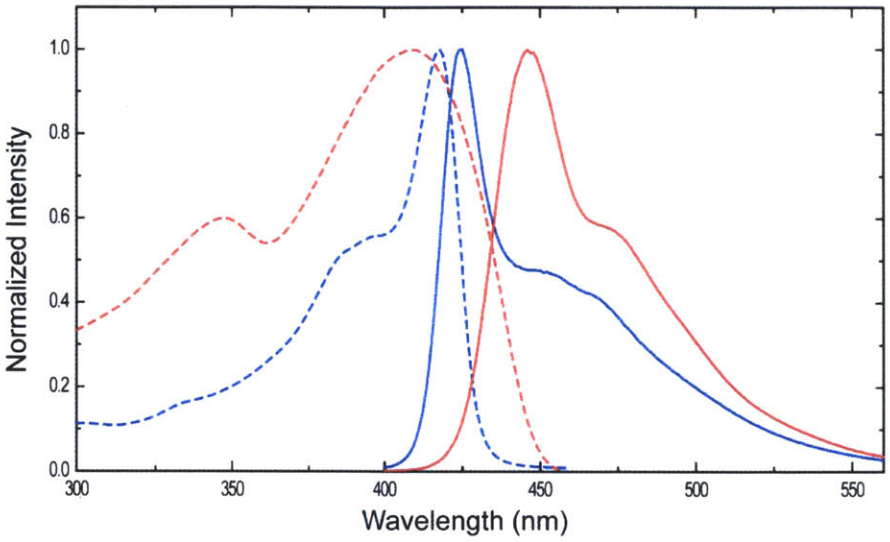

Figure 2-8. Absorption (dotted) and emission (solid) spectra of **P1** (blue, in perfluorodecalin; Q.Y. 0.95) and **P2** (red, in toluene; Q.Y. 0.84).

It is notable that **P1** showed a high quantum yield in perfluorodecalin. Perfluorodecalin[18] is a solvent which was approved by the U.S. Food and Drugs Administration (FDA) for use as a component in a human blood surrogate formulation, Fluosol,™ due to its ability to dissolve up to 50% v/v of oxygen at ambient pressure and 37 °C and its chemical and biological inertness. This finding motivated us to process **P1** as a fluorescent component in a perfluorodecalin emulsion in PBS buffer, details of which are described in Chapter 2 of this thesis.

To compare the properties of **P1** and **P2** with a non-fluorinated polymer with a similar structure, a new polymer, **P3**, featuring a rigid, three-dimensional architecture and dialkyl aryl moiety in the backbone, was synthesized (Scheme 2-7). This polymer displayed lower quantum yield (0.48 in toluene) compared to **P1** and **P2**. Furthermore, whereas the thin-film emission spectra of **P1** and **P2** do not show any noticeable change from their respective solution spectra,

Scheme 2-7. Structure and synthesis of **P3**.

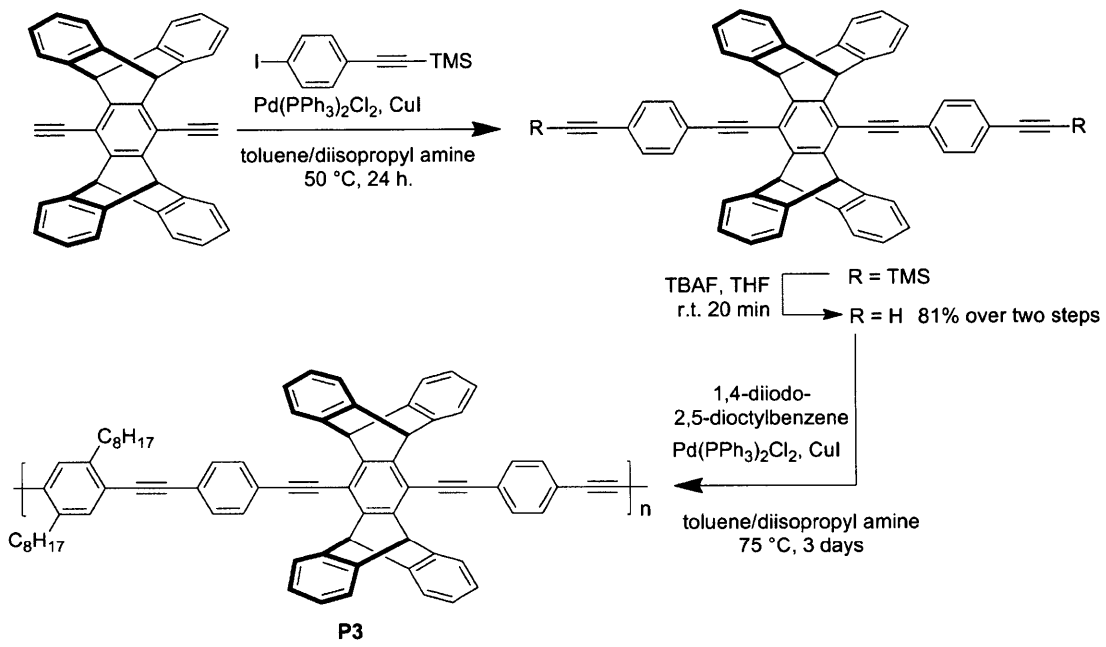

the thin-film emission spectrum of **P3** showed a broad and significantly red-shifted peak, suggesting large degrees of aggregation (Figure 2-9).

Although monomer **10** is soluble in organic solvents including acetone, hexanes, chloroform, ethyl acetate, and THF, and insoluble in non-polar fluorous solvents such as FC-77, perfluoro(methylcyclohexane), and perfluorodecalin, **P1** is soluble in these fluorous solvents but is insoluble in non-fluorous solvents. The exclusive fluorous solubility of **P1** made it difficult to characterize the polymer using standard procedures such as gel permeation chromatography (GPC). DLS measurements conducted on **P1** in both perfluorodecalin and perfluoro(methyl-cyclohexane) were both consistent with the typical persistence length.[16] When **P1** was end-capped with an addition of 1-bromo-4-*tert*-butylbenzene, no *tert*-butyl signals were observed in the proton NMR spectrum, indicating a high degree of polymerization (>20). The organic soluble **P2** could be analyzed by GPC, and was shown to have M_n = 520 kDa, M_w = 2,850 kDa, and PDI = 5.48.

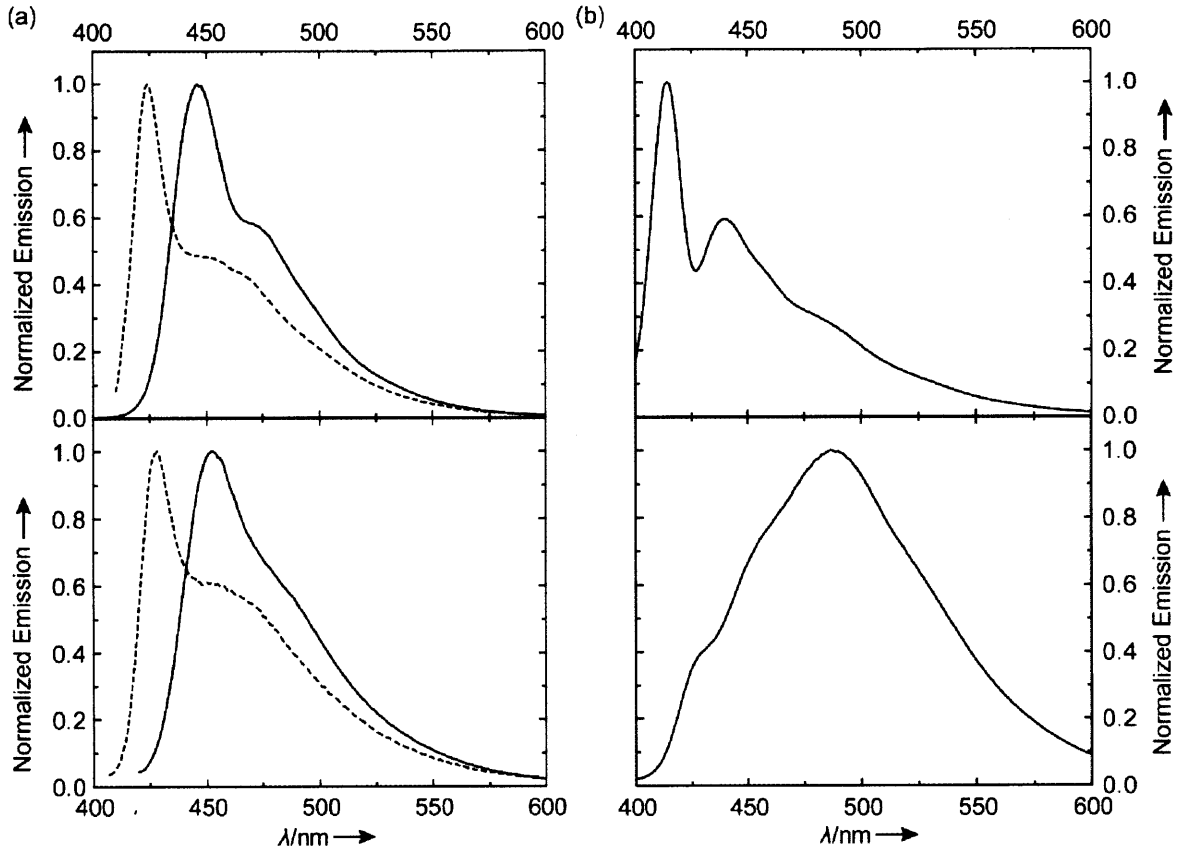

Figure 2-9. (a), top; solution emission spectra of **P1** (dotted) and **P2** (solid) in perfluoro(methylcyclohexane) and toluene, respectively, and bottom; thin-film emission spectra of **P1** (dotted) and **P2** (solid). (b), top; solution emission spectrum of **P3** in toluene, and, bottom; thin-film emission spectrum of **P3**.

Conclusion

In summary, we have synthesized two PPEs from a novel, heavily fluorinated building block, **10**, and established a fluorous biphasic polymerization method involving Sonogashira-Hagihara cross coupling reaction. We have also demonstrated that, depending on the choice of the co-monomer, the solubility properties of the product could be altered drastically. Both polymers from **10** were highly fluorescent both in solution and in thin film. The fluorous phase

soluble PPE, **P1**, was soluble in perfluorodecalin, a solvent approved by the FDA to be used as a component in artificial blood surrogate. Furthermore, the fluorescence quantum yield of the polymer in this solvent was 0.95, which is extraordinarily high even for a fluorescent polymer.

Experimental Section

General

All air- and moisture-sensitive synthetic manipulations were performed under an argon atmosphere using standard Schlenk techniques. Column chromatography was performed using ultra pure silica gel (SILIYCYCLE, 40~63 μm). NMR spectra were obtained on a Varian Mercury-300 spectrometer, and all proton chemical shifts are referenced to residual $CHCl_3$ or THF-d_8, and all fluorine chemical shifts are referenced to an external $CFCl_3$ standard. High-resolution mass spectra were obtained at the MIT Department of Chemistry Instrumentation Facility (DCIF) on a Bruker Daltronics APEX II3 Tesla FT-ICR-MS. Polymer molecular weights and polydispersity indexes were estimated by gel permeation chromatography (GPC) using a HP series 1100 GPC system. Polystyrene standards were used for calibration, and tetrahydrofuran (THF) was used as the eluent at a flow rate of 1.0 mL/min. Fluorescence spectra were measured on a SPEX Fluorolog-τ3 fluorimeter (model FL-321, 450 W Xenon lamp) using right-angle detection for solutions and front-face detection for thin films. Ultraviolet-visible absorption spectra were measured with an Agilent 8453 diode array spectrophotometer and corrected for background signal with a solvent-filled cuvette for solutions and glass slide for thin films. Fluorescence quantum yields of polymer solutions were determined by the optically dilute method[19] using quinine sulfate in 0.1M H_2SO_4, coumarin 6 in ethanol, or 9,10-diphenylanthracene in hexanes as standards and were corrected for solvent refractive index and

absorption differences at the excitation wavelength. Fluorescence quantum yields of polymer thin films were determined using 9,10-diphenylanthracene in poly(methyl methacrylate) (PMMA)(ϕ_F = 0.83).[20] Dynamic light scattering (DLS) data for polymer length distribution was obtained from Wyatt Technologies DynaPro Titan using perfluoro(methylcyclohexane) and perfluorodecalin as solvents.

Materials

All solvents were spectral grade unless otherwise noted. Anhydrous toluene and was obtained using a solvent purification system (Innovative Technologies). Tetrahydrofuran (THF) was dried by refluxing overnight over freshly cut sodium and benzophenone, followed by distillation under argon. Perfluorohexyl iodide ($C_6F_{13}I$) was freshly distilled before use. Diisopropyl amine was distilled over calcium hydride and stored over activated 4Å molecular sieves. Perfluoro(methylcyclohexane) and FC-77 (perfluorooctane) was purified according to literature procedures for fluorocarbons[21] prior to use. All other chemicals were used as received. Solvents for polymerization (perfluoro(methylcyclohexane), toluene, and diisopropyl amine) were degassed via freeze-pump-thaw prior to use.

Synthesis

C_6F_{13}—≡—H

3,3,4,4,5,5,6,6,7,7,8,8,8-tridecafluorooct-1-yne. A flame-dried 50 mL round-bottom flask equipped with distillation apparatus was charged with 5,5,6,6,7,7,8,8,9,9,10,10,10-tridecafluoro-2-methyldec-3-yn-2-ol[22] (35.3 g, 88 mmol) and NaOH pellets (2.5 g, 61 mmol) under argon. The pressure was reduced to 400 mmHg and the flask was heated to 100°C. The crude product was

collected over an hour in a receiving flask in a brine/ice bath. The product was washed 3 times with distilled water and was subsequently dried over $MgSO_4$. Removal of drying agent via filtration gave the title compound (13.4 g, 46%) as a clear liquid. B.p. 92-94°C. ^{1}H NMR (300 MHz, $CDCl_3$): δ 3.07 (t, $J_{H\text{-}F}$ = 5.7 Hz, 1H). ^{19}F NMR (282 MHz, $CDCl_3$): δ -126.69 (2F), -123.39 (2F), -123.25 (2F), -121.83 (2F), -99.76 (2F), -81.33 (3F).

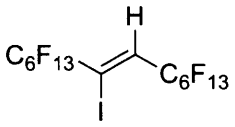

(Z)-1,1,1,2,2,3,3,4,4,5,5,6,6,9,9,10,10,11,11,12,12,13,13,14,14,14-hexacosafluoro-7-iodotetradec-7-ene. 3,3,4,4,5,5,6,6,7,7,8,8,8-tridecafluorooct-1-yne (17.5 g, 50 mmol) and $C_6F_{13}I$ (33.4 g, 75 mmol) were added to a 470 mL Parr bomb under N_2, and the reaction was sealed and heated to 230°C. The pressure of the reaction vessel increased initially to 95-100 psi, and was gradually reduced to 28 psi over 3 hours. The reaction was removed from heat and allowed to cool to room temperature before exposing the reaction chamber to atmosphere. The excess $C_6F_{13}I$ was removed by distillation at 10 mmHg, and the title compound (31.8 g, 80%) was obtained as a clear liquid by distillation at 6 mmHg. B.p. 99-101°C (6 mmHg). ^{1}H NMR (300 MHz, $CDCl_3$): δ 7.14 (t, $J_{H\text{-}F}$ = 12.6 Hz, 1H). ^{19}F NMR (282 MHz, $CDCl_3$): δ -126.62 (4F), -123.35 (6F), -122.22 (2F), -121.18 (2F), -119.25 (2F), -111.34 (4F), -104.21 (2F), -81.21 (6F). HR-MS (EI): calcd for $C_{14}HF_{26}I$ 789.8702; found 789.8723.

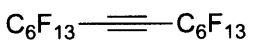

Perfluoro(7-tetradecyne) (1). A flame-dried 100 mL round-bottom flask was charged with anhydrous KOH (10 g, 170 mmol) under argon in the glove box. Outside the glove box, (Z)-1,1,1,2,2,3,3,4,4,5,5,6,6,9,9,10,10,11,11,12,12,13,13,14,14,14-hexacosafluoro-7-iodotetradec-7-ene (27.7 g, 35 mmol) was added, and the flask was equipped with a 15 cm vigreux column and

a short-path distillation apparatus. The pressure was decreased to 6 mmHg, and the reaction mixture was placed in an oil bath pre-heated to 60°C. The reaction was heated slowly to 105°C.** The product collected in the receiving flask was further purified by distillation at 6 mmHg (65-67°C) and the title compound (8.8 g, 38%) was obtained as a clear liquid. B.p. 65-67°C (6 mmHg). ^{1}H NMR (300 MHz, $CDCl_3$): blank. ^{19}F NMR (282 MHz, $CDCl_3$): δ -126.43 (4F), -123.14 (4F), -122.83 (4F), -121.61 (4F), -102.44 (4F), -81.04 (6F).

** WARNING: The reaction is often violent and increasing the temperature at rates above 2°C/min, using a smaller reaction flask, and/or starting the reaction above 6 mmHg can lead to explosion. Extreme caution should be taken when setting up this reaction.

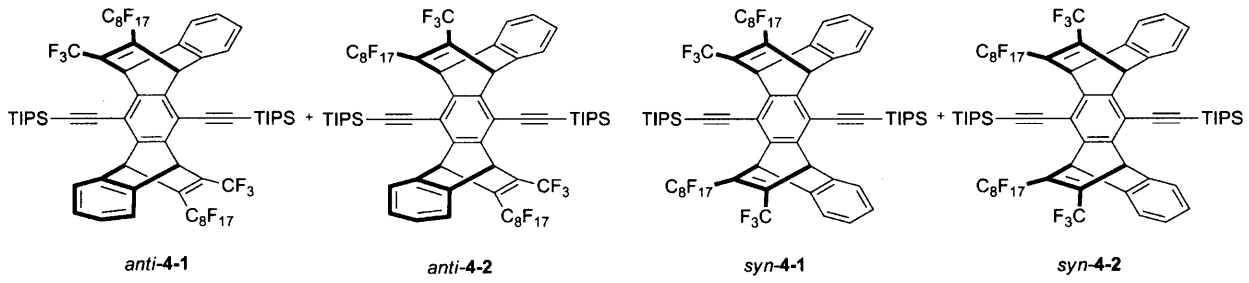

Compound 4. A flame-dried 45 mL pressure tube was charged with **3**[23] (3.0 g, 4.7 mmol), **2**[14] (8.8 g, 17.2 mmol), and xylenes (18 mL). The reaction mixture was degassed by bubbling argon through for 20 minutes while stirring. The reaction vessel was then sealed and heated to 145°C. The color of the reaction changed gradually from deep blue to yellow over 3 days, at which point the reaction was allowed to cool to room temperature. Solvent and excess **2** were removed via distillation. The crude product was recrystallized from hexanes to give a mixture *anti* isomer s(1.27 g, 16%). The mother liquor was concentrated under reduced pressure and recrystallized from acetone to give mixtures of both *syn* and *anti* isomers (3.46 g, 44%). The mother liquor was concentrated in vacuo and purified by column chromatography (silica gel, 100% hexanes) to give a mixture of *syn* isomers (3.05 g, 38%). **Anti** (*anti*-**4** mixture): M.p. > 300°C. ^{1}H NMR (300

MHz, $CDCl_3$): δ 1.28 (m, 42H), (5.92 and 5.97) (s, 4H), 7.12 (dd, $J_{H\text{-}H}$ = 5.4 and 3.3 Hz, 4H), (7.36 and 7.39) (dd. J = 5.4 and 3.3 Hz, 4H). **Syn** (*syn*-**4-2** mixture): M.p. > 300°C. ^{1}H NMR (300 MHz, $CDCl_3$): δ 1.28 (m, 42H), (5.97, 5.97, 5.92, 5.91) (s, 4H), 7.03 (dd, $J_{H\text{-}H}$ = 5.4 and 3.3 Hz, 4H), 7.278(dd. J = 5.4 and 3.3 Hz, 4H).

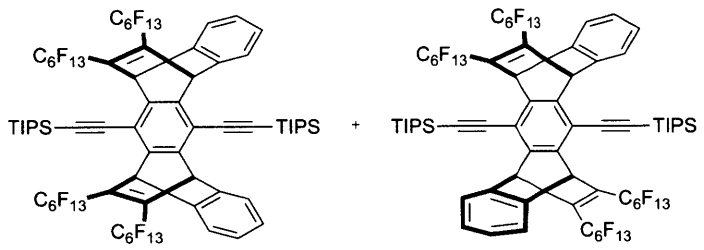

Compound 5. A flame-dried 25 mL pressure tube was charged with **3**[23] (640 mg, 1.0 mmol), **1** (2.0 g, 3.0 mmol), and xylenes (6 mL). The reaction mixture was degassed by bubbling argon through for 20 minutes while stirring. The reaction vessel was then placed in an oil bath at 80°C. After stirring for 20 minutes, the reaction mixture was homogenized with a high-sheer mixer for 20 seconds. The reaction vessel was then sealed and heated to 145°C. The color of the reaction changed gradually from deep blue to yellow over 4 days, at which point the reaction was allowed to cool to room temperature. Solvent and excess **1** were removed via distillation. The crude product was recrystallized in dichloromethane to give the *anti*-**5** (217 mg, 11%). The mother liquor was concentrated and was purified by column chromatography (silica gel, 100% hexanes), followed by recrystallization from acetone to give the *syn*-**5** (1.44 g, 73%) as rod-like crystals and an additional batch of *anti*-**5** (32 mg, combined yield of 13%). **Anti** (*anti*-**5**): M.p. > 300°C. ^{1}H NMR (300 MHz, $CDCl_3$): δ 1.28 (s, 42H), 5.97 (s, 4H), 7.11 (dd, $J_{H\text{-}H}$ = 5.4 and 3.3 Hz, 4H), 7.36 (dd. $_{H\text{-}H}J$ = 5.4 and 3.3 Hz, 4H). 19F NMR (282 MHz, $CDCl_3$): δ -126.73 (4F), -123.41 (4F), -122.33 (4F), -119.58 (4F), -109.62 (4F), -81.33 (6F). HR-MS (EI): calcd for $C_{76}H_{38}F_{52}Si_2$ 1994.1676; found 1994.1624. **Syn** (*syn*-**5**): M.p. > 300°C. ^{1}H NMR (300 MHz, $CDCl_3$): δ 1.28

(s, 42H), 5.97 (s, 4H), 7.03 (dd, J = 5.4 and 3.3 Hz, 4H), 7.27 (dd. J = 5.4 and 3.3 Hz, 4H). ^{19}F NMR (282 MHz, $CDCl_3$): δ -126.77 (4F), -123.47 (4F), -122.50 (4F), -119.83 (4F), -109.50 (2F), -108.30 (2F), -81.47 (6F). HR-MS (EI): calcd for $C_{76}H_{38}F_{52}Si_2$ 1994.1676; found 1994.1624.

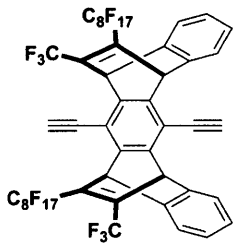

6-1

Compound 6-1. In a flame-dried 100 mL round bottom flask under argon, *syn*-**4** mixture (840 mg, 0.51 mmol) was dissolved in anhydrous THF (20 mL). The flask was cooled to -78°C in dry ice/acetone bath. Tetrabutyl ammonium fluoride (1.2 mL, 1.2 mmol) solution was added dropwise. The reaction was stirred at -78°C for 30 minutes. After warming up to room temperature, the reaction mixture was diluted with 10 mL ethyl acetate and 40 mL hexanes and subsequently passed through a plug of silica gel. The solvents were evaporated under reduced pressure and the crude product was purified by column chromatography (silica gel, 5% CH_2Cl_2 in hexanes as the eluent) followed by recrystallization from ethanol to give **6-1** as needle-like solids (430 mg, 63%). M.p. > 300°C. ^1H NMR (300 MHz, $CDCl_3$): δ 3.73 (s, 2H), 5.85 (s, 2H), 5.91 (s, 2H), 7.04 (dd, $J_{H\text{-}H}$ = 5.3, 3.3 Hz, 4H), 7.37 (dd, $J_{H\text{-}H}$ = 5.3, 3.3 Hz, 4H). ^{19}F NMR (282 MHz, $CDCl_3$): δ -126.49 (2F), -123.05 (2F), -122.19 (6F), -120.84 (2F), -81.04 (3F), -61.57 (3F). HR-MS (ESI): calcd for $C_{54}H_{14}F_{52}$ 1373.0354 $[M+Na]^+$; found 1673.0371.

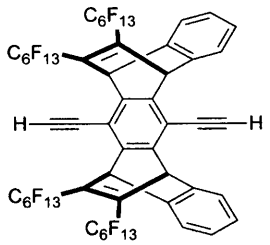

7

Compound 7. In a flame-dried 100 mL round bottom flask under argon, *syn*-**5** (800 mg, 0.41 mmol) was dissolved in anhydrous THF (20 mL). The flask was cooled to -78°C in dry ice/acetone bath. Tetrabutyl ammonium fluoride (0.85 mL, 0.85 mmol) solution was added dropwise. The reaction was stirred at -78°C for 20 minutes. After warming up to room temperature, the reaction mixture was diluted with 10 mL ethyl acetate and 40 mL hexanes and subsequently passed through a plug of silica gel. The solvents were evaporated under reduced pressure and the crude product was purified by column chromatography (silica gel, hexanes as the eluent) to give **7** as white, foamy solids (690 mg, quantitative). M.p. > 300°C. ^{1}H NMR (300 MHz, $CDCl_3$): δ 3.73 (s, 2H), 5.90 (s, 4H), 7.04 (dd, $J_{H\text{-}H}$ = 5.4, 3.1 Hz, 4H), 7.37 (dd, $J_{H\text{-}H}$ = 5.4, 3.1 Hz, 4H). ^{19}F NMR (282 MHz, $CDCl_3$): δ -126.70 (4F), -123.38 (4F), -122.47 (4F), -119.86 (4F), -108.89 (2F), -108.57 (2F), -81.34 (6F). HR-MS (ESI): calcd for $C_{54}H_{14}F_{52}$ 1673.0157 $[M+Na]^+$; found 1673.0192.

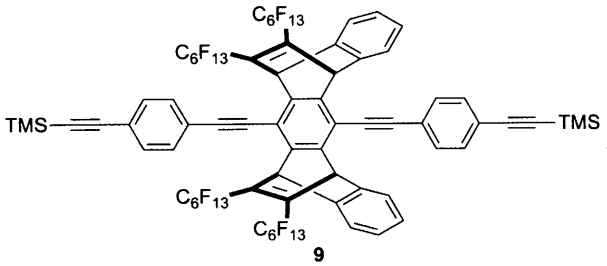

9

Compound 9. Flame-dried 10 mL Schenk flask was charged with **7** (415 mg, 0.251 mmol), 4-iodophenylethynyl trimethylsilane (180 mg, 0.600 mmol), $Pd(PPh_3)_2Cl_2$ (9.0 mg, 0.013 mmol), and copper(I) iodide (5.0 mg, 0.026 mmol). The flask was evacuated and back-filled with argon

three times. Toluene (2 mL) and diisopropyl amine (1 mL), degassed by freeze-pump-thaw, was added via syringe. The reaction mixture was stirred at 40°C for 12 hours. The reaction mixture was poured into 100 mL hexanes / 100 mL aqueous hydrochloric acid (0.1 M). The organic layer was washed with saturated aqueous sodium bicarbonate solution followed by water, dried over $MgSO_4$, and solvent removed under reduced pressure. Crude product was purified by column chromatography (silica gel, gradient from 100% hexanes to 5 % dichloromethane in hexanes) to give **9** as off-white solids (478 mg, 95%). M.p. > 300°C. ^{1}H NMR (300 MHz, $CDCl_3$): δ 0.30 (s, 18H), 5.95 (s, 4H), 7.05 (dd, $J_{H\text{-}H}$ = 5.4, 3.0 Hz, 4H), 7.40 (dd, $J_{H\text{-}H}$ = 5.4, 3.0 Hz, 4H), 7.56 (s, 8H). ^{19}F NMR (282 MHz, $CDCl_3$): δ -126.53 (4F), -123.25 (4F), -122.32 (4F), -119.77 (4F), -108.53 (2F), -108.26 (2F), -81.17 (6F). HR-MS (EI): calcd for $C_{76}H_{38}F_{52}Si_2$ 1994.1676; found 1994.1624.

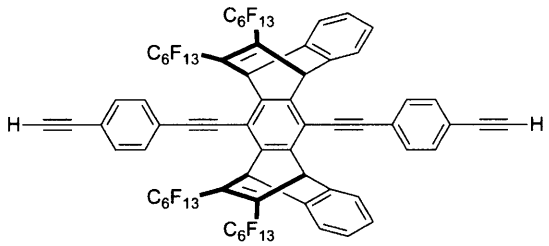

10

Monomer 10. In a 50 mL round bottom flask under argon, **9** (320 mg, 0.160 mmol) was dissolved in 10 mL anhydrous tetrahydrofuran. The solution was cooled to -78°C, and tetrabutylammonium fluoride (1.0 M in tetrahydrofuran, 0.340 mL, 0.340 mmol) was added dropwise. The reaction mixture was stirred at -78°C for 30 minutes and warmed up to room temperature, and subsequently passed over a plug of silica gel, eluting with 25 % ethyl acetate in hexanes. The solvents were removed under reduced pressure, and the crude product was purified by column chromatography (silica gel, 2% dichloromethane in hexanes) to give **10** as an off-white powder (276 mg, 93%). M.p. > 300°C. ^{1}H NMR (300 MHz, $CDCl_3$): δ 3.26 (s, 2H), 5.95

(s, 4H), 7.06 (dd, $J_{H\text{-}H}$ = 5.3, 3.0 Hz, 4H), 7.40 (dd, $J_{H\text{-}H}$ = 5.3, 3.0 Hz, 4H), 7.59 (s, 8H). ^{19}F NMR (282 MHz, $CDCl_3$): δ -126.71 (4F), -123.42 (4F), -122.49 (4F), -119.84 (4F), -108.72 (2F), -108.33 (2F), -81.35 (6F). HR-MS (ESI): calcd for $C_{70}H_{22}F_{52}$ 1873.0783 $[M+Na]^+$; found 1873.0822.

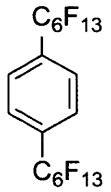

1,4-bis(perfluorohexyl)benzene. A 100 ml Schlenk flask equipped with a stir bar was flame-dried and then charged with 1,4-diiodobenzene (3.30g, 10 mmol), Cu powder (5.08 g, 80 mmol), and 2,2'-bipy (156 mg, 1 mmol). The flask was evacuated and back-filled with argon three times. Anhydrous dimethylsulfoxide (30 mL) was added via a syringe. Perfluorohexyl iodide (6.5 mL, 30 mmol) was added dropwise while stirring. Upon completion of addition, the reaction mixture was heated to 70 °C for 72 hours then removed from heat. The reaction mixture was poured into 100 mL H_2O / 100 mL diethyl ether and stirred vigorously for 30 min. Solid residues were removed by filtration, and the organic layer was washed twice with dilute NH_4OH solution, twice with water, dried over $MgSO_4$. The solvent was removed by evaporation under reduced pressure, and the resulting off-white solids were subjected to sublimation (0.025 mmHg, 70°C) to give the title compound as white solids (5.61 g, 78 %). ^{1}H NMR (300 MHz, $CDCl_3$): δ 7.77 (s, 4H). ^{19}F NMR (282 MHz, $CDCl_3$): δ -126.58 (4F), -123.26 (4F), -122.15 (4F), -121.87 (4F), -111.71 (4F), -81.16 (6F).

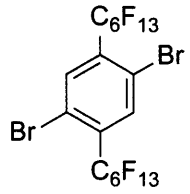

1,4-dibromo-2,5-bis(perfluorohexyl) benzene. A 50 mL round-bottom flask was chaged with 1,4-bis(perfluorohexyl)benzene (2.00 g, 2.80 mmol), trifluoroacetic acid (20.0 mL), and concentrated H_2SO_4 (6.0 mL). The reaction mixture was heated to 60 °C, and *N*-bromosuccinimide (1.50 g, 8.43 mmol) was added in portions (250 mg/hr) over 6 hours. The stirring was continued for 48 hours at 60 °C, and the reaction mixture was poured into iced water. Yellow precipitate was collected by filtration and were recrystallized twice in ethanol to give the title compound as clear crystals (1.27 g, 52%). ^{1}H NMR (300 MHz, $CDCl_3$): δ 7.94 (s, 2H) ^{19}F NMR (282 MHz, $CDCl_3$): δ -126.60 (4F), -123.16 (4F), -122.31 (4F), -119.70 (4F), -108.01 (4F), -81.23 (6F). HR-MS (EI): calcd for $C_{18}H_2Br_2F_{26}$ 871.8090; found 871.8049.

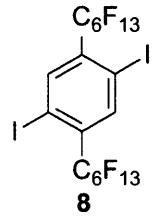

8

1,4-diiodo-2,5-bis(perfluorohexyl) benzene (8). A flame-dried 100 mL round-bottom flask was charged with 1,4-dibromo-2,5-bis(perfluorohexyl) benzene (872 mg, 1.0 mmol), and evacuated and back-filled with argon three times. Anhydrous diethyl ether (8.0 mL) and anhydrous tetrahydrofuran (8.0 mL) were added via syringe. The flask was cooled to -78°C and *tert*-butyllithium (1.5 M in pentanes, 3.0 mL, 4.5 mmol) was added dropwise over 15 minutes. The stirring was continuted for 1.5 hours at -78°C and diiodoethane (900 mg, 3.2 mmol) was added in one portion. The reaction was stirred in the dark at -78°C for an additional hour and was removed from bath. The stirring continued for an additional 16 hours. Water (50 mL) was added

to quench the reaction and the mixture was extracted with diethyl ether (2 X 50 mL). Organic layer was washed twice with NaOH solution (0.2 M), water, then brine, and solvent was removed under reduced pressure. Crude product was recrystallized in ethanol to give **8** (898mg, 93 %). M.p. 129-131°C. ^{1}H NMR (300 MHz, $CDCl_3$): δ 8.14 (s, 2H). 19F NMR (282 MHz, $CDCl_3$): δ -126.31 (4F), -122.88 (4F), -121.83 (4F), -118.83 (4F), -107.47 (4F), -80.93 (6F). HR-MS (EI): calcd for $C_{18}H_2F_{26}I_2$ 965.7825; found 965.7859.

P1. A flame-dried 100 mL Schlenk vessel with teflon screw-on cap under argon was charged with monomer **10** (74.35 mg, 0.0402 mmol), monomer **8** (37.67 mg, 0.0390 mmol), $Pd(PPh_3)_4$ (2.30 mg, 0.0020 mmol), and CuI (0.40 mg, 0.0021 mmol). In a glove box, perfluoromethylcyclohexane (6 mL), toluene (10 mL), and diisopropyl amine (2 mL) were added. The Shlenk vessel was removed from the glove box and was stirred vigorously at 85°C for 3 days. The reaction mixture, which was initially biphasic, became monophasic at c.a. 82°C. After allowing to cool down to room temperature, 10 mL of FC-77 was added. The fluorous (lower) phase, which was fluorescent, was subsequently removed and was washed 3 times with methanol (5 mL each), 3 times with ethyl acetate (5 mL each), and 3 times with acetone (5 mL each). Removal of the fluorous solvents under reduced pressure yielded **P1** as a yellow film, which was detached from the flask via sonication in ethanol (20 mL). Ethanol was then removed under reduced pressure to give **P1** (89.7 mg, 87%) as a bright yellow film. Polymer persistence length = 16.4 nm. ^{1}H NMR (500 MHz, FC-77, C_6D_6 external lock): δ 8.15-7.26 (br, 14H), 6.89 (br, 4H), 6.23 (br, 4H).

P2. A flame-dried 100 mL Schlenk vessel with teflon screw-on cap under argon was charged with monomer **10** (28.60 mg, 0.01505 mmol), monomer **11**[6] (11.17 mg, 0.01500 mmol), $Pd(PPh_3)_4$ (0.80 mg, 0.00069 mmol), and CuI (0.20 mg, 0.0011 mmol). In a glove box, perfluoromethylcyclohexane (5 mL), toluene (10 mL), and diisopropyl amine (5 mL) were added. The Shlenk vessel was removed from the glove box and was stirred vigorously at 70°C for 3 days. The reaction mixture, which was initially biphasic, became monophasic at c.a. 65°C. After allowing to cool down to room temperature the fluorous layer, which was not fluorescent, was removed. The organic layer was divided into two portions and each portion was added to 50 mL methanol. Yellow precipitates were collected via centrifugation, and the process was repeated three times with methanol, followed by three times with acetone to give **P2** (27.6 mg, 78%) as bright yellow solids after drying under vacuum. Mn = 520 kDa; PDI = 5.48; DP = 219 (THF-GPC). ^{1}H NMR (500 MHz, $CDCl_3$): δ 7.67 (br, 8H), 7.44 (br, 4H), 7.11 (br, 6H), 6.00 (br, 4H), 4.12 (br, 4H), 1.93 (br, 4H), 1.61 (br, 4H), 1.44 (br, 4H), 1.26 (br, 36H), 0.84 (t, 6H). ^{19}F NMR (282 MHz, $CDCl_3$): δ -126.66 (4F), -123.37 (4F), -122.38 (4F), -119.71 (4F), -108.72 (2F), -108.19 (2F), -81.32 (6F).

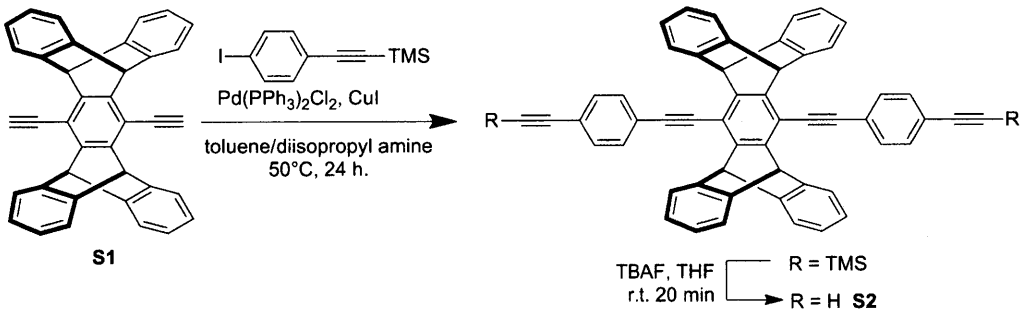

Monomer S2. Flame-dried 10 mL Schenk flask was charged with **S1** (180 mg, 0.376 mmol), 4-iodophenylethynyl trimethylsilane (237 mg, 0.790 mmol), $Pd(PPh_3)_2Cl_2$ (13.2 mg, 0.019 mmol), and copper(I) iodide (7.2 mg, 0.038 mmol). The flask was evacuated and back-filled with argon

three times. Toluene (2 mL) and diisopropyl amine (0.5 mL), degassed by freeze-pump-thaw, was added via syringe. The reaction mixture was stirred at 60°C for 16 hours. The reaction mixture was then precipitated into methanol (50 mL). The solids were further cleaned by re-precipitation in methanol three times, followed by re-precipitation in acetone three times. The resulting off-white solids were suspended in 10 mL anhydrous tetrahydrofuran under argon. Tetrabutylammonium fluoride (1.0 M in tetrahydrofuran, 0.770 mL, 0.770 mmol) was added dropwise. The reaction mixture was stirred at room temperature for 15 minutes, and subsequently passed over a plug of silica gel, eluting with 50 % dichloromethane in hexanes. The solvents were removed under reduced pressure, and the crude product was purified by column chromatography (silica gel, 30% dichloromethane in hexanes) to give **S2** as an off-white powder (203 mg, 81% over two steps). M.p. > 300°C. ^{1}H NMR (300 MHz, $CDCl_3$): δ 3.27 (s, 2H), 5.86 (s, 4H), 6.96 (dd, J = 5.1, 3.3 Hz, 8H), 7.38 (dd, J = 5.1, 3.3 Hz, 8H), 7.65 (d, J = 5.1 Hz, 4H), 7.75 (d, J = 5.1 Hz, 4H). ^{13}C NMR (300 MHz, $CDCl_3$): δ 52.52, 79.55, 83.46, 87.08, 96.54, 114.92, 122.65, 124.00, 124.07, 125.57, 141.90, 132.58, 144.33, 144.92.

P3. A flame-dried 100 mL Schlenk vessel with teflon screw-on cap under argon was charged with monomer **S2** (69.92 mg, 0.103 mmol), 1,4-diiodo-2,5-dioctylbenzene (55.43 mg, 0.100 mmol), $Pd(PPh_3)_4$ (5.8 mg, 0.050 mmol), and CuI (1.3 mg, 0.070 mmol). In a glove box, toluene (16 mL), and diisopropyl amine (4 mL) were added. The Shlenk vessel was removed from the glove box and was stirred at 75°C for 3 days. The reaction was then precipitated into 100 mL methanol. Yellow precipitates were collected via centrifugation, and the process was repeated three times with methanol, followed by three times with acetone to give **P3** (66.7 mg, 68%) as bright yellow solids after drying under vacuum. Mn = 73.7 kDa; PDI = 10.5; DP = 75 (THF-

GPC). ^{1}H NMR (500 MHz, THF-d_8): δ 7.92 (br, 4H), 7.78 (br, 4H), 7.52 (br, 2H), 7.41 (br, 8H), 6.95 (br, 8H), 6.00 (br, 4H), 1.30-1.60 (br, 24H), 1.44 (br, 4H), 0.98 (br, 10H).

NMR Spectra

*^{1}H NMR Spectrum of **6-1**($CDCl_3$/TMS)*

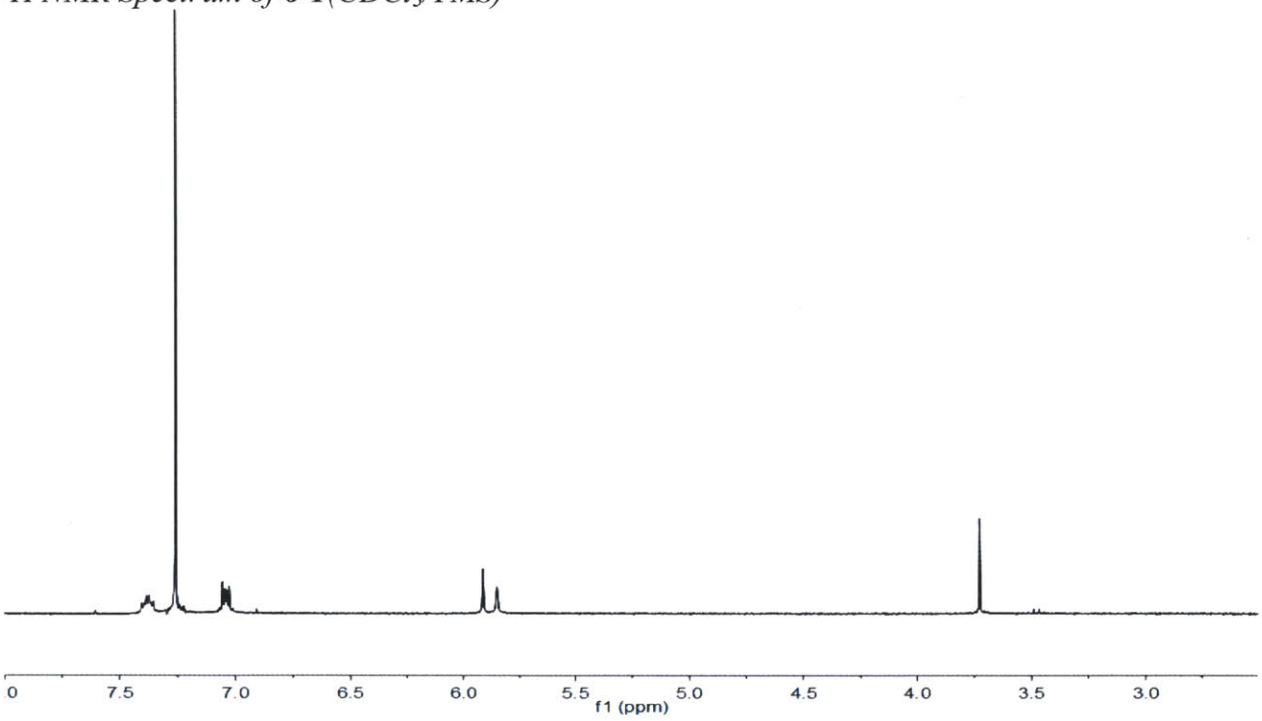

*^{1}H NMR Spectrum of **6-2**($CDCl_3$/TMS)*

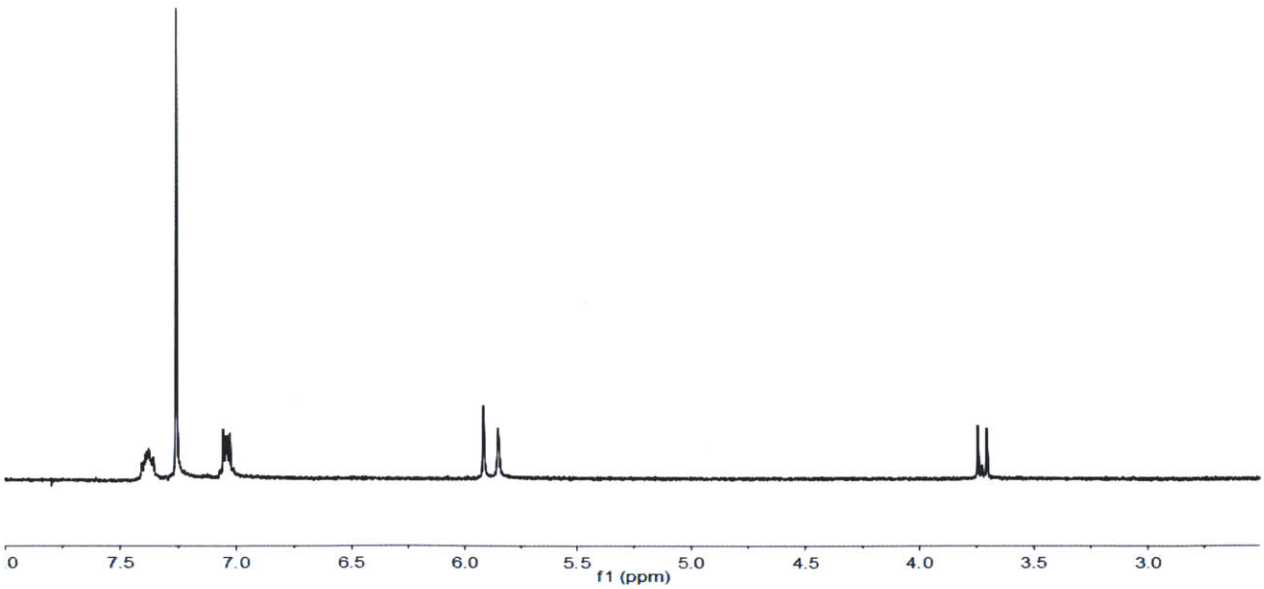

^{1}H NMR Spectrum of 7($CDCl_3$/TMS)

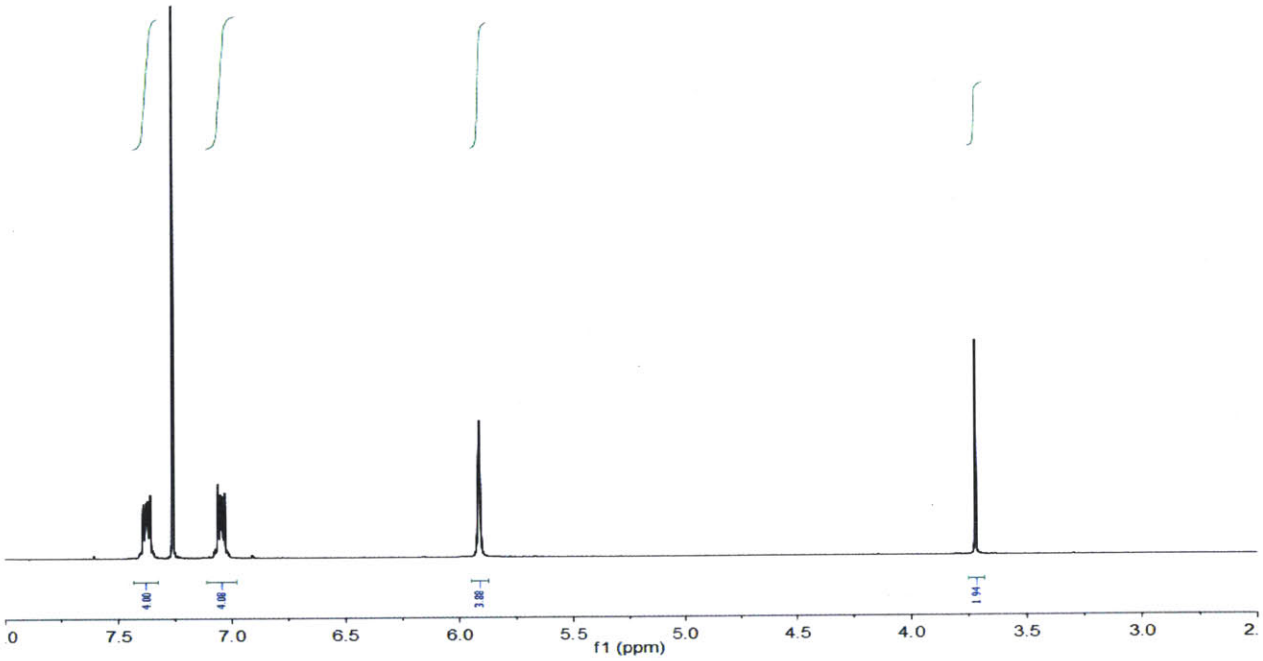

^{19}F NMR Spectrum of 7($CDCl_3$/TMS)

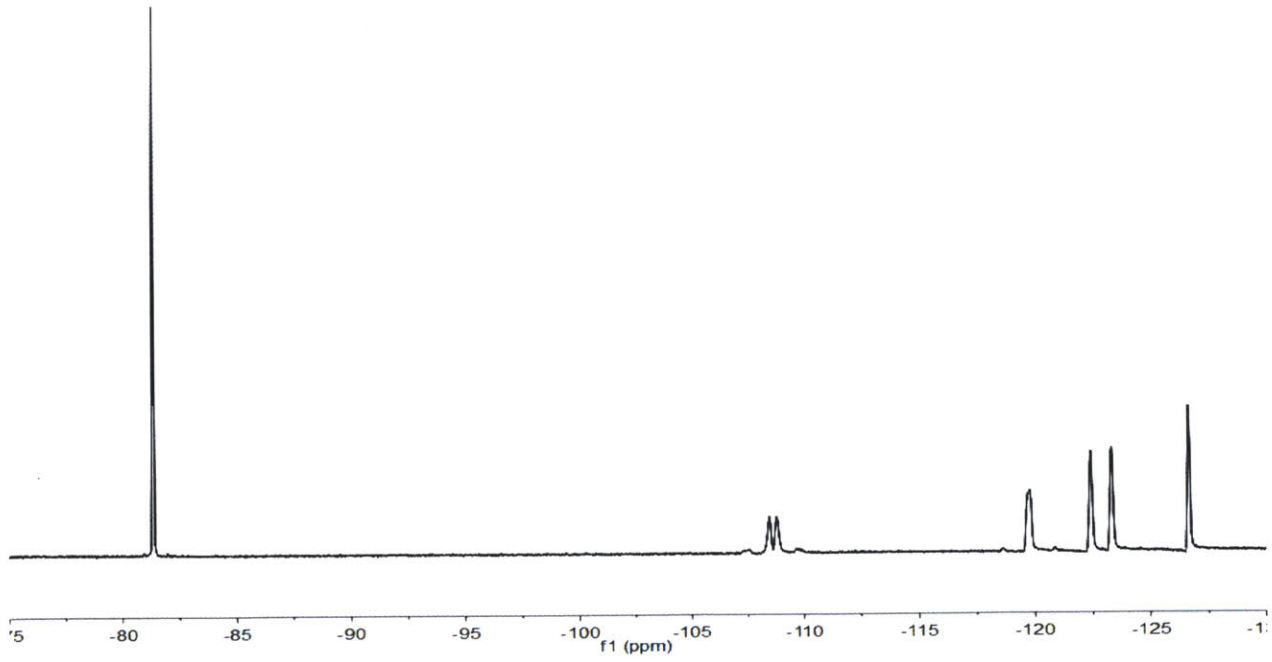

*^{1}H NMR Spectrum of **9**($CDCl_3$/TMS)*

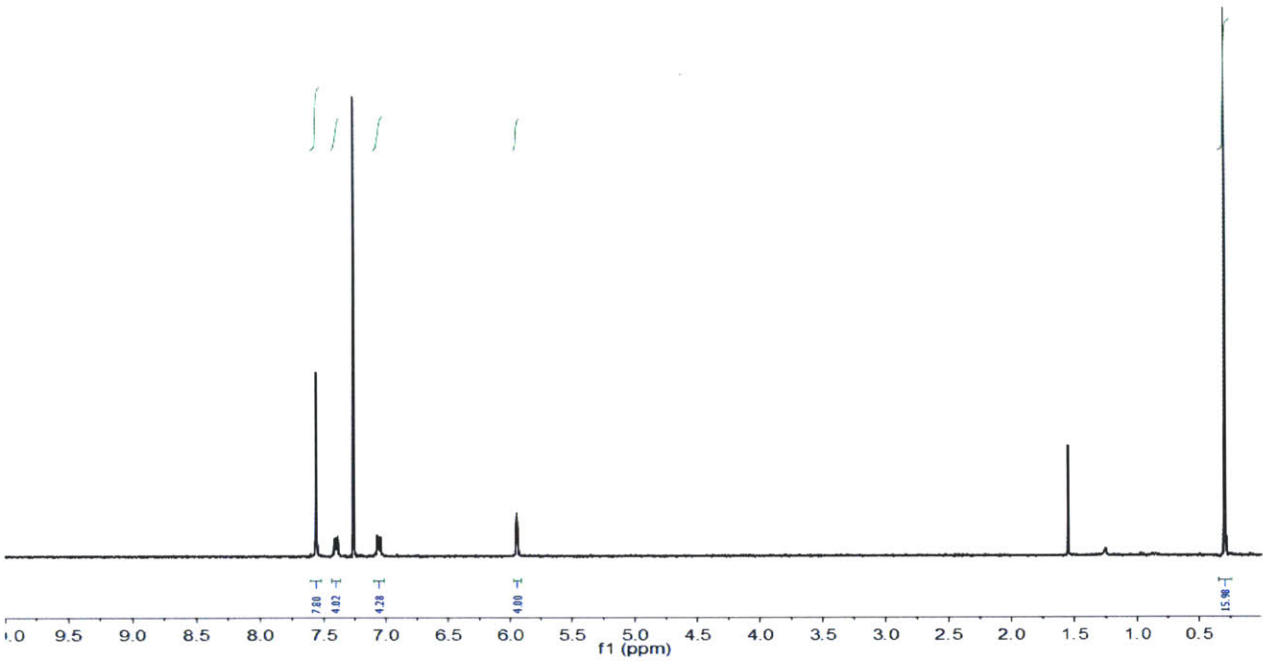

*^{19}F NMR Spectrum of **9**($CDCl_3$/TMS)*

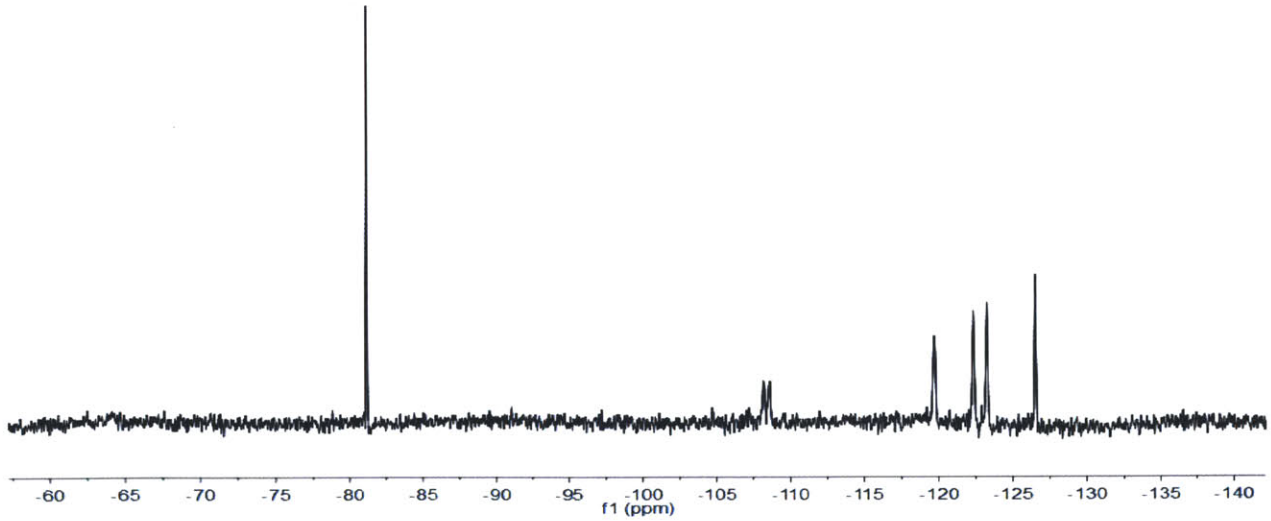

*^{1}H NMR Spectrum of **10**($CDCl_3$/TMS)*

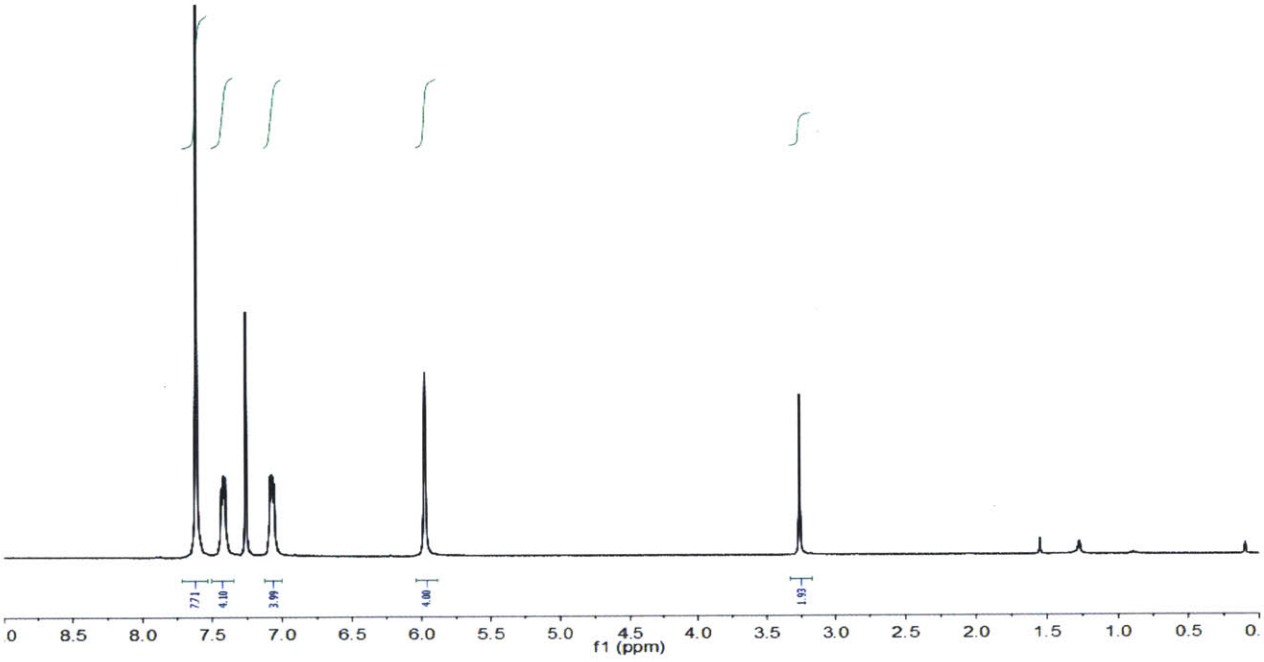

*^{19}F NMR Spectrum of **10** ($CDCl_3$/TMS)*

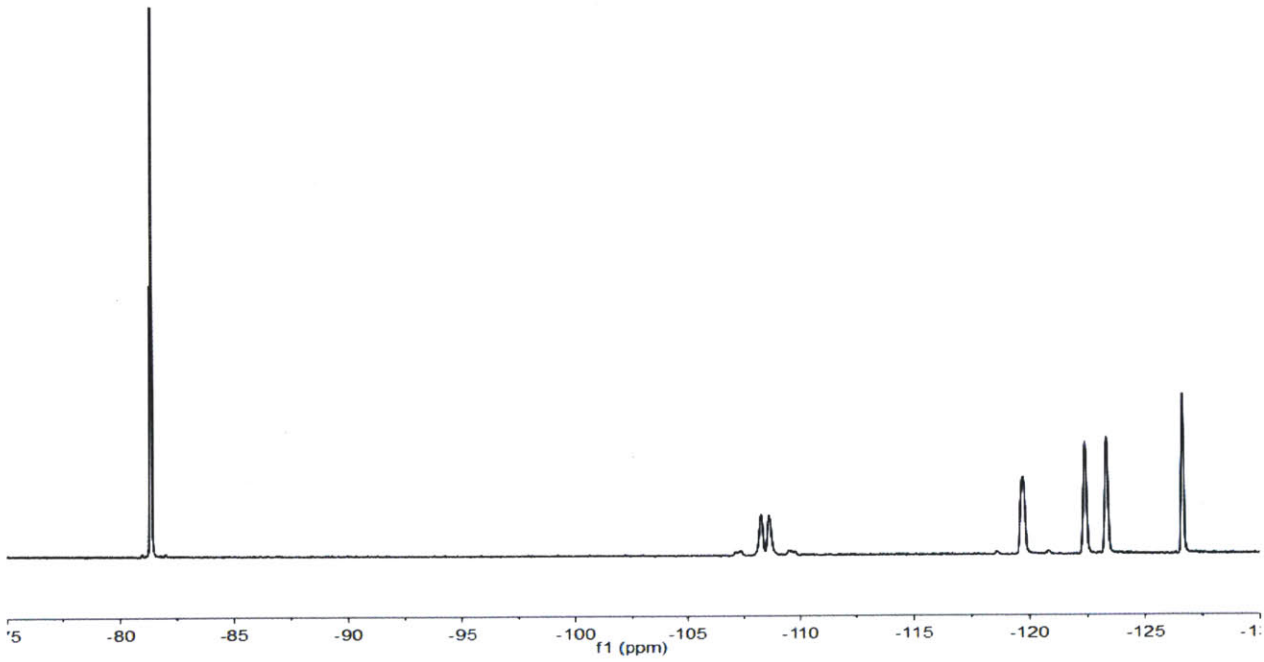

*^{1}H NMR Spectrum of **S2**($CDCl_3$)*

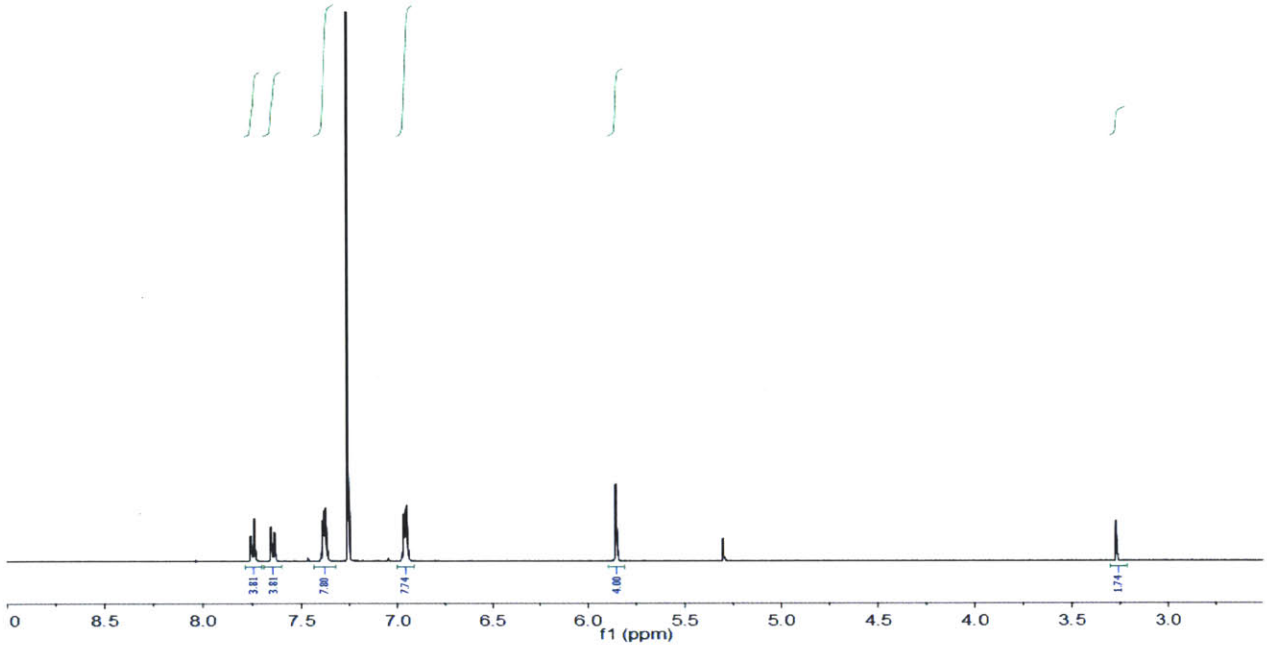

*^{13}C NMR Spectrum of **S2**($CDCl_3$)*

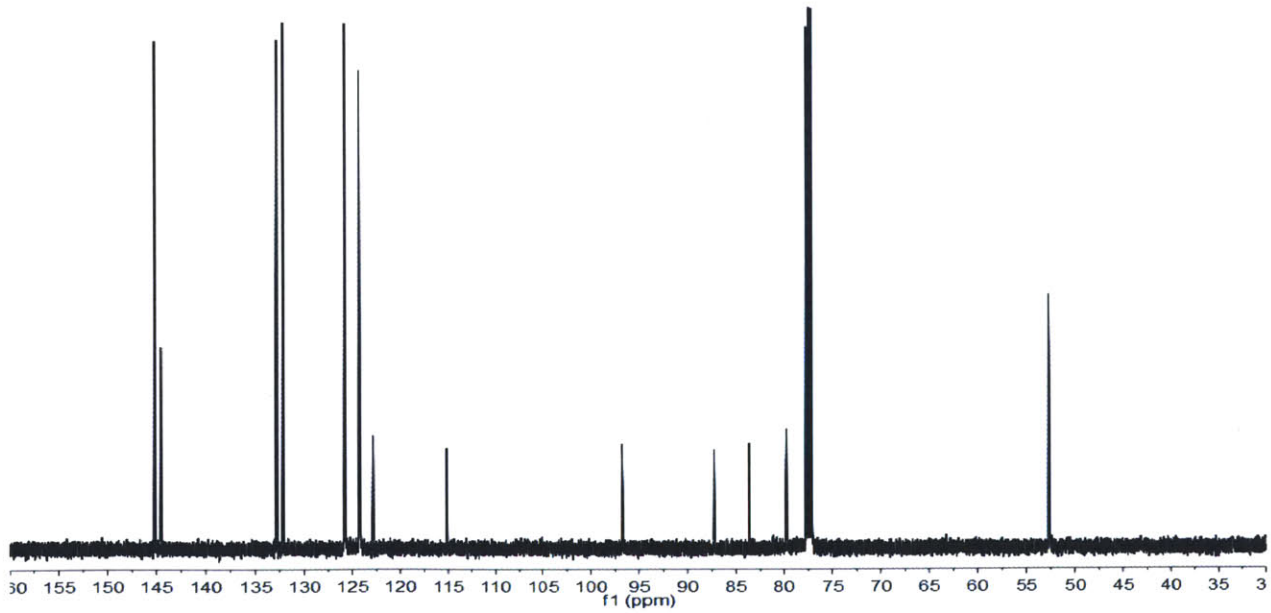

^{1}H NMR Spectrum of FC-77 (solvent only) with C_6D_6 External Lock

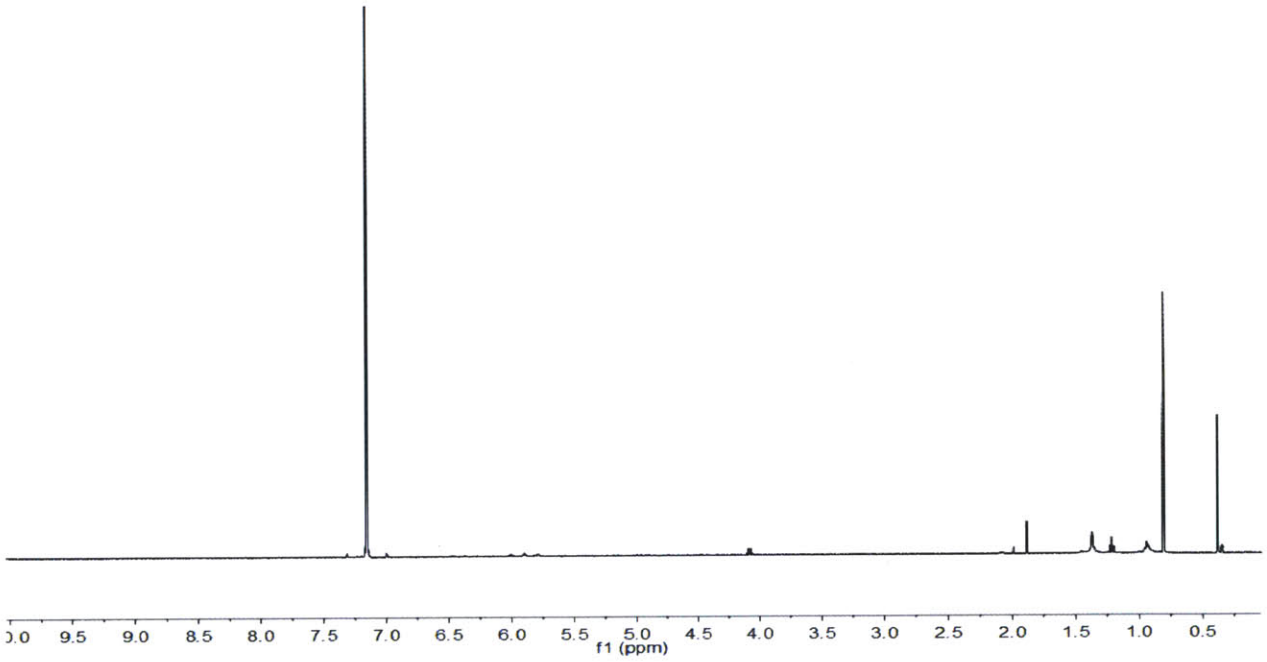

*^{1}H NMR Spectrum of **P1** in FC-77 (solvent only) with C_6D_6 External Lock*

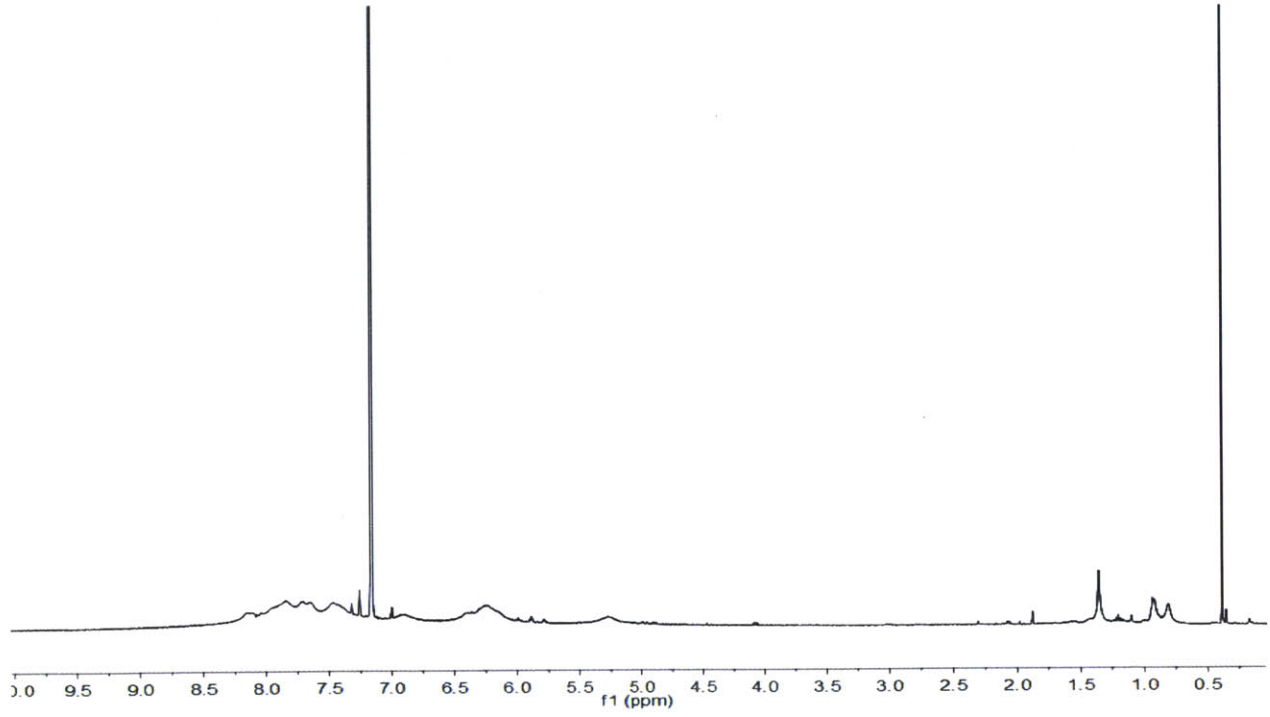

*^{1}H NMR Spectrum of **P2** in $CDCl_3$*

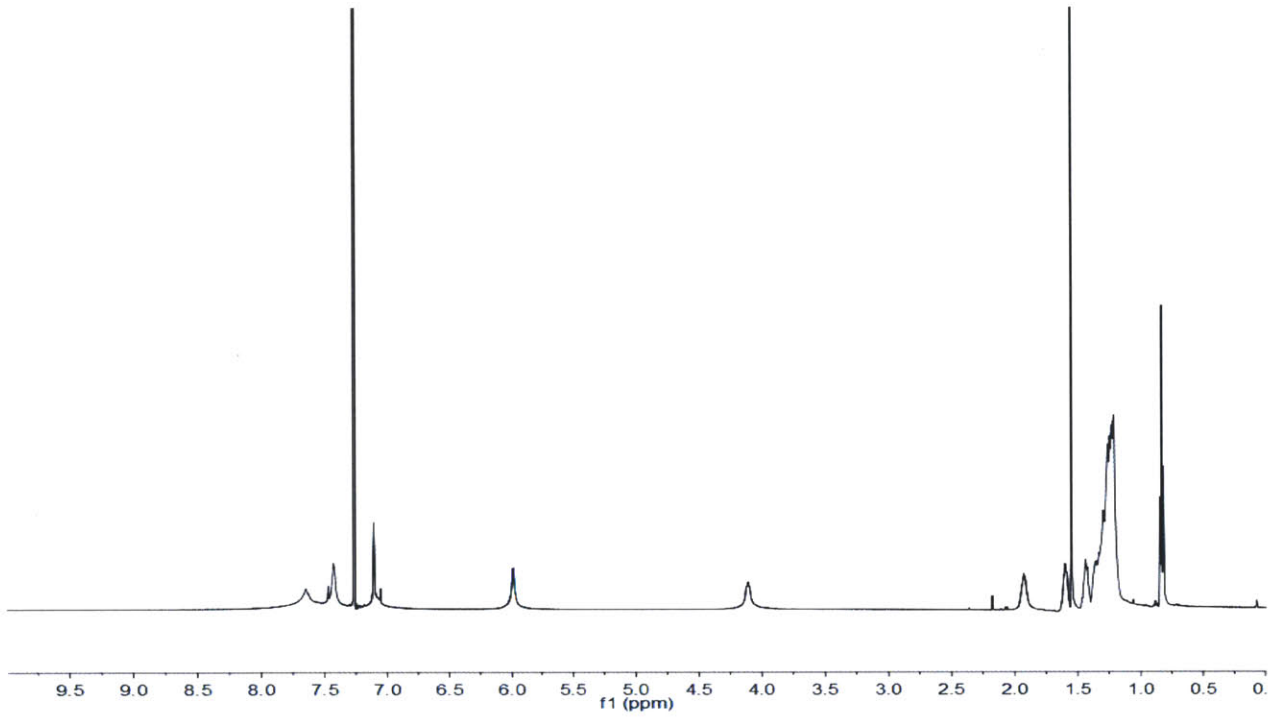

*^{19}F NMR Spectrum of **P2** in $CDCl_3$*

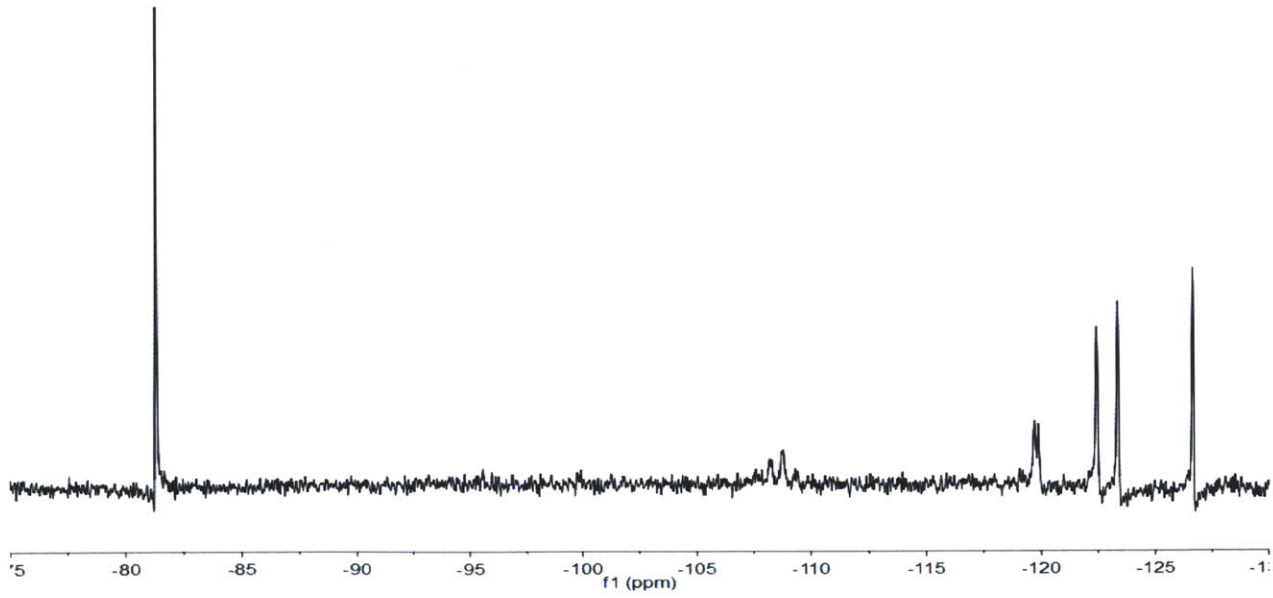

*^1H NMR Spectrum of **P3** in THF-d_8*

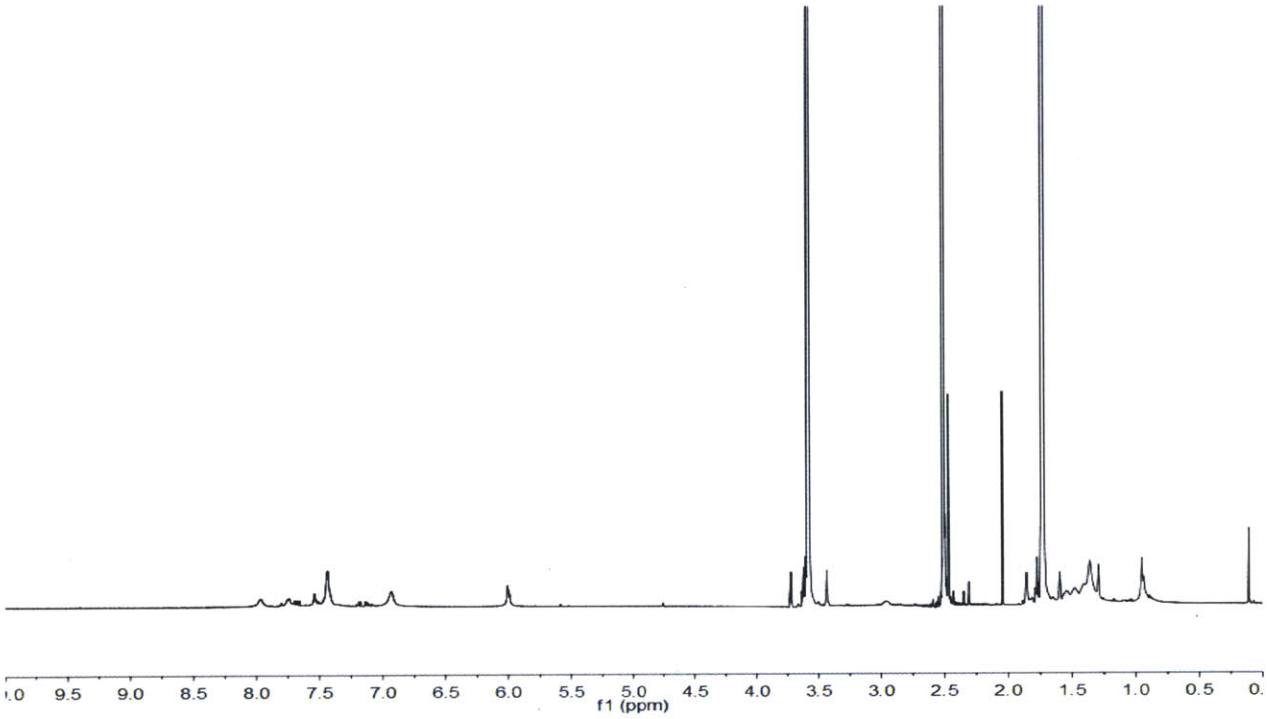

Table 2-2. Crystal data and structure refinement for **10**.

Compound	10	
Identification code	11183	
Empirical formula	C70 H22 F52	
Formula Weight	1850.862	
Temperature	100(2) K	
Wavelength	0.71073 Å	
Crystal system	Triclinic	
Space group	*P*1	
Unit cell dimensions	a = 14.7185(11) Å b = 16.0923(12) Å c = 16.5895(12) Å	α = 69.4790(10)° β = 88.2100(10) ° γ = 71.6190(10) °
Volume	3478.25 $Å^3$	
Z	2	
Density (calculated)	1.767 g/cm^3	
Absorption coefficient	0.201 mm^{-1}	
F(000)	1820	
Crystal size	0.12 mm × 0.25 mm × 0.30 mm	
Theta range for data collection	2.26 to 30.52 °	
Index ranges	-20 ≤ h ≤ 20, -22 ≤ k 22, -23 ≤ k ≤ 23	
Reflections collected	86526	
Independent reflections	19989	
Completeness to theta = 30.52°	99.5%	
Absorption correction	Multi-scan	
Max. and min. transmission	0.9763 and 0.9421	
Refinement method	Full-matrix least-squares on F^2	
Data/restraints/parameters	19989 / 645 / 1208	
Goodness-of-fit on F^2	1.017	

References

1. (a) McQuade, D. T.; Pullen, A. E.; Swager, T. M., Conjugated polymer-based chemical sensors. *Chem. Rev.* **2000,** *100* (7), 2537-2574; (b) Swager, T. M.; Thomas, S. W.; Joly, G. D., Chemical sensors based on amplifying fluorescent conjugated polymers. *Chem. Rev.* **2007,** *107* (4), 1339-1386.

2. Grimsdale, A. C.; Chan, K. L.; Martin, R. E.; Jokisz, P. G.; Holmes, A. B., Synthesis of Light-Emitting Conjugated Polymers for Applications in Electroluminescent Devices. *Chem. Rev.* **2009,** *109* (3), 897-1091.

3. Facchetti, A.; Letizia, J. A.; Salata, M. R.; Tribout, C. M.; Ratner, M. A.; Marks, T. J., n-channel polymers by design: Optimizing the interplay of solubilizing substituents, crystal packing, and field-effect transistor characteristics in polymeric bithiophene-imide semiconductors. *J. Am. Chem. Soc.* **2008,** *130* (30), 9679-9694.

4. (a) Gunes, S.; Neugebauer, H.; Sariciftci, N. S., Conjugated polymer-based organic solar cells. *Chem. Rev.* **2007,** *107* (4), 1324-1338; (b) Hsu, C. S.; Cheng, Y. J.; Yang, S. H., Synthesis of Conjugated Polymers for Organic Solar Cell Applications. *Chem. Rev.* **2009,** *109* (11), 5868-5923.

5. Bunz, U. H. F., Poly(aryleneethynylene)s: Syntheses, properties, structures, and applications. *Chem. Rev.* **2000,** *100* (4), 1605-1644.

6. Swager, T. M.; Gil, C. J.; Wrighton, M. S., Fluorescence Studies of Poly(P-Phenyleneethynylene)S - the Effect of Anthracene Substitution. *J. Phys. Chem* **1995,** *99* (14), 4886-4893.

7. (a) Swager, T. M.; Amara, J. P., Synthesis and properties of poly(phenylene ethynylene)s with pendant hexafluoro-2-propanol groups. *Macromolecules* **2005,** *38* (22), 9091-9094; (b)

Swager, T. M.; Thomas, S. W., Trace hydrazine detection with fluorescent conjugated polymers: A turn-on sensory mechanism. *Adv. Mater.* **2006,** *18* (8), 1047-1050; (c) Swager, T. M.; Yang, J. S., Fluorescent porous polymer films as TNT chemosensors: Electronic and structural effects. *J. Am. Chem. Soc.* **1998,** *120* (46), 11864-11873; (d) Swager, T. M.; Yang, J. S., Porous shape persistent fluorescent polymer films: An approach to TNT sensory materials. *J. Am. Chem. Soc.* **1998,** *120* (21), 5321-5322.

8. (a) Bunz, U. H. F.; Kim, I. B.; Wilson, J. N., Mannose-substituted PPEs detect lectins: A model for Ricin sensing. *Chem. Comm.* **2005,** (10), 1273-1275; (b) Kim, J.; Lee, K.; Cho, J. C.; DeHeck, J., Synthesis and functionalization of a highly fluorescent and completely water-soluble poly(para-phenyleneethynylene) copolymer for bioconjugation. *Chem. Comm.* **2006,** (18), 1983-1985; (c) Schanze, K. S.; Pinto, M. R., Amplified fluorescence sensing of protease activity with conjugated polyelectrolytes. *Proc. Nat. Acad. Sci. USA* **2004,** *101* (20), 7505-7510; (d) Swager, T. M.; Wosnick, J. H.; Liao, J. H., Layer-by-layer poly(phenylene ethynylene) films on silica microspheres for enhanced sensory amplification. *Macromolecules* **2005,** *38* (22), 9287-9290; (e) Swager, T. M.; Wosnick, J. H.; Mello, C. M., Synthesis and application of poly(phenylene ethynylene)s for bioconjugation: A conjugated polymer-based fluorogenic probe for proteases. *J. Am. Chem. Soc.* **2005,** *127* (10), 3400-3405; (f) Whitten, D.; Kumaraswamy, S.; Bergstedt, T.; Shi, X. B.; Rininsland, F.; Kushon, S.; Xia, W. S.; Ley, K.; Achyuthan, K.; McBranch, D., Fluorescent-conjugated polymer superquenching facilitates highly sensitive detection of proteases. *Proc. Nat. Acad. Sci. USA* **2004,** *101* (20), 7511-7515; (g) Whitten, D.; Rininsland, F.; Xia, W. S.; Wittenburg, S.; Shi, X. B.; Stankewicz, C.; Achyuthan, K.; McBranch, D., Metal ion-mediated polymer superquenching for highly sensitive detection of kinase and phosphatase activities. *Proc. Nat. Acad. Sci. USA* **2004,** *101* (43), 15295-15300; (h) Whitten, D. G.;

Achyuthan, K. E.; Bergstedt, T. S.; Chen, L.; Jones, R. M.; Kumaraswamy, S.; Kushon, S. A.; Ley, K. D.; Lu, L.; McBranch, D.; Mukundan, H.; Rininsland, F.; Shi, X.; Xia, W., Fluorescence superquenching of conjugated polyelectrolytes: applications for biosensing and drug discovery. *J. Mater. Chem.* **2005,** *15* (27-28), 2648-2656.

9. Whitten, J. E.; Kim, Y.; Swager, T. M., High ionization potential conjugated polymers. *J. Am. Chem. Soc.* **2005,** *127* (34), 12122-12130.

10. Kirsch, P., *Modern fluoroorganic chemistry : synthesis, reactivity, applications*. Wiley-VCH: Weinheim, 2004; pp 203-234.

11. Huheey, J. E., Electronegativity of Groups. *J. Phys. Chem.* **1965,** *69* (10), 3284-3291.

12. (a) Zhang, W.; Curran, D. P., Synthetic applications of fluorous solid-phase extraction (F-SPE). *Tetrahedron* **2006,** *62* (51), 11837-11865; (b) Curran, D. P.; Luo, Z. Y.; Zhang, Q. S.; Oderaotoshi, Y., Fluorous mixture synthesis: A fluorous-tagging strategy for the synthesis and separation of mixtures of organic compounds. *Science* **2001,** *291* (5509), 1766-1769; (c) Curran, D. P., Fluorous reverse phase silica gel. A new tool for preparative separations in synthetic organic and organofluorine chemistry. *Synlett* **2001,** (9), 1488-1496.

13. Swager, T. M.; Kim, Y.; Zhu, Z. G., Hyperconjugative and inductive perturbations in poly(p-phenylene vinylenes). *J. Am. Chem. Soc.* **2004,** *126* (2), 452-453.

14. Wagaman, M. W.; Bellmann, E.; Cucullu, M.; Grubbs, R. H., Synthesis of substituted bicyclo[2.2.2]octatrienes. *J. Org. Chem.* **1997,** *62* (26), 9076-9082.

15. Gladysz, J. A.; Curran, D. P.; Horváth, I. T., *Handbook of fluorous chemistry*. Wiley-VCH: Weinheim, 2004; p 546.

16. Cotts, P. M.; Swager, T. M.; Zhou, Q., Equilibrium flexibility of a rigid linear conjugated polymer. *Macromolecules* **1996,** *29* (23), 7323-7328.

17. Hildebrand, J. H.; Cochran, D. R. F., Liquid-Liquid Solubility of Perfluoromethylcyclohexane with Benzene, Carbon Tetrachloride, Chlorobenzene, Chloroform and Toluene. *J. Am. Chem. Soc.* **1949,** *71* (1), 22-25.

18. (a) Lowe, K. C.; Davey, M. R.; Power, J. B., Perfluorochemicals: their applications and benefits to cell culture. *Trends Biotechnol* **1998,** *16* (6), 272-277; (b) King, A. T.; Mulligan, B. J.; Lowe, K. C., Perfluorochemicals and Cell-Culture. *Bio-Technol* **1989,** *7* (10), 1037-1042.

19. Demas, J. N.; Crosby, G. A., Measurement of Photoluminescence Quantum Yields - Review. *J. Phys. Chem.* **1971,** *75* (8), 991-1024.

20. Osaheni, J. A.; Jenekhe, S. A., Electroactive and Photoactive Rod-Coil Copolymers - Design, Synthesis, and Supramolecular Regulation of Photophysical Properties. *J. Am. Chem. Soc.* **1995,** *117* (28), 7389-7398.

21. Glew, D. N.; Reeves, L. W., Purification of Perfluoro-Normal-Heptane and Perfluoromethylcyclohexane. *J. Phys. Chem.* **1956,** *60* (5), 615-615.

22. Aboughazaleh, B.; Laurent, P.; Blancou, H.; Commeyras, A., Addition of Perfluoroalkyl Iodides R(F)I (C(N)F(2n+1), N=4,6,8) to 2-Methyl-3-Butyn-2-Ol Activated by Zinc in Different Solvents - Application to the Synthesis of Perfluoroalkynes. *J. Fluorine Chem.* **1994,** *68* (1), 21-24.

23. Anthony, J. E.; Brooks, J. S.; Eaton, D. L.; Parkin, S. R., Functionalized pentacene: Improved electronic properties from control of solid-state order. *J. Am. Chem. Soc.* **2001,** *123* (38), 9482-9483.

CHAPTER 3

Properties and Sensory Applications of Fluorous Poly(*para*-Phenyleneethynylene)

Introduction

Since the late 1990s, fluorescent conjugated polymers (CPs) have been recognized as an important class of materials for sensory applications.[1] The advantages of CPs over traditional small-molecules in sensory applications is that the extended π-conjugated structure of CPs, often described as "molecular wires,"[2] features large signal amplification in fluorescence-based sensing due to facile diffusion of excitons through the polymer backbone. Small energy perturbations, such as those caused by analyte binding event, on a monomer unit can therefore produce observable changes in the emissive properties of the entire polymer chain (Figure 3-1). Such efficient delocalization is observed in both solution[3] and in solid state,[4] allowing for both solution-phase and solid-phase sensing.

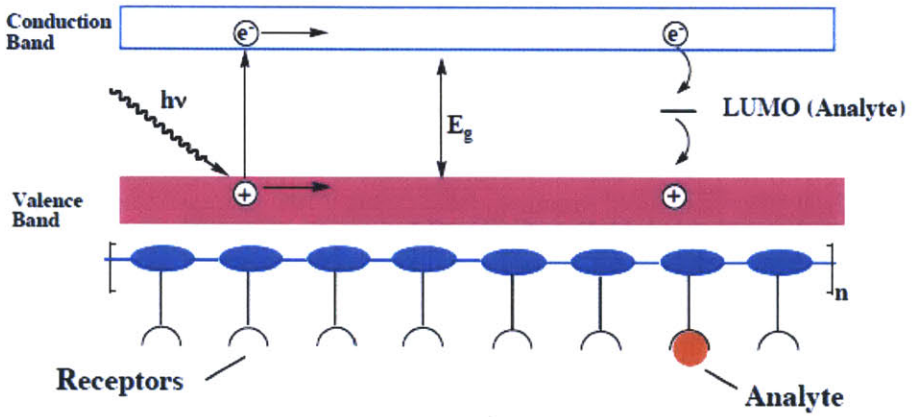

Figure 3-1. Schematic representation of sensing activity of a CP chain. Excitons migrating along the polymer backbone are quenched when a non-emissive pathway for recombination is provided by an analyte.

Electron-rich PPEs, such as the one shown in Figure 3-2, with rigid three-dimensional architecture have been previously synthesized by our group and have been shown to be excellent sensors of electron-deficient aromatics.[4-5] The fluorescence of these polymers in thin film show

strong quenching response to nitroaromatic compounds, including TNT at equilibrium vapor pressure (10 ppb).

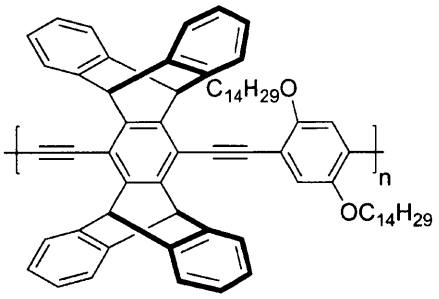

Figure 3-2. Structure of an electron-rich PPE with efficient quenching response to TNT.

An electron-poor PPE with [2.2.2] bicyclic architecture with pendant $-CF_3$ groups has also been previously reported. The polymer in solution was demonstrated to be efficiently quenched by electron-rich aromatic systems such as indole. From thin films of this polymer, however, a novel emissive signal was observed upon exposure to indole vapor, which was attributed to exciplex formation.[6] In some cases, [2.2.2] bicyclic structures were reported to undergo thermal and/or photophysical decomposition via retro Diels-Alder reaction, creating lower band-gap anthryl defects along the polymer chains (Figure 3-3).[7] The emissions from the defect sites were prominent in thin films while negligible in solution. This is probably due to enhanced interchain exciton migration in solid state. Stable electron-poor PPEs, which can detect electron-rich analytes in vapor phase, are therefore of interest.

Thin-films of PPEs have been coated on to solids supports, such as silica microspheres,[8] in order to achieve emissive water-soluble and water-dispersible platforms. While this approach has potentials biological imaging and sensing applications, difficulties of modifying polymer-coated bead surfaces poses a major challenge. Furthermore, solubility properties of the solid supports vary heavily depending on the nature of the polymer coating the outermost surface, and

presence of water-soluble side chains is required on PPEs in order to make PPE-coated particles soluble in water. Novel water-soluble PPE-based emissive platforms, therefore, are of interest for their potential of expanding the applications of these highly fluorescent materials.

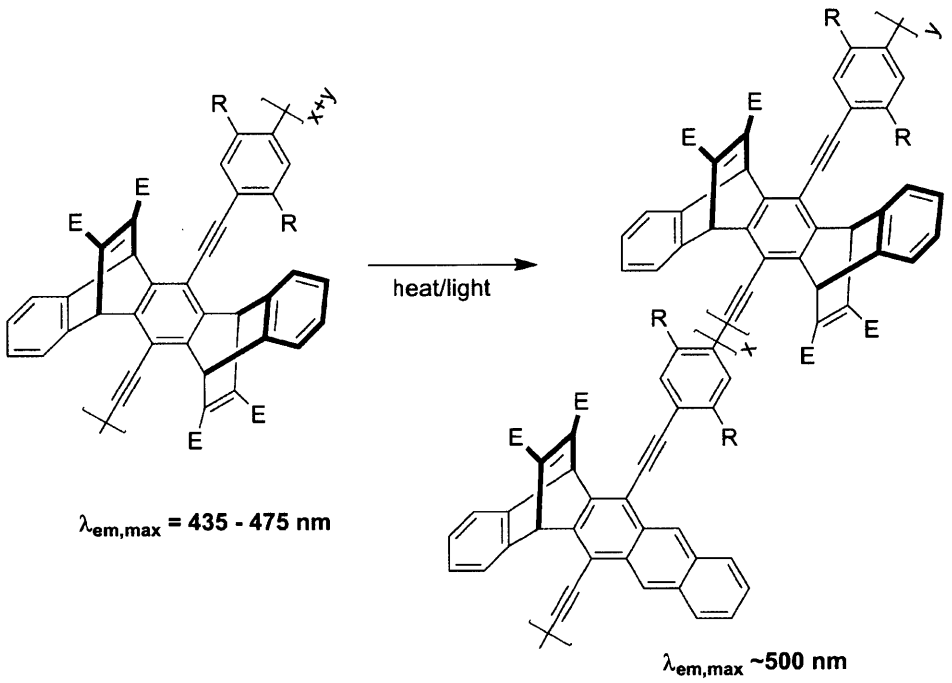

Figure 3-3. Anthryl defect formation in PPEs via retro Diels-Alder reaction.

In this chapter, quenching studies of thin films of **P1** (Chapter 2) is discussed, followed by the synthesis of fluorescent fluorous emulsions in PBS buffer (pH 7.4). The thin films of **P1** are photophysically and chemically stable, displaying excellent stability under UV irradiation and upon exposure to basic vapors such as indole and aniline. Fluorescence of **P1** is efficiently quenched by vapors of electron-rich aromatic molecules such as indole, aniline, and phenol. Furthermore, **P1** could be processed into fluorocarbon-in-water emulsions, preliminary studies of which suggest that it is possible to modify the surface of the emulsion for potential imaging applications.

Results and Discussion

Thin Film Properties

Thin films of **P1** spun-cast from perfluoro(methylcyclohexane) solutions onto glass were studied. Films cast from solutions with concentrations above 0.05 mg/ml gave emission signals with a relatively intense and broad shoulder, likely due to aggregation. Furthermore, emission from these films was too high for consistent measurement. Formation of aggregation was initially associated with the fluorous nature of the polymer resulting in unfavorable interactions with glass substrate surface. Treatment of glass surfaces with *1H,1H,2H,2H*-perfluorodecyltrichlrosilane prior to spin-casting, however, did not lead to reduction of the intensity of the shoulder. When films were cast onto untreated glass from solutions with concentrations of 0.025 mg/ml, the emission spectrum resembled that of the polymer in fluorous solutions. The studies discussed in this section are from thin-films cast from 0.025 mg/ml solutions of **P1** in perfluoro(methylcyclohexane). The optical densities of films prepared in this manner were 0.014 ± 0.001.

Water droplet contact angle, the angle at which water/air interface meets a solid surface, is a useful measurement for determination of relative surface energies of solid substrates. Among various methods of measuring contact angles, the dynamic sessile drop method measures both the maximum and minimum contact angle achievable on a solid substrate by dynamically adding and removing small volumes of water to and from the droplet. Water contact angle measurements using this method showed that thin films of **P1** had surface energies on par with that of Teflon (Figure 3-4). Both advancing and receding contact angle values were similar to those of Teflon-coated aluminum foil substrates. Prolonged exposure of the thin film to water droplets, however, led to detachment of the film from the surface of glass slides.

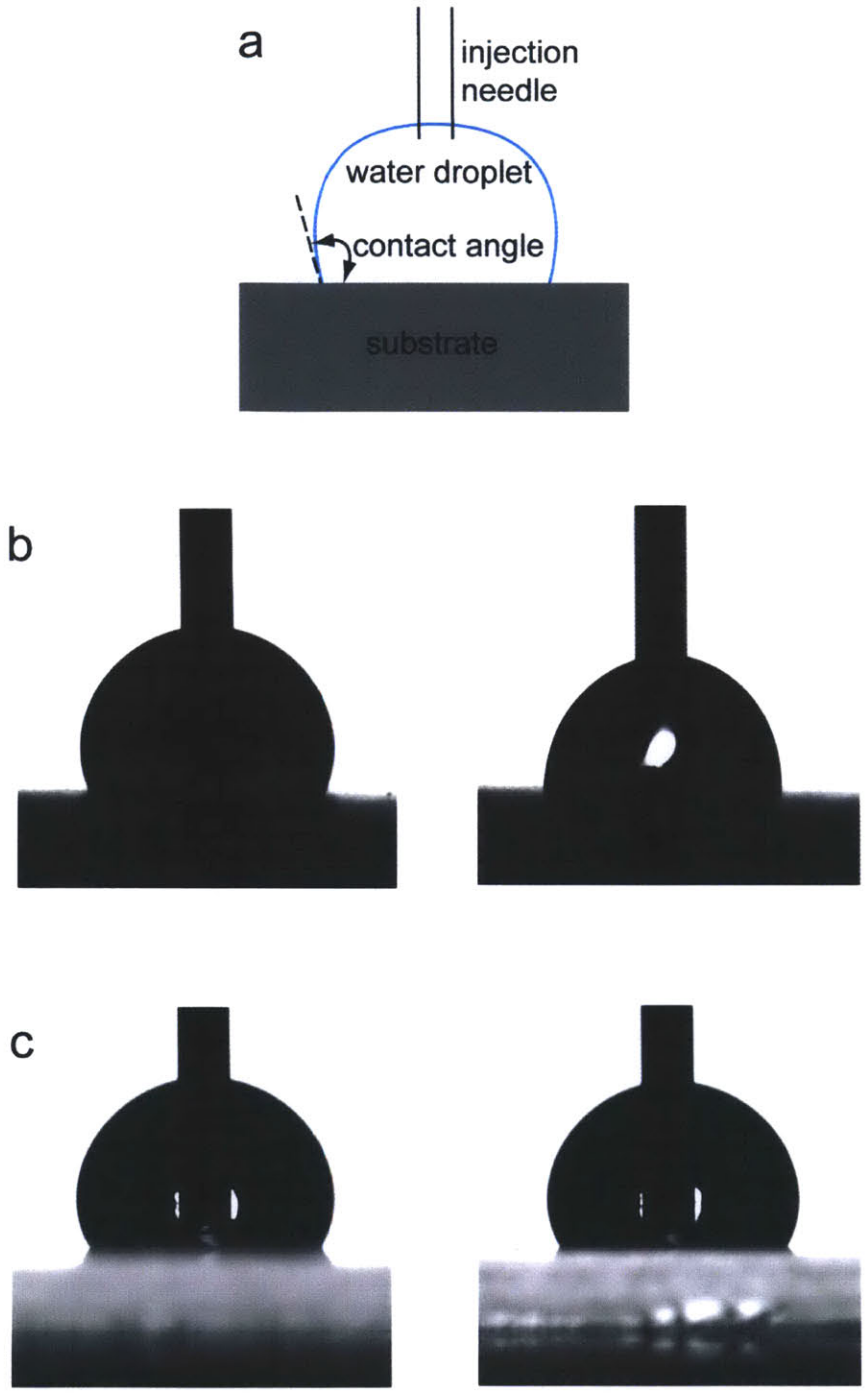

Figure 3-4. Schematic representation of dynamic sessile measurement (a), and side-long view of advancing (left) and receding (right) water droplets on Teflon (b) and **P1** thin film (c).

Prior to thin-film quenching studies, the polymer's solid state photostability was tested by exposing the films to continuous UV irradiation at 395 nm (Figure 3-5). At maximum excitation intensity (6.0 mW), the 97.5% of fluorescence intensity remained after a 15-minute exposure. At excitation intensities where all photophysical measurements discussed in this chapter were conducted, 98.6% of fluorescence intensity remained after 15 minutes. These values are higher than those reported for typical PPEs.[6]

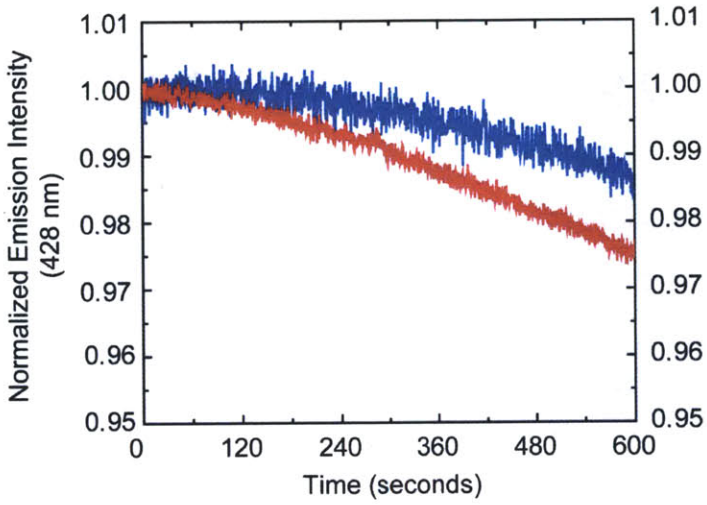

Figure 3-5. Time-dependent fluorescence intensity of a thin-film of **P1** under continuous irradiation at its absorption maximum using maximum excitation intensity (red) and at excitation intensity used in sensing studies (blue).

Thin Film Fluorescence Studies

With photostable and highly emissive thin films with very low surface energy in hand, we set out to test the stability of the films under exposure to chemical vapors and the potential for using **P1** as a sensor for electron-rich aromatic substrates. The fluorescence response of thin films of **P1** to various analytes in vapor phase was monitored by inserting a thin film into a

sealed 20 mL quartz cuvette at room temperature containing small quantities of solid (indole and phenol) and liquid (benzene, toluene, hexafluorobenzene, and aniline) analytes so that the film was not in direct contact with an analyte. The films were then continuously irradiated at 395 nm over a specific period of time while monitoring the emission intensity at the emission maximum (428 nm) at 0.5-second intervals. The fluorescence intensities were normalized to the value measured before the films were exposed to the analyte. Full emission spectra (410-650 nm) were also acquired before and after exposure to monitor the shape of the emission curves for possible defect formation.

Fluorescence response of **P1** thin films to indole, phenol, and aniline vapor are shown in Figure 3-6. Upon exposure to indole (vapor pressure = 0.012 mmHg), the fluorescence of the thin film was reduced to ~60 % of original intensity immediately and to ~14% over 15 minutes (Figure 3-6a). Emission from anthryl defects were not observed during the quenching studies, indicating that the [2.2.2] bicyclic core structure of **P1** remained intact.

Fluorescence change of the thin film upon exposure to phenol vapor (vapor pressure = 0.35 mmHg) is shown in Figure 3-6b. Quenching is less efficient compared to indole, with fluorescence reduction of ~20% over 15 minutes. The emission spectra before and after 15-minute exposure to phenol indicate that there is a slight blue-shift (4 nm) in the emission maximum.

Aniline (vapor pressure = 0.70 mmHg) induced a very efficient quenching response from a thin film of **P1** (Figure 3-6c). Fluorescence of the thin film was reduced to nearly 8% of the original intensity upon exposure, and eventually to 3% over 15-minutes. The higher rate and the larger degree of quenching compared to indole could be attributed to the higher equilibrium vapor pressure of aniline.

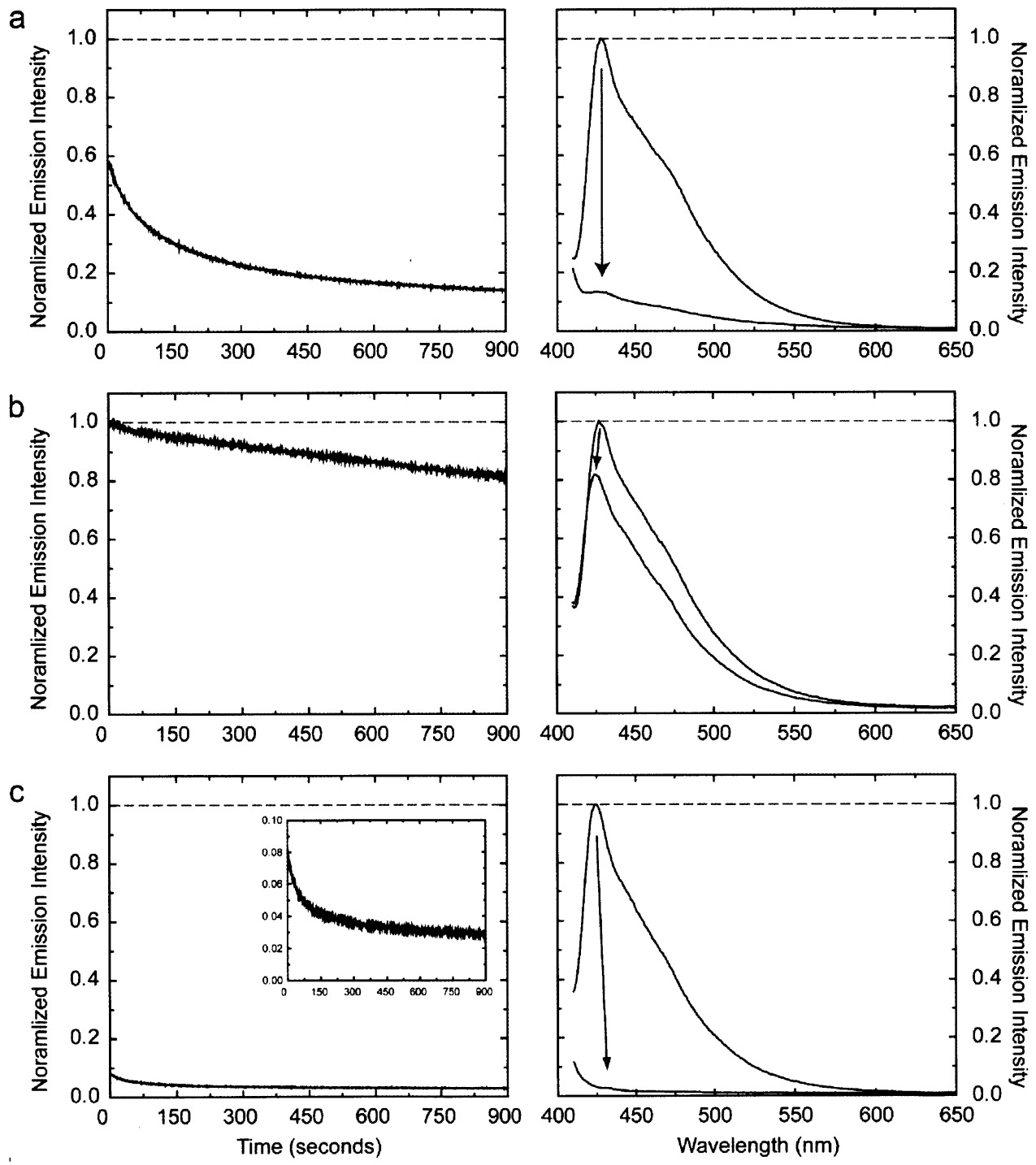

Figure 3-6. Fluorescence response of thin-films of **P1** to indole (a), phenol (b), and aniline (c) at equilibrium vapor pressures. Grey dashed line indicates the intensity of fluorescence prior to exposure.

Fluorescence response to toluene, benzene, and hexafluorobenzene are shown in Figure 3-7. Exposure to toluene (vapor pressure = 26 mmHg) vapor (Figure 3-7a) led to a gradual enhancement in fluorescence to 130% of the original intensity over 15 minutes. The emission spectra acquired before and after the 15-minute exposure demonstrate that only the emission maximum is enhanced, while there is no noticeable change in the rest of the emission curve. This suggests that the enhancement is coming from deaggregation of the polymer by toluene uptake.

The fluorescence enhancement is more prominent with the more volatile benzene (vapor pressure = 75 mm Hg) (Figure 3-7b). Nearly 40% increase was observed over 3 minutes, and the enhanced fluorescence was maintained in presence of benzene. After removal of benzene, original emission intensity was restored in a few seconds.

Given the response of **P1** to toluene and benzene vapors, it was anticipated that similar behavior could be observed from exposure of the thin film to hexafluorobenzene (vapor pressure = 95 mmHg). Hexafluorobenzene has been reported to dissolve fluorous polymers such as poly(hexafluoropropylene) and poly(methacrylate)s bearing perfluoroalkyl chains.[9] When a thin film of **P1** was exposed to hexafluorobenzene vapor, however, no enhancement of fluorescence was observed (Figure 3-7c). Upon exposure, there was about 5% reduction in fluorescence over 2.5 minutes, followed by slow recovery of fluorescence to 97.5% of original intensity over 15 minutes.

In summary, electron-rich aromatic compounds, such as indole, phenol, and aniline, caused quenching of fluorescence from thin films of **P1**. Toluene and benzene enhanced fluorescence, probably by swelling the thin film. In the case of hexafluorobenzene, small initial quenching response was followed with a recovery of fluorescence. None of these analytes caused formation of novel emission peaks, suggesting that **P1** in solid state is stable to these vapors.

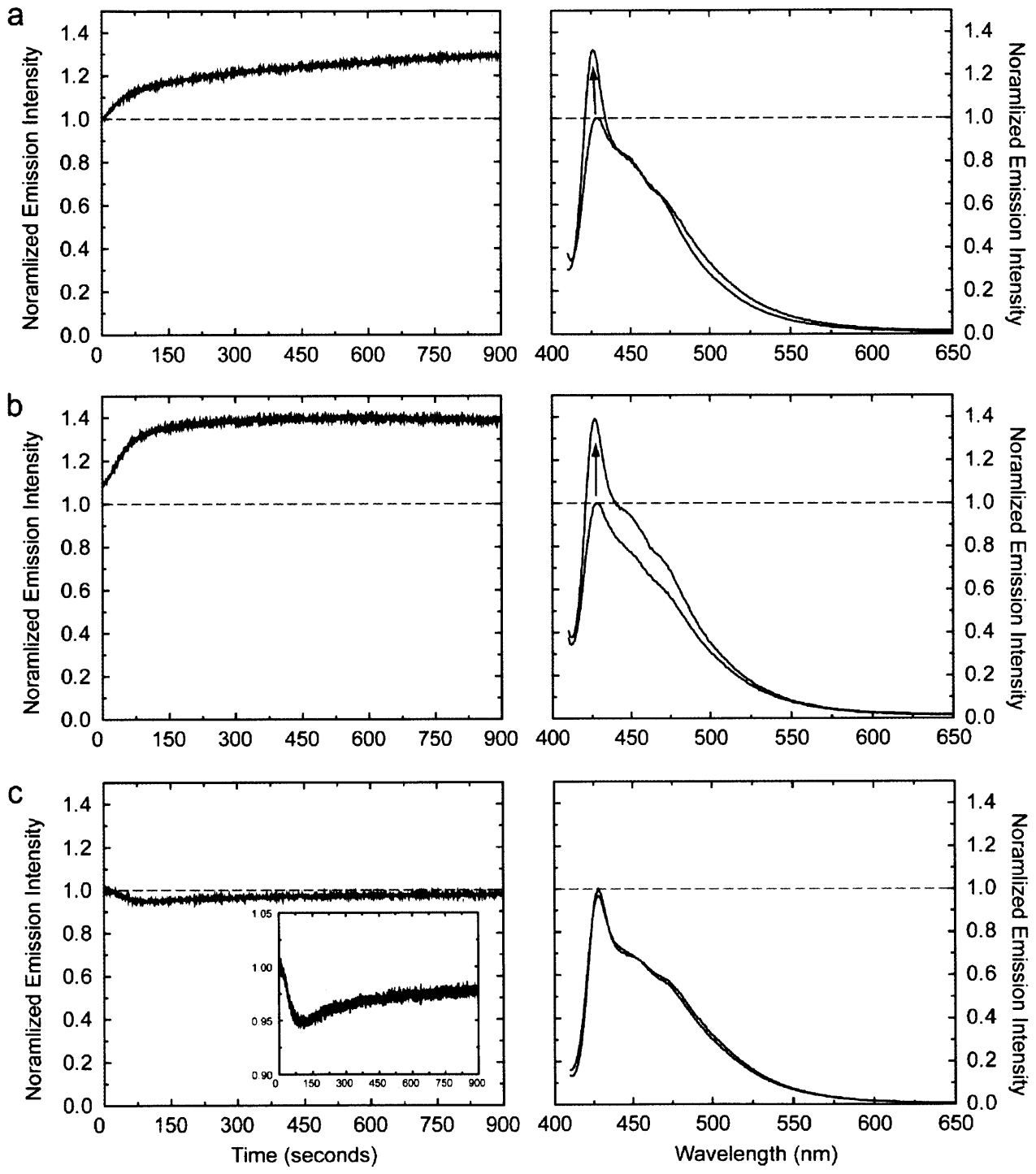

Figure 3-7. Fluorescence response of thin-films of **P1** to toluene (a), benzene (b), and hexafluorobenzene (c) at equilibrium vapor pressures. Grey dashed line indicates the intensity of fluorescence prior to exposure.

Fluorescent Aqueous Fluorous Phase Emulsion

In order to make possible sensory applications of our fluorous-phase soluble fluorescent polymer in aqueous environments, we set out to process fluorous solutions of **P1** into stable emulsion in water with easily modifiable functional groups adorning the surface.

Various fluorocarbon-in-water emulsions formed with[10] and without[11] surfactants have previously been reported. The majority of research effort involving these emulsions focuses on the coarsening mechanism of the emulsion and formulation of biocompatible and stable surfactants which would prevent coarsening in both *in vitro* and *in vivo* settings. The focus of this section is the synthesis of fluorescent fluorocarbon-in-water emulsions with chemically modifiable surface.

Perfluorodecalin,[12] which has been approved by the FDA for use as a component in human blood surrogate, Fluosol-DA,[13] (page 650) was chosen as the fluorous component of the emulsion due to its non-toxic nature. Furthermore, **P1** displayed a quantum yield of 0.95 in perfluorodecalin (see Chapter 1). When a solution of **P1** in perfluorodecalin was added slowly to a hot solution of *2H,2H,3H,3H*-perfluorononanoic acid (0.01 M) in 1X PBS buffer (pH 7.4) under probe sonication, a turbid and strongly fluorescent solution was obtained. After cooling and filtering off excess *2H,2H,3H,3H*-perfluorononanoic acid crystals, the solution was analyzed via DLS, which showed presence of spherical emulsion with an average diameter of 245.8 ± 43.9 nm.

Figure 3-8 shows the absorption and emission spectra and a photograph of the emulsion in PBS buffer. The absorption and emission spectra (Figure3-8a) were identical to that of **P1** in fluorous solution. The emulsion was highly fluorescent, with a quantum yield of 0.58. Surface potential (Z-potential) measurement is a useful method of determining stability of colloidal

particles in water, because higher surface charge will discourage aggregation of particles. Colloids with surface potential of ± 40 mV and higher are considered to have good stability.[14] Surface potential measurements of the emulsion of perfluorodecalin solution of **P1** in PBS buffer gave – 57 ± 13 mV, the sign of which was consistent with the presence of carboxylate moieties on the surface and the degree which indicated that the surfaces of the emulsion are sufficiently charged to confer good stability to the overall emulsion.

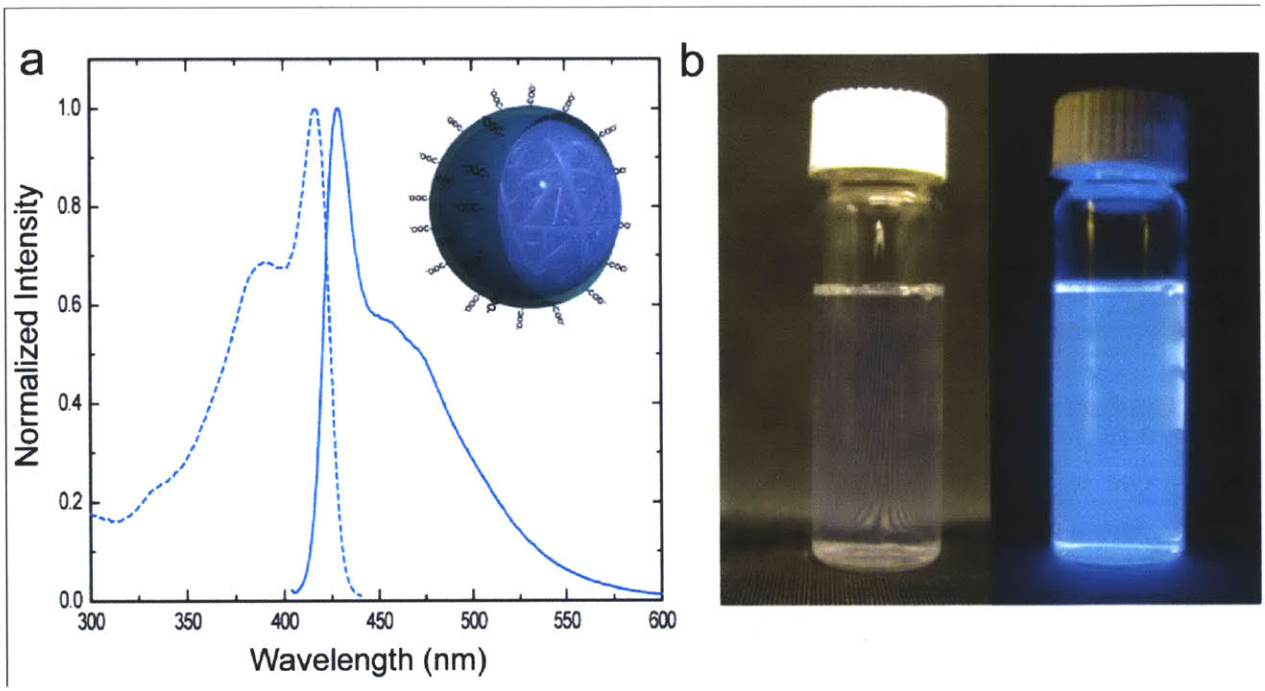

Figure 3-8. (a) Absorption (dotted) and emission (solid) spectra of the emulsion of perfluorodecalin solution of **P1** in PBS buffer. The inset shows a pictorial representation of an emulsion particle. (b) Photograph of the emulsion with (right) and without (left) irradiation with hand-held laboratory UV lamp (long wave).

Increasing surfactant concentration in attempts to decrease the emulsion size resulted in a greater Z-potential without a significant decrease in emulsion size. Doubling surfactant concentration to 0.02 M gave Z-potential of – 79 ± 11 mV (1.4-fold increase) with emulsion size

of 242.1 ± 23.6 nm (no statistically significant difference). Further increasing concentrations of the *2H,2H,3H,3H*-perfluorononanoic acid caused significant amount of surfactant precipitating upon cooling, with little fluorescence remaining in the solution. Phosphate surfactant with perfluorooctyl groups (8:2 monoPAPS[15]) had lower solubility in PBS buffer compared to *2H,2H,3H,3H*-perfluorononanoic acid, and emulsions synthesized with this surfactant gave micron-scale emulsions (3-4 μm) with – 42 ± 6 mV Z-potential.

Emulsion Surface Modification

With carboxylate groups covering the surface of fluorescent fluorous emulsions, we set out to investigate the possibility of modifying the surface via amide bond-fomring reaction. We chose biotin, since derivatives of biotin that can be readily conjugated to carboxylic acid moieties are readily available along with various dye-labeled streptavidin, a protein with a high

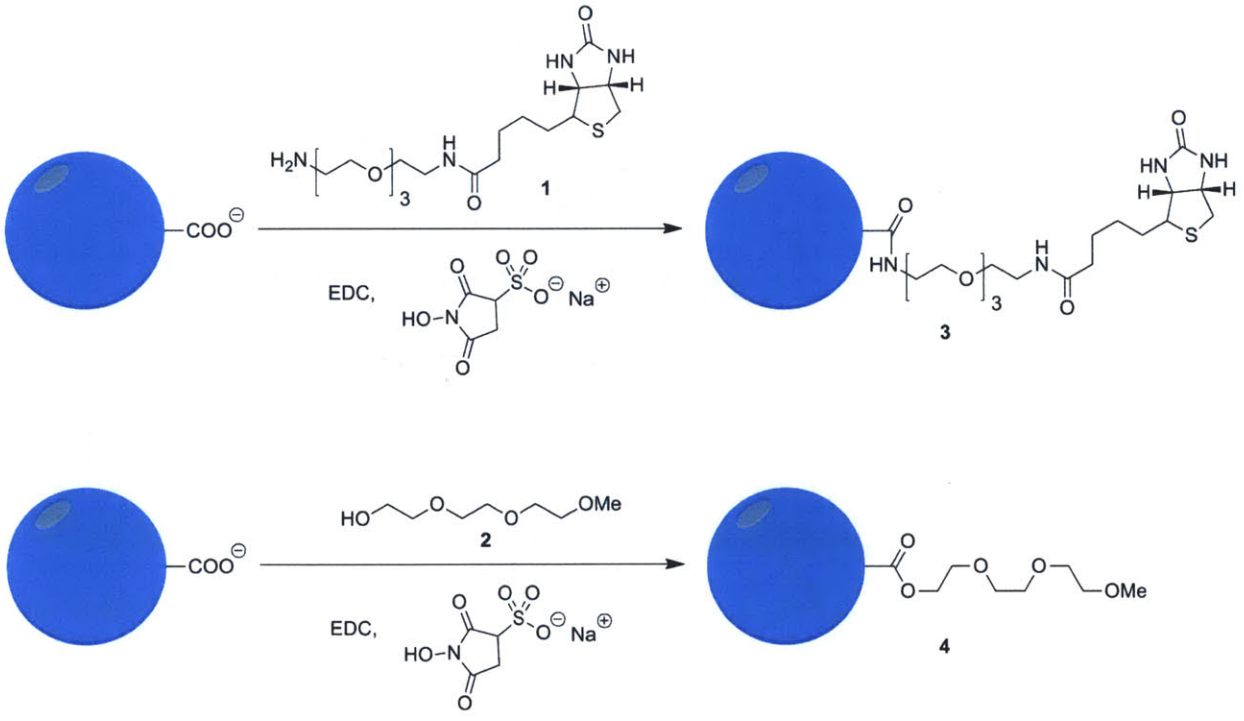

Scheme 3-1. Surface modification of emulsions.

affinity for biotin.[16] Streptavidin is consisted of four equivalent monomeric units,[17] each of which has an equal affinity for biotin. We therefore expected that successful modification of emulsions with biotin tags would produce an observable change.

Treatment of the emulsion with (+)-biotinyl-3,6,9-trioxaundecanediamine (Amine-PEG_3-Biotin; **1**, Scheme 3-1) in presence of 1-ethyl-3-(3-dimethylaminopropyl) carbodiimide) (EDC) and *N*-hydroxysulfosuccinimide (sulfo-NHS) in PBS buffer (pH 7.4), followed by dialysis of the resulting solution against PBS gave solutions without significant reduction in fluorescence (**3**, Scheme 3-1). Treatment of the emulsion with 2-(2-(2-methoxyethoxy)ethoxy)ethanol (**2**) under the same conditions gave solutions with reduced fluorescence (**4**), along with formation of fluorescent precipitates.

Both emulsions were treated with streptavidin labeled with Texas Red® dye, and subsequently subjected to dialysis against PBS buffer. The resulting solutions were imaged with confocal microscopy. Figure 3-9 and 3-10 shows images of emulsion **4** and **3**, respectively, treated with the dye-labeled streptavidin.

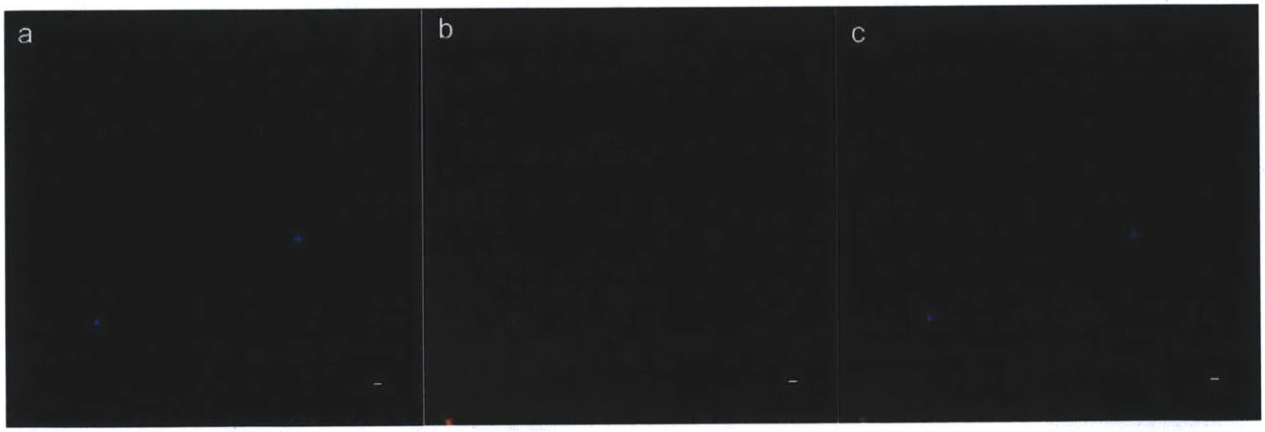

Figure 3-9. Confocal fluorescence microscope images of **4** treated with dye-labeled streptavidin, with excitation wavelength of 364 nm (a) and 564 nm (b). Image c is an overlay of a and b. White bar indicates 5 μm.

Even without the presence of biotin on the surface, the blue emission of the emulsion and the red emission from Texas Red® appear to be co-localized, with the blue emission coming from the core and the red coming from the outer edges of the emulsion. The spherical shape of the emulsion is maintained (Figure 3-9a), suggesting simple adsorption of streptavidin on the negatively charged emulsion surface.

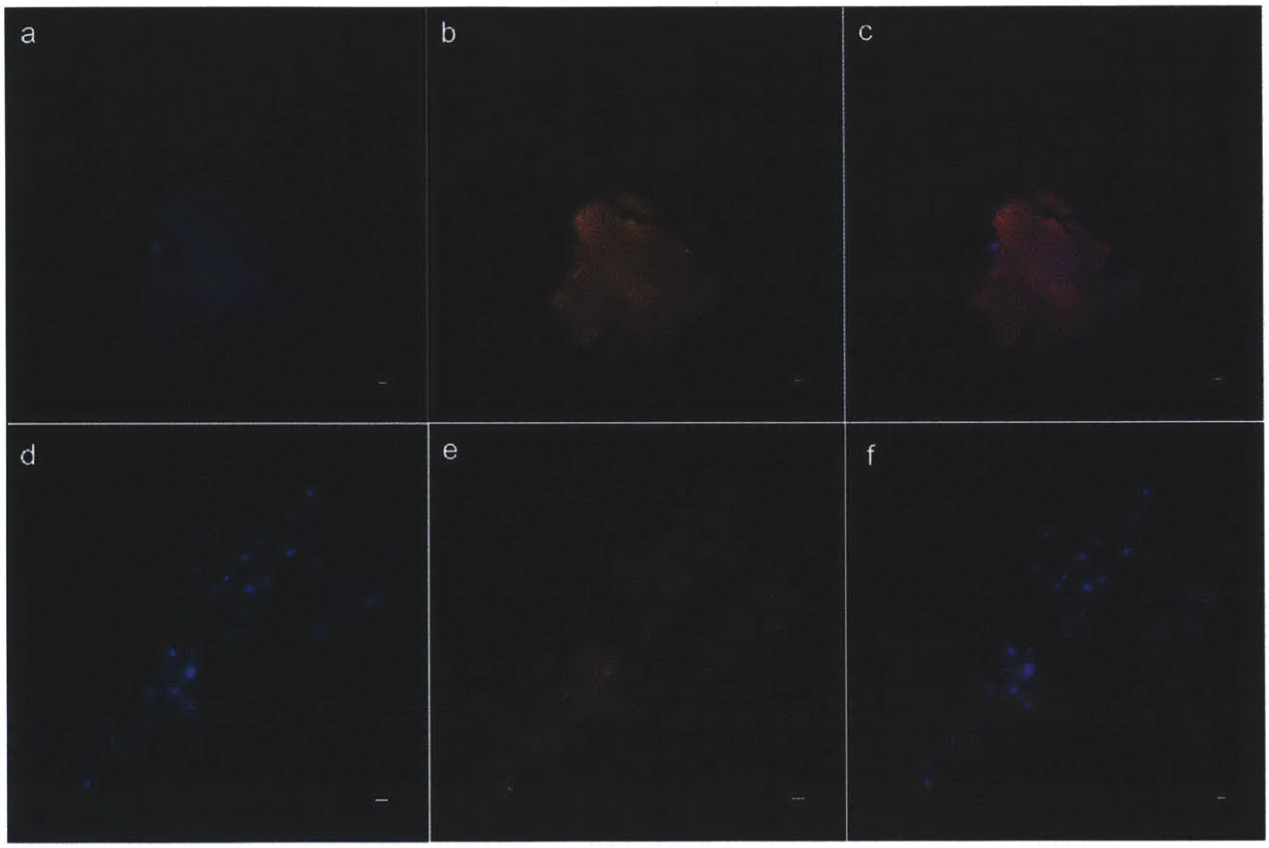

Figure 3-10. Confocal fluorescence microscope images of emulsion **3** treated with dye-labeled streptavidin, with excitation wavelength of 364 nm (a, d) and 564 nm (b, e). Image c is an overlay of a and b, and image f is an overlay of d and e. White bar indicates 5 μm.

In the case of biotin-labeled emulsion (**3**), large degrees of aggregation and loss of spherical shape of the emulsion were observed upon treatment with streptavidin, with emission from both the emulsion and Texas Red® co-localizing (Figure 3-10 c and f). While the results

are preliminary and significantly more control studies need to be conducted in order to confirm surface modification, these observations suggest that the surface modification of the carboxylate-coated emulsion maybe possible via peptide coupling reactions and the modified emulsions have potentials in bioimaging applications. It can be expected that, with the emergence of novel fluorocarbon-in-water emulsion formulations, fluorescent fluorous emulsions with various molecular tags on their surfaces would be possible.

Conclusion

We have processed the fluorous fluorescent polymer, **P1**, into thin films and fluorocarbon-in-water emulsions. The thin films show good stability under UV irradiation, and display efficient quenching response to electron-rich aromatic systems such as indole and aniline. Importantly, emissive signals from anthryl defects, which are known to occur in various PPEs with a [2.2.2] bicyclic structure under UV irradiation or exposure to chemical vapors, are not observed. The photophysical and chemical stability of **P1** are promising characteristics for potential application of the polymer in sensory devices as the active material.

The emulsion of perfluorodecalin solution of **P1** in PBS buffer forms a homogenous mixture with absorption and emission spectra identical to the parent polymer in fluorous solution. Furthermore, an excellent quantum yield of 0.58 was achieved in an aqueous environment. Preliminary results from EDC-mediated amide bond forming reactions on the emulsion show promise in the potential for these emissive emulsions to be used in biosensing and imaging applications.

Experimental Section

General

Fluorescence spectra were measured on a SPEX Fluorolog-τ3 fluorimeter (model FL-321, 450 W Xenon lamp) using right-angle detection for solutions and front-face detection for thin films. Ultraviolet-visible absorption spectra were measured with an Agilent 8453 diode array spectrophotometer and corrected for background signal with a solvent-filled cuvette for solutions and glass slide for thin films. Fluorescence quantum yields of fluorescent emulsions were determined by the optically dilute method[18] using quinine sulfate in 0.1M H_2SO_4 as the standard and were corrected for solvent refractive index and absorption differences at the excitation wavelength. The emulsion size and Z-potential was obtained from Malvern Zeta Sizer Nano ZS90.

Thin films were prepared by carefully dropping 0.025 mg/ml solution of **P1** onto microscope slide cover slips and subsequently spinning the cover slip at 2000 rpm for 20 seconds. The films were dried under air for 10 minutes prior to photophysical measurements. The thin films were inserted into a Teflon cuvette lid featuring a cover slip holder. The holder with the cover slip was initially inserted into an empty cuvette for initial emission acquisition. It was then inserted into a 20 mL quartz cuvette containing small amounts of analyte at the bottom in order to prevent the analytes from coming in direct contact with the thin film. Time-dependent emission intensity was monitored at 428 nm at 0.5-second intervals with excitation at 395 nm.

Fluorescence confocal microscopy was conducted with Leica TCS SP2 confocal microscope with pinhole set at 120 μm. Emission from emulsion were monitored at 375-450 nm, and emission from Texas Red® was monitored at 600-750 nm.

Materials

All solvents were spectral grade unless otherwise noted. Perfluoro(methylcyclohexane) was purified according to literature procedures for fluorocarbons[19] prior to use. All other chemicals were used as received.

Emulsion Synthesis

Table 3-1. Emulsion synthesis conditions and the resulting emulsion properties.

[P1] in PFD (mg/ml)	*Volume of PFD solution (mL)*	*Volume of 1X PBS buffer*	*Surfactant*	*Surfactant Concentration*	*Emulsion size*	*Emulsion Z-potential*
2	0.01	5.0 mL	**S1**	0.01 M	245.8 ± 43.9 nm	-57 ± 13 mV
2	0.01	5.0 mL	**S1**	0.02 M	242.1 ± 23.6 nm	-79 ± 11 mV
2	0.01	5.0 mL	**S2**	0.0025 M	3~4 μm	-42 ± 6 mV

S1: *2H,2H,3H,3H*-perfluorononanoic acid, **S2**: 8:2 monoPAPS[15]

In a 50 mL round-bottom flask, surfactant (Table 3-1, columns 4 and 5) in 5.0 mL PBS buffer was heated to 75°C while stirring. After complete dissolution of the surfactant, **P1** (10 μL, 2 mg/ml in perfluorodecalin) was added. The flask was then removed from heat and was sonicated with a probe sonicator at 3 Watts (rms) for 5 minutes. The solution was subsequently allowed to cool to room temperature. Excess surfactant was removed via filtration. The size distribution and Z-potentials of the emulsions are shown in Table 3-1 (columns 6 and 7).

Biotin Modification of Emulsion Surface

Emulsion was synthesized from 0.01M *2H,2H,3H,3H*-perfluorononanoic acid in PBS buffer (see above). 5 mL of this emulsion was treated with Amine-PEG_3-Biotin (4.2 mg, 0.01 mmol) or triethyleneglycol monomethyl ether (2 μl, 1.3 mmol), EDC (0.16 mg, 0.01 mmol), and sulfo-NHS (11 mg, 0.05 mmol). The reaction mixture was stirred vigorously overnight, and

subsequently dialyzed against PBS buffer over 12 hours, while introducing fresh PBS buffer in 3-hour intervals. To this mixture, 0.1 mg/ml streptavidin Texas Red® conjugate (0.1 ml) was added. The resulting mixture was dialyzed against PBS buffer over 12 hours, while introducing fresh PBS buffer in 3-hour intervals.

The dialyzed solution was dropped onto a microscope slide. The cover slip was fixed onto the slide with 5-minute epoxy prior to imaging.

Reference

1. (a) McQuade, D. T.; Pullen, A. E.; Swager, T. M., Conjugated polymer-based chemical sensors. *Chem. Rev.* **2000,** *100* (7), 2537-2574; (b) Swager, T. M.; Thomas, S. W.; Joly, G. D., Chemical sensors based on amplifying fluorescent conjugated polymers. *Chem. Rev.* **2007,** *107* (4), 1339-1386; (c) Wang, K.; Huang, H. M.; Tan, W. H.; An, D.; Yang, X. H.; Huang, S. S.; Zhai, Q.; Zhou, L.; Jin, Y., Design of a modular-based fluorescent conjugated polymer for selective sensing. *Angew. Chem. In. Ed.* **2004,** *43* (42), 5635-5638.

2. Zhou, Q.; Swager, T. M., Fluorescent chemosensors based on energy migration in conjugated polymers: The molecular wire approach to increased sensitivity. *J. Am. Chem. Soc.* **1995,** *117* (50), 12593-12602.

3. Zhou, Q.; Swager, T. M., Methodology for Enhancing the Sensitivity of Fluorescent Chemosensors - Energy Migration in Conjugated Polymers. *J. Am. Chem. Soc.* **1995,** *117* (26), 7017-7018.

4. (a) Swager, T. M.; Yang, J. S., Fluorescent porous polymer films as TNT chemosensors: Electronic and structural effects. *J. Am. Chem. Soc.* **1998,** *120* (46), 11864-11873; (b) Swager, T. M.; Yang, J. S., Porous shape persistent fluorescent polymer films: An approach to TNT sensory materials. *J. Am. Chem. Soc.* **1998,** *120* (21), 5321-5322.

5. (a) Williams, V. E.; Yang, J. S.; Lugmair, C. G.; Miao, Y. J.; Swager, T. M., Design of novel iptycene-containing fluorescent polymers for the detection of TNT. *Detection and Remediation Technologies for Mines and Minelike Targets Iv, Pts 1 and 2* **1999,** *3710*, 402-408; (b) Miao, Y. J.; Yang, J. S.; Swager, T. M., Fluorescence sensory polymers containing rigid non-planar aromatic scaffolds. *Abstr. Pap. Am. Chem. Soc.* **1998,** *216*, U171-U171; (c) Williams, V.;

Yang, J. S.; Swager, T. M., Design of porous shape persistent fluorescent polymer films for the detection of TNT. *Abstr Pap Am Chem S* **1998,** *216*, U354-U355.

6. Whitten, J. E.; Kim, Y.; Swager, T. M., High ionization potential conjugated polymers. *J. Am. Chem. Soc.* **2005,** *127* (34), 12122-12130.

7. (a) Meskers, S. C. J.; Satrijo, A.; Swager, T. M., Probing a conjugated polymer's transfer of organization-dependent properties from solutions to films. *J. Am. Chem. Soc.* **2006,** *128* (28), 9030-9031; (b) Swager, T. M.; Satrijo, A., Anthryl-doped conjugated polyelectrolytes as aggregation-based sensors for nonquenching multicationic analytes. *J. Am. Chem. Soc.* **2007,** *129* (51), 16020-16028.

8. Swager, T. M.; Wosnick, J. H.; Liao, J. H., Layer-by-layer poly(phenylene ethynylene) films on silica microspheres for enhanced sensory amplification. *Macromolecules* **2005,** *38* (22), 9287-9290.

9. Lowry, R. E.; Brown, D. W.; Wall, L. A., Radiation-Induced Polymerization of Hexafluoropropylene at High Temperature and Pressure. *J. Poly. Sci. A.* **1966,** *4* (Part A-1), 2229-2240.

10. (a) Weers, J. G.; Arlauskas, R. A.; Tarara, T. E.; Pelura, T. J., Characterization of fluorocarbon-in-water emulsions with added triglyceride. *Langmuir* **2004,** *20* (18), 7430-7435; (b) Holtze, C.; Rowat, A. C.; Agresti, J. J.; Hutchison, J. B.; Angile, F. E.; Schmitz, C. H. J.; Koster, S.; Duan, H.; Humphry, K. J.; Scanga, R. A.; Johnson, J. S.; Pisignano, D.; Weitz, D. A., Biocompatible surfactants for water-in-fluorocarbon emulsions. *Lab on a Chip* **2008,** *8* (10), 1632-1639.

11. Kabalnov, A. S.; Makarov, K. N.; Shcherbakova, O. V., Solubility of Fluorocarbons in Water as a Key Parameter Determining Fluorocarbon Emulsion Stability. *J. Fluorine Chem.* **1990,** *50* (3), 271-284.

12. King, A. T.; Mulligan, B. J.; Lowe, K. C., Perfluorochemicals and Cell-Culture. *Bio-Technol* **1989,** *7* (10), 1037-1042.

13. Marieb, E. N., *Human anatomy & physiology*. 4th ed.; Benjamin/Cummings: Menlo Park, Calif., 1998.

14. Zeta Potential of Colloids in Water and Waste Water, ASTM Standard D 4187-82, American Society for Testing and Materials, 1985.

15. D'eon, J. C.; Mabury, S. A., Production of perfluorinated carboxylic acids (PFCAs) from the biotransformation of polyfluoroalkyl phosphate surfictants (PAPS): Exploring routes of human contamination. *Environ. Sci. Technol.* **2007,** *41* (13), 4799-4805.

16. Chaiet, L.; Wolf, F. J., The Properties of Streptavidin, a Biotin-Binding Protein Produced by Streptomycetes. *Archives of Biochemistry and Biophysics* **1964,** *106*, 1-5.

17. Green, N. M., Avidin. *Adv. Protein. Chem.* **1975,** *29*, 85-133.

18. Demas, J. N.; Crosby, G. A., Measurement of Photoluminescence Quantum Yields - Review. *J. Phys. Chem.* **1971,** *75* (8), 991-1024.

19. Glew, D. N.; Reeves, L. W., Purification of Perfluoro-Normal-Heptane and Perfluoromethylcyclohexane. *J. Phys. Chem.* **1956,** *60* (5), 615-615.

CHAPTER 4

Heavily Fluorinated Poly(*para*-Phenylenevinylene)s

Introduction

While polymers, such as the one discussed in Chapter 2 of this thesis, in which phenylene units are conjugated to ethynylene units (*poly*(phenyleneethynylene)s, or PPEs), have various advantages in sensory applications, those polymers in which phenylene units conjugated to vinylene units (*poly*(phenylenevinylene)s, or PPVs)[1] (page 343-351) are distinct in that they generally have lower band gaps and higher crystallinity than their ethynylene counterparts (Figure 4-1).[2] PPVs have been extensively investigated for applications in electroluminescent devices,[3] organic photovoltaic devices,[4] field-effect transistors,[5] and sensing.[6]

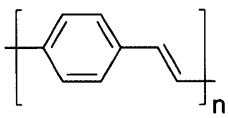

Figure 4-1. Core structure of PPV.

Many electron-rich PPVs are known. MEH-PPV (Figure 4-2a) is a highly soluble PPV derivative studied extensively for its light-emitting properties and facile processibility. The polymer has also found a wide use as a component in organic photovoltaic devices and as an organic light-emitting diode (OLED). Another electron-rich PPV with bulkier side chains for reduction of aggregation-induced self-quenching in thin film has been used in devices for the detection of explosives (Figure 4-2b).[7]

Compared to the wide availability of various electron-rich (donor) PPVs, there is a relative scarcity of corresponding electron-deficient (acceptor) PPVs. The most prevalent method of preparing electron-deficient PPVs reported thus far involve installment of electron-withdrawing groups such as $-CF_3$[8] or $-CN$[9] on the vinyl groups of the PPV backbone. These polymers and oligomers still feature electron-donating alkoxy groups on the phenyl groups of the polymer backbone. Furthermore, the increased steric demand along the vinyl groups gives rise to

undesirable conformational deviation from planarity, causing disruption in transport properties of the polymers.[10]

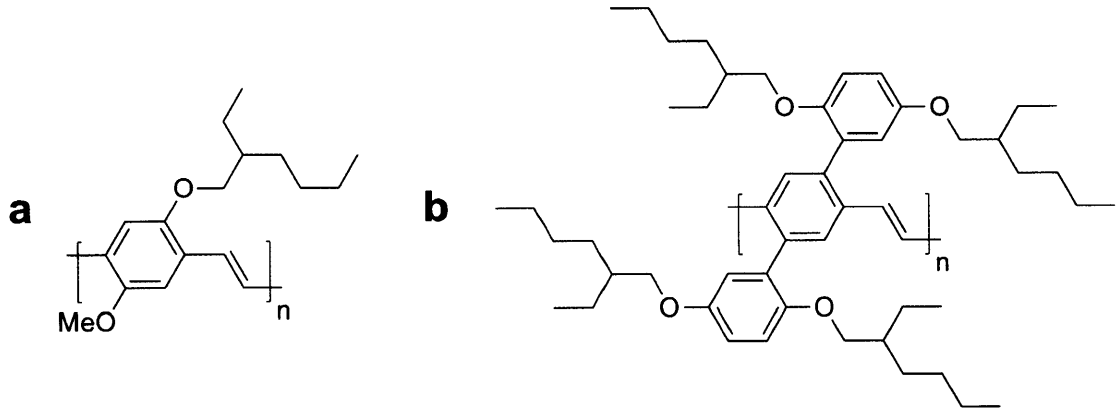

Figure 4-2. Structure of MEH-PPV (a) and a PPV for lasing-based TNT sensing (b).

Our group has previously reported *poly*-[2,5-bis(trifluoromethyl)-*p*-phenylenevinylene] (CF3-PPV; Figure 4-3), which was shown to have high resistance to oxidation, maintaining 100% of its fluorescence intensity even after 120 minutes of continuous UV irradiation. This polymer, however, showed poor solubility in dichloroethane or chloroform, and only partial solubility in THF and DMF.

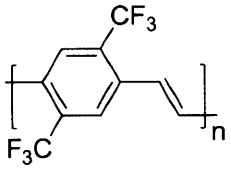

Figure 4-3. Structure of CF3-PPV.

The high photostability of the CF3-PPV and its solubility profile led us to investigate the effects of substituting trifluoromethyl groups with longer perfluoroalkyl chains. It was expected that higher fluorine content may render the resulting PPV soluble in the fluorous phase, allowing for facile processing of the material.

Results and Discussion

Monomer Synthesis

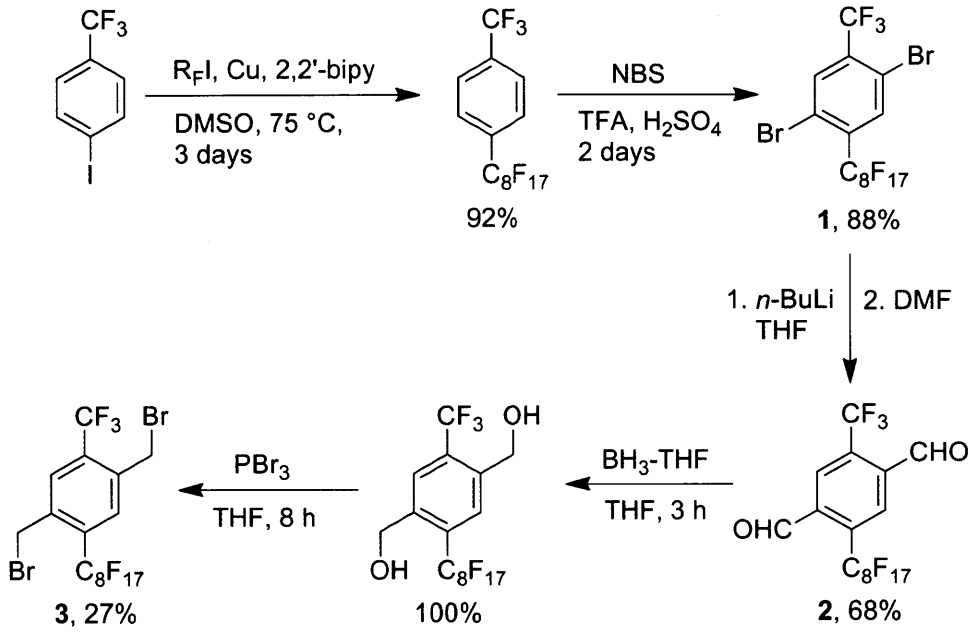

Scheme 4-1. Synthesis of monomer **3**.

Scheme 4-1 outlines the synthesis of PPV monomers containing perfluoroalkyl chains of various lengths. Copper-mediated coupling between 4-iodobenzotrifluoride and perfluorooctyl and perfluorodecyl iodide proceeded smoothly to give corresponding 4-(perfluoroalkyl) benzotrifluoride in good yields. Slow addition of NBS to the product in hot trifluoroacetic acid/sulfuric acid mixtures gave the corresponding 1,4-dibromo-2-(perfluoroalkyl)-5-(trifluoromethyl)benzene (**1**) cleanly after sublimation. Compound **1** was soluble in THF at room temperature, but was insoluble at -78°C. Lithiation was therefore carried out with a slow addition of solutions of **1** in THF to *n*-butyllithium solution at -78 °C. Cannulation of this lithiation mixture into solution of DMF in THF gave compound **2** in a moderate yield. Reduction with BH_3-THF gave the corresponding benzyl alcohols, which were converted to monomer **3** by treatment with PBr_3.

Gilch Polymerization

Monomer **3** was soluble in THF at room temperature, but was insoluble at lower temperatures. Treatment of a suspension of **3** in THF at -78 °C with freshly prepared potassium *tert*-butoxide in THF, followed by gradually warming the reaction mixture to room temperature overnight gave a brown, slightly fluorescent solution. Attempts to precipitate the product by pouring the reaction mixture into methanol gave a clear brown solution from which no precipitation was observed upon standing over several days.

It was found that FC-770 (perfluoro(*N*-propyl morpholine)) was miscible with THF above c.a. -20 °C, and FC-770 was envisioned as a solvent capable of accommodating alkoxide bases in anionic polymerization reactions. Treatment of an FC-770 solution of monomer **3** at -15 °C with a THF solution of potassium *tert*-butoxide gave, upon warming up to room temperature overnight, a cloudy reaction mixture. Removal of FC-770 under reduced pressure followed by washing with methanol gave yellow solids with green fluorescence. The product was insoluble in common organic solvents, as well as in perfluoro(methylcyclohexane), FC-770 (perfluorooctanes), and FC-770, even under refluxing conditions. A weakly fluorescent solution was obtained by extracting the product with boiling hexafluorobenzene. Although the solubility was not high enough for NMR characterization, absorption and emission spectra of the product could be recorded in hexafluorobenzene and are shown in Figure 4-4a.

The absorption emission spectra were suggestive of a formation of a PPV structure. Surprisingly, differential scanning calorimetry measurement (DSC) from 25 °C to 375 °C displayed no shift in slope typically observed at the glass transition temperature (T_g) of polymers (Figure 4-4b). Furthermore, no endotherm/exotherm corresponding to degradation of the sample

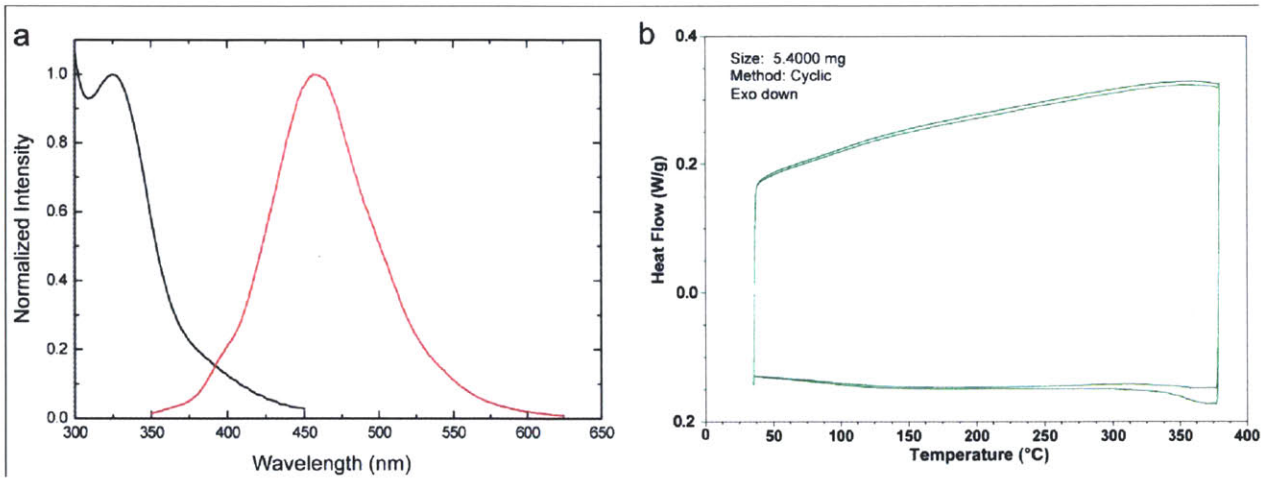

Figure 4-4. (a) Absorption (black) and emission (red) spectra of polymerization products of **3** and its differential scanning calorimetry (25 °C to 375 °C) (b).

was observed. More surprisingly, scanning to 375 °C three times yielded nearly identical traces. The absorption and emission data, along with DSC measurements indicate that the obtained material is a highly heat-stable fluorescent polymer with a very high T_g.

Second Generation Monomer and Polymer Synthesis

In attempts to synthesize PPVs soluble in the fluorous phase, we set out to further increase the fluorine content by installing two perfluoroalkyl groups per monomeric unit, the synthesis of which is outlined in Scheme 4-2. Monomers with two perfluorohexyl chains per

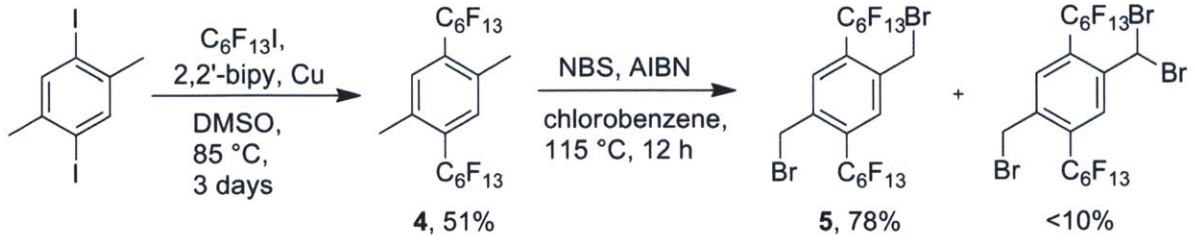

Scheme 4-2. Synthesis of bis(perfluorohexyl) monomer, **5**.

repeat unit were synthesized from 1,4-diiodo-2,5-dimethyl benzene, the treatment of which with an excess of perfluorohexyl iodide under copper-mediated coupling conditions mentioned in the previous section gave 1,4-dimethyl-2,5-bis(perfluorohexyl)benzene (**4**) in a moderate yield. Radical bromination with NBS and AIBN in chloroform and carbon tetrachloride gave trace amounts of desired product, with the major product being the mono-brominated species. The reaction proceeded smoothly in refluxing chlorobenzene to give monomer **5** in a good yield with a small fraction of over-brominated byproduct.

Treatment of **5** with potassium *tert*-butoxide solution in THF in identical polymerization conditions as mentioned previously gave similar yellow solids with green fluorescence. The product was insoluble in common organic solvents and in perfluoro(methylcyclohexane), FC-77, and FC-770. It was slightly soluble in hexafluorobenzene at room temperature.

Absorption, emission, and excitation spectra of the product in hexafluorobenzene are shown in Figure 5. The absorption maximum is identical to the product of polymerization of monomer **3**. The emission spectra, however, is slightly blue-shifted (by 12 nm). The excitation spectra recorded at the emission maximum show a maximum at 360 nm, which is 35 nm red-shifted from the absorption maximum. This suggests that the short the product contains mainly short-chain polymers that dominate absorption, while a small fraction of longer-chain polymers present are responsible for majority of the emission at 446 nm.

The properties of polymers from monomers **3** and **5** indicate that substitution of trifluroomethyl groups in CF3-PPV (Figure 3) with longer perfluoroalkyl chains give emissive materials with very high thermal stability. While these properties are rare among emissive polymers and therefore very attractive, the lack of solubility of these materials poses a major barrier for further investigation. One method of approaching polymer solubility problems

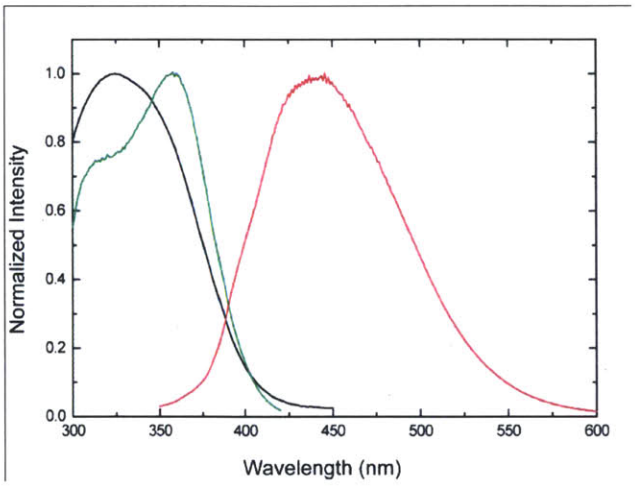

Figure 4-5. Absorption (black) and emission (red) spectra of polymerization products of monomer **5**. Green curve is the excitation spectra recorded while monitoring emission at 446 nm.

involves synthesis of soluble "pre-polymers" from which the desired polymer could readily be generated after processing the pre-polymer into desired platform. Elsenbaumer reported usage of bis-sulfoxide-containing monomer to synthesize soluble, non-conjugated polymer. Casting a thin film of this polymer and subsequent thermal elimination of sulfenic acid gave the desired conjugated polymer (Scheme 4-3).

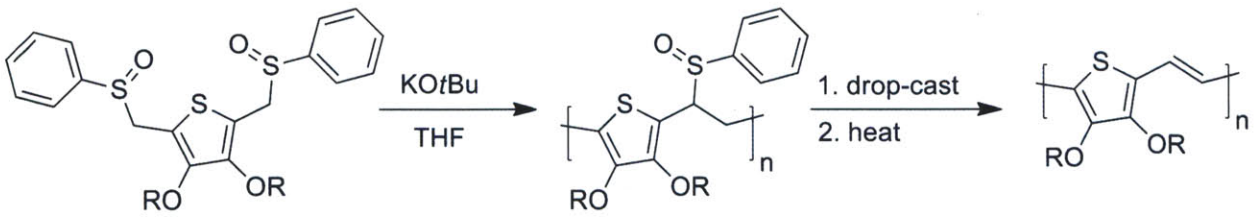

Scheme 4-3. Bis-sulfoxide pre-polymer approach to CPs.

Bromines on monomer **3** could be smoothly substituted with thiophenolates. Oxidation of this compound with *m*CPBA, however, gave solids insoluble in chloroform, THF, hexanes, and ethyl acetate, and also insoluble in fluorous solvents.

Conclusion

Various monomers for the syntheses of perfluoroalkylated PPVs have been explored. Our studies suggest that the desired PPVs are insoluble in both fluorous and non-fluorous solvents and exhibit extremely high thermal stability. The lack of solubility, which is an asset for emissive materials in device applications, severely limits the processibility of the polymer. To address the lack of solubility of the desired polymer, the bis-sulfoxide pre-polymer approach was investigated. Unfortunately, the bis-sulfoxide monomers also exhibited very limited solubility, and attempts at anionic polymerization on the monomer led to no conversion, probably due to the highly electron-deficient nature of the molecule.

Experimental Section

General. All air- and moisture-sensitive synthetic manipulations were performed under an argon atmosphere using standard Schlenk techniques. Column chromatography was performed using ultra pure silica gel (SILIYCYCLE, 40~63 μm). NMR spectra were obtained on a Varian Mercury-300 spectrometer, and all proton chemical shifts are referenced to residual $CHCl_3$ or THF-d_6, and all fluorine chemical shifts are referenced to an external $CFCl_3$ standard. High-resolution mass spectra were obtained at the MIT Department of Chemistry Instrumentation Facility (DCIF) on a Bruker Daltronics APEX II3 Tesla FT-ICR-MS. Fluorescence and excitation spectra were measured on a SPEX Fluorolog-τ3 fluorimeter (model FL-321, 450 W Xenon lamp) using right-angle detection for solutions and front-face detection for thin films. Ultraviolet-visible absorption spectra were measured with an Agilent 8453 diode array spectrophotometer and corrected for background signal with a solvent-filled cuvette for solutions and glass slide for thin films.

Materials. All solvents were spectral grade unless otherwise noted. Anhydrous toluene and was obtained using a solvent purification system (Innovative Technologies). Tetrahydrofuran (THF) was dried by refluxing overnight over freshly cut sodium and benzophenone, followed by distillation under argon. FC-770 (mixture of perfluoro(*N*-alkyl morpholine)) was distilled over calcium hydride and stored under argon. Dimethylsulfoxie (DMSO) was dried by distillation under reduced pressure (10 Torr) over CaH_2 and stored under argon over 4A molecular sieves. Perfluoro(methylcyclohexane) and FC-77 (perfluorooctane) was purified according to literature procedures[11] prior to use. Solvents for polymerization (FC-770 and THF) were degassed via freeze-pump-thaw directly prior to use. Perfluorohexyl iodide ($C_6F_{13}I$) and perfluorooctyl iodide

($C_8F_{17}I$), clear liquids which turn purple upon storage, were freshly distilled prior to use. 2,2'-bipyridyl was recrystallized from hexanes and dried under vacuum. *N*-bromosuccinimide (NBS) was recrystallized from water and dried under vacuum. 2,2'-Azobis(isobutyronitrile) (AIBN) was recrystallized from chloroform and dried under vacuum in the dark. All other chemicals were used as received.

Synthesis

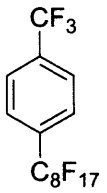

1-(perfluorooctyl)-4-(trifluoromethyl)benzene. The synthesis is modified from a literature procedure.[12] To a flame-dried 100 mL round-bottom flask equipped with an addition funnel was charged 4-iodobenzotrifluoride (2.5 g, 9.2 mmol), copper powder (4.7 g, 74 mmol), 2,2'-bipyridyl (110 mg, 0.7 mmol), and anhydrous DMSO (30 mL). The reaction mixture was stirred vigorously and heated to 75°C. Perfluorooctyl iodide (10.0 g, 18.4 mmol) was added dropwise over 10 minutes at 75°C. The reaction mixture was stirred at 75°C for 3 days. After cooling to room temperature, the reaction mixture was poured into a mixture of 200 mL water and 200 mL diethyl ether. The cloudy mixture was stirred vigorously for 1hour and then the solids were filtered and washed with 50 mL diethyl ether. The organic layers were combined and washed 3 times with 100 mL 1.0 N ammonium hydroxide and then twice with 100 mL water. The organic layer was then dried over $MgSO_4$ and the solvent was removed under reduced pressure. The resulting solids were sublimed (10 mTorr, 70°C) for 16 hours to give the title compound as white crystalline solids (5.01 g, 97%). ^{1}H NMR (300 MHz, THF-d_8): δ 7.87 (d, $J_{H\text{-}H}$ = 8.5 Hz, 2H),

7.95 (d, $J_{H\text{-}H}$ = 8.5 Hz, 2H). ^{19}F NMR (282 MHz, THF-d_8): δ -127.29 (2F), -123.75 (2F), -122.74 (6F), -122.21 (2F), -112.04 (2F), -82.25 (3F), -64.22 (3F).

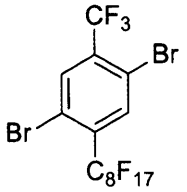

1,4-dibromo-2-(perfluorooctyl)-5-(trifluoromethyl)benzene (1). The synthesis is modified from a literature procedure.[12] To 200 mL round-bottom flask was added 1-(perfluorooctyl)-4-(trifluoromethyl)benzene (4.0 g, 7.1 mmol), TFA (40 mL), and 96% sulfuric acid (12 mL). Equip with a reflux condenser and heat to 80°C. *N*-Bromosuccinimide (NBS) (4.01 g, 21.3 mmol) was added in small portions over 6 hours. Upon completion of addition, the reaction was allowed to stir for additional 48 hours. The reaction mixture was then cooled to room temperature and poured into ice/water mixture. White precipitates were filtered, dried, and washed with ethanol. The resulting crude material was sublimed (0.025 mmHg, 80°C) to give the title compound (3.2g, 63%) as white crystalline solids. ^{1}H NMR (300 MHz, THF-d_8): δ 8.16 (s, 1H), 8.24 (s, 1H). ^{19}F NMR (282 MHz THF-d_8): δ -126.76 (2F), -123.23 (2F), -122.30 (4F), -121.96 (2F), -119.73 (2F), -107.66 (2F), -81.74 (3F), -64.27 (3F).

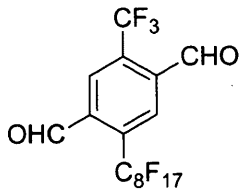

2-(perfluorooctyl)-5-(trifluoromethyl)terephthalaldehyde (2). A flame-dried 50 mL round-bottom flask was charged with 20 mL anhydrous THF, followed by *n*-BuLi (11 mL, 1.6 M in hexanes, 18 mmol). The reaction mixture was cooled to -78°C. 1,4-dibromo-2-(perfluorooctyl)-5-(trifluoromethyl)benzene (**1**) (5.8 g, 8.0 mmol) dissolved in 20 mL THF was added dropwise over 20 minutes. The reaction mixture was then stirred at -78°C for 30 minutes and then was

cannulated slowly into a separate flame-dried flask containing DMF (4.4 mL, 56 mmol) and THF (20 mL) at 0°C. The reaction was removed from cooling bath and was stirred at room temperature for 3 hours. The reaction was then quenched by addition of 0.1 N HCl and diluted with addition of 100 mL water and 50 mL diethyl ether. The aqeuous layer was further extracted with diethyl ether (2 × 50 mL) and combined organic layers were dried over $MgSO_4$ and the solvent was removed under reduced pressure. Flask column chromatography (silica gel, gradient from 9:1 hexanes/dichloromethane to 8:2 hexanes/dichloromethane) gave the title compound (3.4 g, 69%) as white solids. ^{1}H NMR (300 MHz, THF-d_8): δ 8.44 (s, 1H), 8.51 (s, 1H), 10.35 (m, 1H), 10.38 (q, 1H). ^{19}F NMR (282 MHz THF-d_8): δ -126.76 (2F), -123.29 (2F), -122.29 (4F), -121.66 (2F), -120.70 (2F), -103.77 (2F), -81.73 (3F), -67.95 (3F).

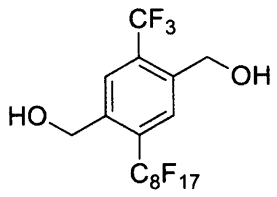

(2-(perfluorooctyl)-5-(trifluoromethyl)-1,4-phenylene)dimethanol. Flame-dried 200 mL round-bottom flask was charged with **2** (3.2 g, 5.2 mmol) and anhydrous THF (52 mL). At 0°C, BH_3-THF (21 mL, 1.0 M in THF, 21 mmol) was added dropwise. White precipitates began to form. The reaction was then removed from cooling bath and stirred for 3 hours at room temperature. 0.3 M NaOH was then added carefully until all solids dissolved. The resulting reaction mixture was diluted with water (100 mL) and was extracted with diethyl ether (3 × 50 mL). The organic layer was dried over $MgSO_4$ and the solvent was removed under reduced pressure. Flask column chromatography (silica gel, 9:1 hexanes/ethyl acetate) gave the title compound (3.2 g, quantitative) as white solids. ^{1}H NMR (300 MHz, THF-d_8): δ 4.80 (m, 6H),

8.09 (s, 1H), 8.24 (s, 1H). ^{19}F NMR (282 MHz THF-d_8): δ -126.77 (2F), -123.26 (2F), -122.33 (4F), -121.94 (2F), -121.30 (2F), -106.46 (2F), -81.66 (3F), -62.05 (3F).

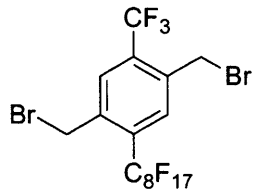

1,4-bis(bromomethyl)-2-(perfluorooctyl)-5-(trifluoromethyl)benzene (3). A flame-dried 100 mL round-bottom flask was charged with (2-(perfluorooctyl)-5-(trifluoromethyl)-1,4-phenylene)dimethanol (3.3 g, 5.2 mmol). PBr_3 was then added dropwise, and the reaction was stirred at room temperature for 10 hours. After quenching with careful addition of saturated $NaHCO_3$ solution, the reaction mixture was diluted with water and extracted with diethyl ether. The organic layer was dried over $MgSO_4$ and the solvent was removed under reduced pressure. Flask column chromatography (silica gel, 9.5:0.5 hexanes/ethyl acetate) gave the title compound (1.1 g, 27%) as white solids. ^{1}H NMR (300 MHz, $CDCl_3$): δ 4.60 (s, 2H), 4.63 (s, 1H), 7.79 (s, 1H), 7.90 (s, 1H). ^{19}F NMR (282 MHz $CDCl_3$): δ -126.33 (2F), -122.92 (2F), -122.05 (4F), -121.46 (2F), -120.80 (2F), -106.96 (2F), -80.95 (3F), -60.69 (3F).

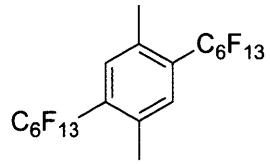

1,4-dimethyl-2,5-bis(perfluorohexyl)benzene. To a flame-dried 50 mL Schlenk flask was charged 1,4-diiodo-2,5-dimethylbenzene[13] (2.0 g, 5.6 mmol, 1.0 eq), copper powder (mesh, 2.2 g, 34 mmol, 6.0 eq), 2,2'-bipyridyl (90 mg, 0.56 mmol, 0.10 eq), and anhydrous DMSO (25 mL). The reaction mixture was stirred vigorously and heated to 85°C. Perfluorohexyl iodide (10 g, 22 mmol, 4.0 eq) was added dropwise over 10 minutes (fast addition often resulted in a highly exothermic reaction). The reaction mixture was stirred at 85°C for 3 days. After cooling to room temperature, the reaction mixture was

poured into a mixture of 100 mL water and 100 mL diethyl ether. The cloudy mixture was stirred vigorously for 1 hour and then the solids were filtered and washed with 20 mL diethyl ether. The organic layers were combined and washed 3 times with 50 mL 0.1 N ammonium hydroxide and then twice with 50 mL water. The organic layer was then dried over $MgSO_4$ and the solvent was removed under reduced pressure in presence of a small amount of silica. Flash column chromatography (silica gel, 100 % hexanes) of the dry solids gave 1,4-dimethyl-2,5-bis(perfluorohexyl)benzene as white solids (2.1 g, 51%). ^1H NMR (300 MHz, $CDCl_3$): δ 2.50 (t, J_{H-F} = 2.7 Hz, 6H), 7.42 (s, 2H). 19F NMR (282 MHz, $CDCl_3$): δ -126.38 (m, 4F), -123.01 (s, 4F), -121.96 (s, 4F), -121.03 (s, 4F), -107.36 (t, J_{F-H} = 15.1 Hz, 4F), -81.04 (t, J_{F-F} = 10.2 Hz, 6F).

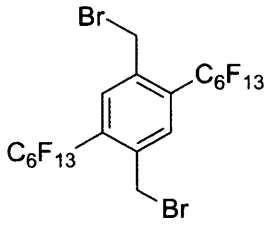

1,4-bis(bromomethyl)-2,5-bis(perfluorohexyl)benzene (5). Flame-dried 50 mL round-bottom flask equipped with a reflux condenser was charged with 1,4-dimethyl-2,5-bis(perfluorohexyl)benzene (1.50 g, 2.02 mmol, 1.00 eq), NBS (1.20 g, 6.74 mmol, 3.34 eq), and AIBN (20 mg, 0.12 mmol, 0.060 eq) under argon. Chlorobenzene (20 mL) was then added and the reaction was stirred at 115°C for 42 hours. After cooling to room temperature, solvent was removed under reduced pressure. Flash column chromatography (silica gel, 100% hexanes) of the resulting crude solids gave 1,4-bis(bromomethyl)-2,5-bis(perfluorohexyl)benzene as a white powder (1.41 g, 78%). NMR: JL4-152-2H (1H for mono brominated product). ^1H NMR (300 MHz, $CDCl_3$): δ 4.60 (s, 4H), 7.81 (s, 3H). ^{19}F NMR (282 MHz $CDCl_3$): δ -126.29 (2F), -122.89 (2F), -121.69 (2F), -121.46 (2F), -120.81 (2F), -107.59 (2F), -80.94 (3F).

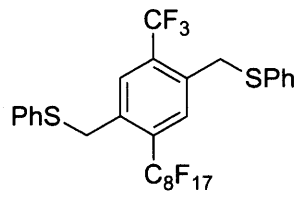

((2-(perfluorooctyl)-5-(trifluoromethyl)-1,4-phenylene)bis(methylene))bis(phenylsulfane). Flame-dried Schelnk vessel was charged with **3** (1.29 g, 1.49 mmol) and THF (10 mL). In a separate flask, NaH (184 mg, 60% w/w suspension in mienral oil, 4.50 mmol) was suspended in THF (5 m) and the flask was charged with thiophenol (460 μL, 4.50 mmol) at 0°C. After cessation of gas evolution, the latter solution was transferred dropwise to the solution of **3** in THF at 0°C over 15 minutes. The reaction mixture was stirred vigorously over an hour and quenched with a slow addition of water (50 mL). The resulting mixture was extracted with diethyl ether (3×40 mL). The organic layer was then dried over $MgSO_4$ and the solvent was removed under reduced pressure in presence of a small amount of silica. Flash column chromatography (silica gel, 7:3 hexanes/ethyl acetate) of the dry solids gave the title compound as a white solid (0.87 g, 72%). ^1H NMR (300 MHz, $CDCl_3$): δ 2.50 (t, $J_{H\text{-}F}$ = 2.7 Hz, 6H), 7.42 (s, 2H). 19F NMR (282 MHz, $CDCl_3$): δ -126.38 (m, 4F), -123.01 (s, 4F), -121.96 (s, 4F), -121.03 (s, 4F), -107.36 (t, $J_{F\text{-}H}$ = 15.1 Hz, 4F), -81.04 (t, $J_{F\text{-}F}$ = 10.2 Hz, 6F). HR-MS (ESI): calcd for $C_{29}H_{16}F_{20}S_2$ 831.0272 $[M+Na]^+$; found 831.0279.

General Method of Polymerization – THF as Solvent

Monomer (0.2 mmol) was dissolved in THF (10 mL) in a flame-dried Schlenck vessel and cooled to -78°C. Freshly prepared KO*t*Bu (90 mg) in THF (1 mL) was added dropwise. The reaction, which initially turned bright yellow, was allowed to warm up to room temperature overnight, during which the color of reaction turned orange-brown. The reaction mixture was poured into 0.1 N HCl, and precipitates were collected by centrifugation. The solids were washed with methanol and were subjected to Soxhlet

extraction with chloroform and hexanes to remove non-fluorous impurities, followed by extraction with hexafluorobenzene.

General Method of Polymerization – FC-770 as Solvent

Monomer (0.2 mmol) was dissolved in -770 (10mL) in a flame-dried Schlenck vessel and cooled to -15°C. Freshly prepared KO*t*Bu (90 mg) in THF (1 mL) was added dropwise. The reaction, which initially turned bright yellow, was allowed to warm up to room temperature overnight, during which the color of reaction turned orange-brown. Solvents were removed under reduced pressure, and the solids were washed with water and methanol, and were subjected to Soxhlet extraction with chloroform and hexanes to remove non-fluorous impurities, followed by extraction with hexafluorobenzene.

References

1. Skotheim, T. A.; Elsenbaumer, R. L.; Reynolds, J. R., *Handbook of conducting polymers*. 2nd ed.; M. Dekker: New York, 1998; p 4-1.

2. (a) Granier, T.; Thomas, E. L.; Gagnon, D. R.; Karasz, F. E.; Lenz, R. W., Structure Investigation of Poly(P-Phenylene Vinylene). *J. Poly. Sci. Pol. Phys.* **1986,** *24* (12), 2793-2804; (b) Granier, T.; Thomas, E. L.; Karasz, F. E., Paracrystalline Structure of Poly(Paraphenylene Vinylene). *J. Polym. Sci. Pol. Phys.* **1989,** *27* (3), 469-487.

3. Grimsdale, A. C.; Chan, K. L.; Martin, R. E.; Jokisz, P. G.; Holmes, A. B., Synthesis of Light-Emitting Conjugated Polymers for Applications in Electroluminescent Devices. *Chem. Rev.* **2009,** *109* (3), 897-1091.

4. (a) Gunes, S.; Neugebauer, H.; Sariciftci, N. S., Conjugated polymer-based organic solar cells. *Chem. Rev.* **2007,** *107* (4), 1324-1338; (b) Hsu, C. S.; Cheng, Y. J.; Yang, S. H., Synthesis of Conjugated Polymers for Organic Solar Cell Applications. *Chem. Rev.* **2009,** *109* (11), 5868-5923.

5. Parker, I. D.; Gymer, R. W.; Harrison, M. G.; Friend, R. H.; Ahmed, H., Fabrication of a Novel Electrooptical Intensity Modulator from the Conjugated Polymer, Poly(2,5-Dimethoxy-P-Phenylene Vinylene). *Appl. Phys. Lett.* **1993,** *62* (13), 1519-1521.

6. Swager, T. M.; Thomas, S. W.; Joly, G. D., Chemical sensors based on amplifying fluorescent conjugated polymers. *Chem. Rev.* **2007,** *107* (4), 1339-1386.

7. Swager, T. M.; Rose, A.; Zhu, Z. G.; Madigan, C. F.; Bulovic, V., Sensitivity gains in chemosensing by lasing action in organic polymers. *Nature* **2005,** *434* (7035), 876-879.

8. Lux, A.; Holmes, A. B.; Cervini, R.; Davies, J. E.; Moratti, S. C.; Gruner, J.; Cacialli, F.; Friend, R. H., New CF3-substituted PPV-type oligomers and polymers for use as hole blocking layers in LEDs. *Synth. Met.* **1997,** *84* (1-3), 293-294.

9. (a) Oelkrug, D.; Tompert, A.; Gierschner, J.; Egelhaaf, H. J.; Hanack, M.; Hohloch, M.; Steinhuber, E., Tuning of fluorescence in films and nanoparticles of oligophenylenevinylenes. *J. Phys. Chem. B* **1998,** *102* (11), 1902-1907; (b) Swager, T. M.; Moslin, R. M.; Andrew, T. L.; Kooi, S. E., Anionic Oxidative Polymerization: The Synthesis of Poly(phenylenedicyanovinylene) (PPCN2V). *J. Am. Chem. Soc.* **2009,** *131* (1), 20-21.

10. Fahlman, M.; Bredas, J. L., Theoretical study of torsion and its effect on the structural and electronic properties of cyano-substituted poly(p-phenylene vinylene) and its derivatives. *Synth. Met.* **1996,** *78* (1), 39-46.

11. Glew, D. N.; Reeves, L. W., Purification of Perfluoro-Normal-Heptane and Perfluoromethylcyclohexane. *J. Phys. Chem.* **1956,** *60* (5), 615-615.

12. Whitten, J. E.; Kim, Y.; Swager, T. M., High ionization potential conjugated polymers. *J. Am. Chem. Soc.* **2005,** *127* (34), 12122-12130.

13. Swager, T. M.; McQuade, D. T.; Kim, J., Two-dimensional conjugated polymer assemblies: Interchain spacing for control of photophysics. *J. Am. Chem. Soc.* **2000,** *122* (24), 5885-5886.

CHAPTER 5

Regiospecific Synthesis of Gold Nanorod-SWCNT Heterojunctions

Adapted from
Yossi Weizmann, Jeewoo Lim, David M. Chenoweth, and Timothy M. Swager
Nano Lett. **2010**, *10*, 2466-2469*

*Initial synthesis of the materials was conducted by YW. TEM imaging and determination of product distribution were done by JL. Characterizations of materials by AFM and Raman spectroscopy were done by YW and DMC.

Introduction

High aspect ratio building blocks such as gold nanorods and carbon nanotubes (CNTs) have the potential to be used as "wires" for construction of interconnected arrays of electronic materials at the nano level. Gold nanorods and CNTs possess large surface areas along with highly directional electronic conduction pathways, characteristics which are of particular utility in creating materials for resistivity-based sensory applications.[1] A wide range of methods for functionalization of carbon nanotubes which allow for immobilization[2] of tailored metallic and/or semiconducting nanoparticles on the sidewalls of nanotubes is known. Regioselectivity (end functionalization versus sidewall functionalization), however, remains a major problem.[1f, 6]

The formation of heterojunctions between carbon nanotubes and metals has received increased attention due to the potential of allowing single carbon nanotube strands to be incorporated directly into devices in electronic and materials applications. Previous heterojunction fabrication methods have relied on vapor phase growth of materials directly onto nanotubes, solid-phase reactions at elevated temperatures >450 °C, or ablative techniques using intense electron beam irradiation to destroy the nanotube wall around a metallic core.[1a, b, 1j]

Heterojunctions between gold nanorods and CNTs have previously been reported. The approach involved attachment of gold nanoparticles (Au-NP) "seeds" to CNTs, followed by gold nanorod growth from the nanoparticles.[3] The attachment of Au-NPs to CNTs, however, could not be controlled, resulting in multiple random attachment on both surfaces and termni of CNTs. Gold nanorod growth from this hybrid material gave unpredictable patterns.[6] Harsh experimental conditions and the difficulties in precise positioning of the metal junctions have limited the widespread utility of these methods.[1a, b, 1f, 1j] Methods for the regioselective synthesis of well-defined Au-nanorod/CNT/Au-nanorod nanocomposites would represent a major step forward in the controlled functionalization of SWCNTs with precisely defined metallic heterojunctions.

This chapter describes an operationally simple method for the regiospecific synthesis of terminally-linked Au-nanorod/SWCNT/Au-nanorod nanostructures. Our method allows for the growth of Au-nanorods from the termini of single-walled CNTs (SWCNTs), creating precisely positioned metallic heterojunctions. These nanocomposites are synthesized in solution and are found to be very stable under a variety of experimental conditions.

Results and Discussion

The Au-nanorod/SWCNT/Au-nanorod synthesis is depicted schematically in Scheme 5-1. In order to remove carbon particles and metal impurities and introduce carboxylic acid groups to the surface, HiPco SWCNTs were treated with a mixture of concentrated sulfuric and nitric acid (3:1, 98% and 70%, respectively), subjected to bath sonication for 35 min. at 40 °C, and then oxidized with a mixture of concentrated sulfuric acid and hydrogen peroxide (4:1, 98% and 30%, respectively, 35 minutes).[4] Previous studies have demonstrated treatment with mixtures of strong acids leads to chemical shortening of SWCNTs, along with oxidation at the nanotube ends (resulting in formation of carboxylic acid groups), and can also introduce oxidative defects along the nanotube sidewall.[4]

The oxidized SWCNTs were incubated with Triton X-100/PEG (M_r = 10,000) in an aqueous solution and sonicated for 4 hours in an ice bath. This process results in a stable dispersion of SWCNTs wrapped by the surfactant. The surfactant also acts as a "protective sheath," preventing non-specific surface adsorption and/or undesired covalent functionalization of defects on nanotube sidewalls.[5] The oxidized termini of the shielded SWCNTs were then coupled to the monofunctionalized 1.4 nm Au-nanoparticles (Au-NPs) bearing a

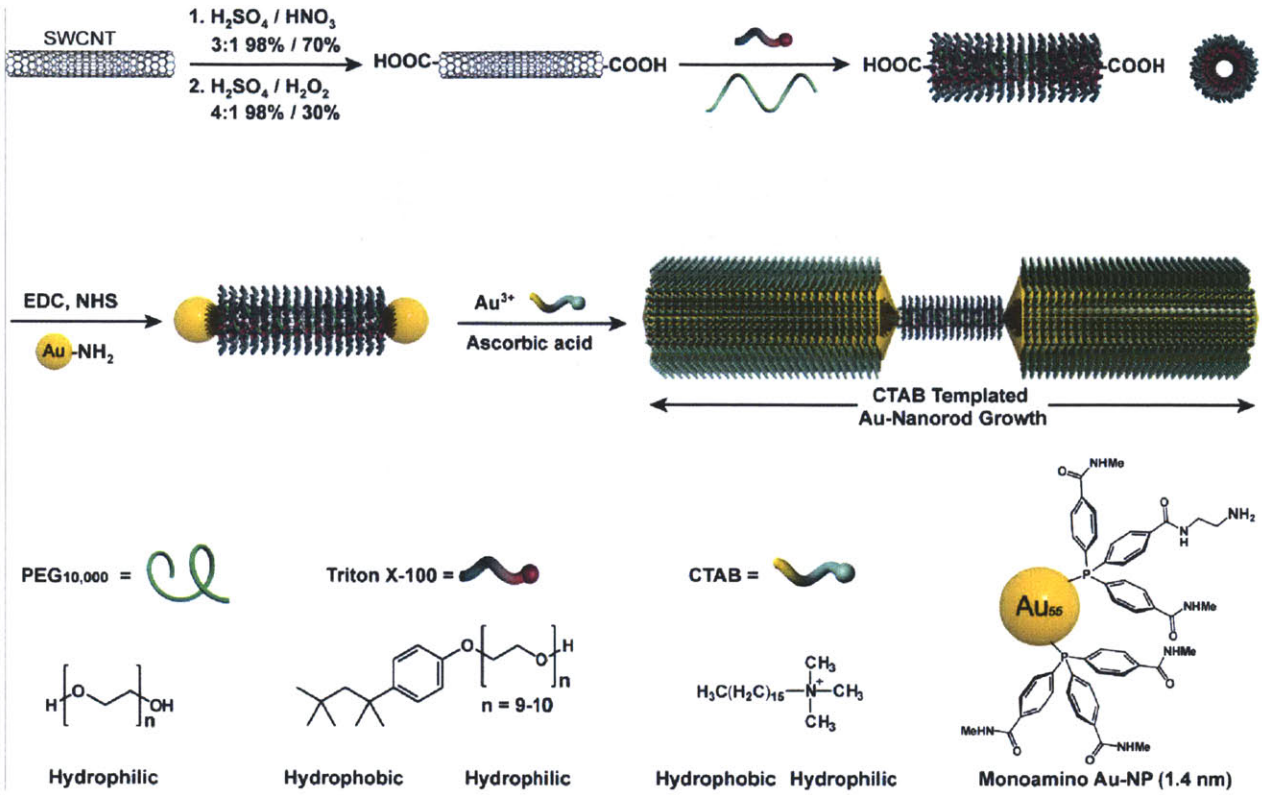

Scheme 5-1. Schematic of the synthesis of Au-nanorod/SWCNT/Au-nanorod hybrid material.

single primary amine group per nanoparticle. Efficient coupling was achieved using 1-(3-dimethylaminopropyl)-3-ethylcarbodiimide hydrochloride (EDC) and *N*-hydroxysulfosuccinimide (sulfo-NHS), resulting in SWCNTs functionalized with Au-NPs at their termini. The Au-NP diameter (~1.4 nm) is slightly larger than the diameter of HiPco SWCNTs (~0.7-1.2 nm), and the steric bulk of the Au-NPs provides a basis for monofunctionalization of the nanotube ends. The resulting Au-NP conjugated SWCNTs were used to seed the growth of Au-nanorods from the termini of the SWCNTs. Catalytic enlargement of the Au-nanoparticles was achieved using $HAuCl_4$ and CTAB as a template.[6]

Characterization of the Au-nanorod/SWCNT/Au-nanorod nanostructures was performed using a combination of transmission electron microscopy (TEM) (Figure 5-1), atomic force

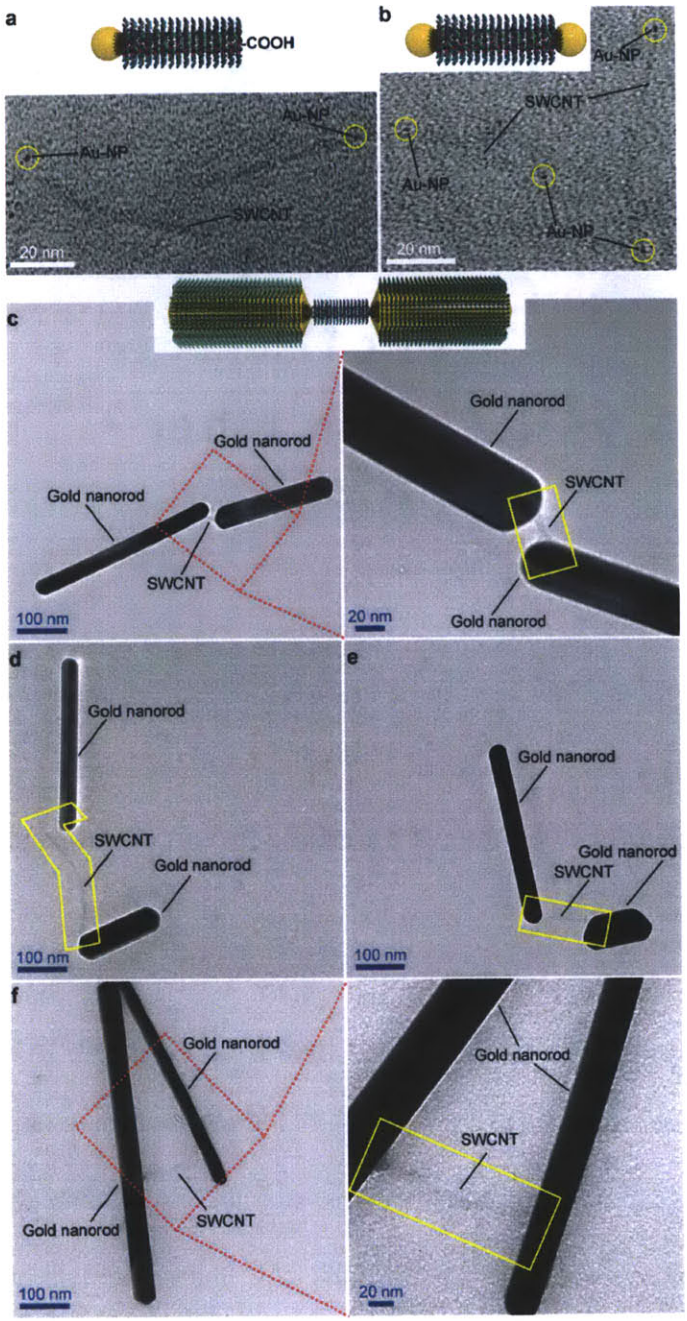

Figure 5-1. TEM images of Au-NP/SWCNT/Au-NP (a and b), and Au-nanorod/SWCNT/Au-nanorod assembly (c-f).

microscopy (AFM) (Figure 5-2a-c and Figure 5-3), and confocal Raman spectroscopy (Figure 5-2d) before and after Au-nanorod growth. AFM images revealed that, prior to Au-nanorod growth,

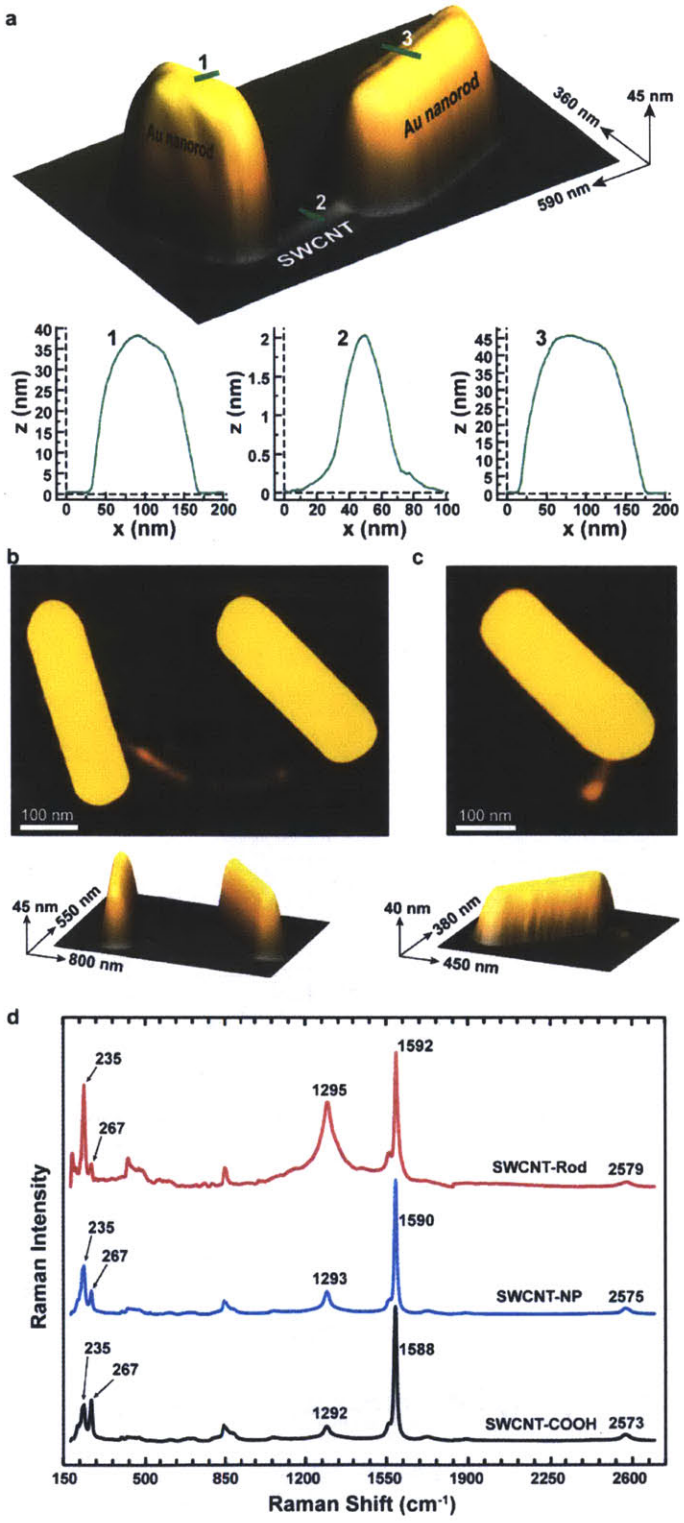

Figure 5-2. AFM images and cross-section profiles (a-c) and confocal Raman spectroscopy (d) of Au-nanorod/SWCNT/Au-nanorod assembly.

the surfactant-wrapped SWCNTs were well dispersed as unbundled monomeric species with average lengths of ~200 nm (Figure 5-3). The regiospecific Au-NP conjugation to the termini of the SWCNTs was confirmed by TEM and Figure 1a and 1b show images of individual SWCNTs labeled with a single gold nanoparticle at one end and at both ends, respectively. A rare occurrence is shown in Figure 5-1a, where two SWCNT's in close proximity to one another are mono-functionalized with Au-NPs. Mono-functionalized nanotubes represented <10% of the structures observed prior to Au-nanorod growth. The bis-functionalized SWCNTs were the predominant structures, representing ~90% of the structures observed by TEM and are shown in Figure 5-1b. The relative abundance of each type of assembly is summarized in Figure 5-5.

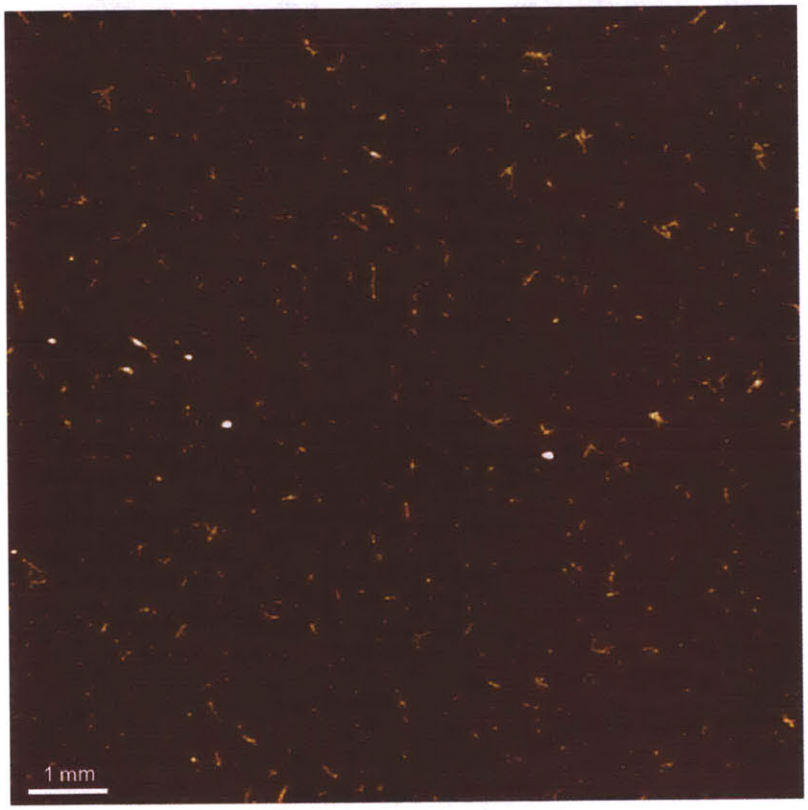

Figure 5-3. AFM images and Au-NP/SWCNT/Au-NP prior to Au-nanorod growth.

Dispersed individual nanotubes are difficult to see with TEM, since their local electron density is similar to the amorphous carbon supports on which microscopy is conducted. However, the individual Au-NPs attached directly to the tube termini are clearly visible and provide enough contrast ratio to unambiguously identify SWCNTs.

Figure 5-1c-e are TEM images of the Au-nanorod / SWCNT / Au-nanorod nanostructures obtained after Au-nanorod growth from the Au-NP functionalized SWCNT termini and the distribution of observed nanostructures are shown in Figure 5b. Au-nanorod lengths of ~200-400 nm are observed to be attached directly to the termini of short (~10 nm) and long (~100-250 nm) SWCNTs. The nanorod growth pattern and direction is also affected by nearby structures (i.e. SWCNT termini), and a majority of connections of the SWCNTs to the ends of the Au-nanorods suggest that the nanorod growth is mainly in a direction opposite from the point of Au-NP conjugation. Some (~24%) of the SWCNT structures contained perpendicularly connected Au-nanorods, which are presumed to be produced from the seed-mediated growth in two directions orthogonal to the lengthwise axis of the SWCNTs (Figure 5b).[6a] Additionally, we observed a few (~15%) structures where a SWCNT has one terminus connected to a single Au-nanorod and the other to a large Au-nanoparticle (Figure 5-4) produced by non-directional growth of the Au-NP. We expect that as improved methods for controlling Au-nanorod growth are investigated, even more homogenous materials could be achieved.

The Au-nanorod/SWCNT/Au-nanorod nanostructures were further characterized by AFM (Figure 5-2a-c). Long nanorods 40-45 nm in height and 200-400 nm in length, with SWCNT 0.7-2.2 nm in height and 10-500 nm in length, were observed after drop-casting of the solution onto freshly cleaved mica surface. A topographical AFM image of a gold nanorod-linked SWCNT is shown in Figure 2a with the associated height profiles. Figure 2a shows an individual

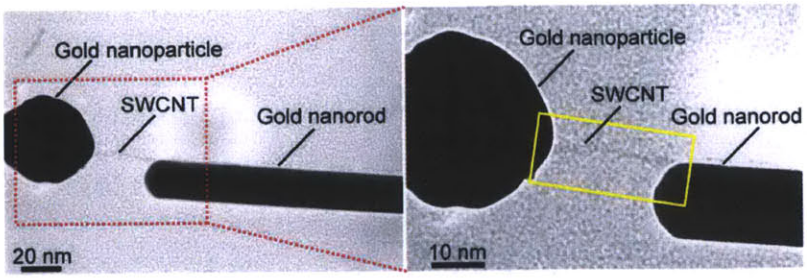

Figure 5-4. TEM images and Au-nanorod/SWCNT/enlarged Au-NP assembly.

nanostructure where two Au-nanorods are attached regiospecifically to the termini of a SWCNT. The Au-nanorod height and length dimensions range from 40×200 nm to 45×300 nm. The SWCNT fixed between the two Au-nanorods has a height of ~2.2 nm and a length of ~100 nm (Figure 5-2a). Figure 2b shows the AFM image of a perpendicularly connected Au-nanorod/SWCNT/Au-nanorod nanostructure. The height and length dimensions of the Au-nanorods varied from 40×400 nm to 45×400 nm. The SWCNT positioned between the two rods has a height of ~0.7-1.2 nm and a length of ~500 nm. The Au-nanorod on the left is perpendicularly connected to the SWCNT terminus whereas the other nanorod is connected in an end-to-end fashion with the SWCNT. Figure 5-2c shows a SWCNT with one end connected to a Au-nanorod and the other terminated by an Au-NP which failed to seed a nanorod. Inhibition of nanorod growth could be attributed to interference from nearby objects.[6]

Further characterization of the Au-nanorod/SWCNT/Au-nanorod nanocomposites at each step in the synthesis was performed by laser scanning Raman confocal microscopy. Previously reported resonance Raman studies have demonstrated that SWCNTs filled with metallic silver displayed an altered Fermi level with silver behaving as an electron donor increasing the electron carrier density.[7] Utilizing laser scanning confocal Raman microscopy and a laser excitation

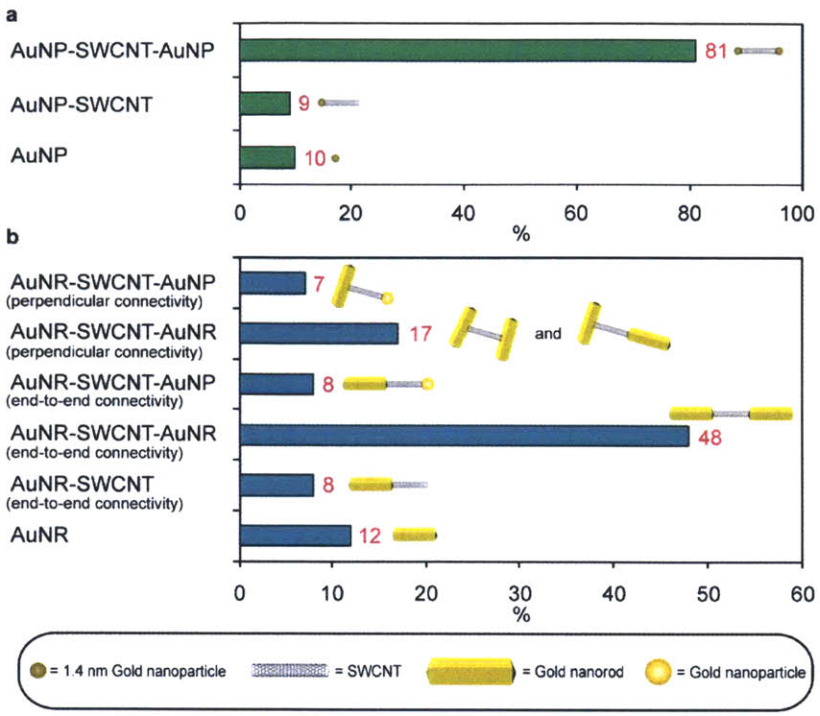

Figure 5-5. Summary of distribution of various structures before and after gold nanorod growth as counted from TEM images.

wavelength of 784.4 nm (1.58 eV), we characterized our Au-nanorod/SWCNT/Au-nanorods after oxidation, after Au- NP conjugation, and after Au-nanorod growth (Figure 5-2d).

Gold nanorod growth results in significant changes in the Raman spectra and the RBM region showed major peaks at 235, and 267 cm^{-1}. The RBM peak at 235 cm^{-1} shows a significant increase in intensity after Au-nanorod growth whereas the peak at 267 cm^{-1} shows a significant decrease, implying an increased isolation of individual SWCNTs by Au-nanorods.[7a] The intensity of the D-band increases with significant broadening upon Au-nanorod formation and shows a slight ~4 cm^{-1} shift to higher frequency from 1588 cm^{-1} consistent with previous studies of SWCNTs on silver surfaces.[8] Increases in the D/G ratio upon Au-nanorod formation reflects a modification of the nanotube surface and/or a plasmonic enhancement of scattering from sights proximate to the Au-nanorods. Additionally, the peak in the G' region shows a 6 cm^{-1} shift to

higher wavenumbers. Control spectra for CTAB, CTAB-coated gold nanorods, and 1.4 nm gold nanoparticles are shown in Figure 5-6. The control spectra show no significant resolvable signals above the baseline when compared to the spectra in Figure 5-3d.

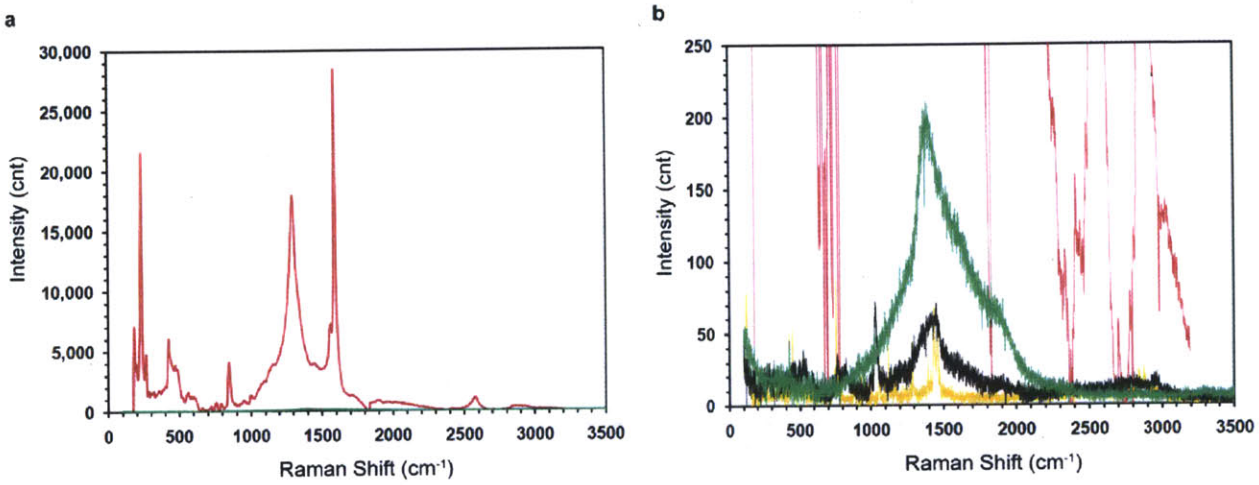

Figure 5-6. Confocal Raman spectra of Au-nanorod/SWCNT/Au-nanorods (red, left), Au-nanorods (green), 1.4 nm Au-nanoparticles (black), CTAB (yellow) using a laser excitation wavelength of 784.4 nm (1.58 eV). (a) Full scale spectrum. (b) Expanded view of y-axis intensity from 0-250 counts showing the Au-nanorods (green), 1.4 nm Au-nanoparticles (black), and CTAB spectra in the baseline.

Conclusion

An operationally simple and controllable method for the regioselective synthesis of well-defined Au-nanorod/SWCNT/Au-nanorod nanostructures represents a major step forward in the controlled functionalization of SWCNTs with precisely defined metallic heterojunctions. Control of gold nanorod length, growth direction, and alignment are under investigation in addition to the use of alternate metals such as silver as well as the use of multiwalled CNTs as a seed scaffold.

Applications utilizing the optical and electronic properties are under investigation and range from field effect transistors to chemical sensors and Raman active nanoscale devices.

Experimental Section

Materials

Unless otherwise noted, all the starting materials were obtained from commercial suppliers and used without further purification. Purified HiPco Single-Wall Carbon Nanotubes were purchased from Unidym, Inc. Purified MWCNT; hexadecyltrimethylammonium bromide, 99% (CTAB); *N*-hydroxysulfosuccinimide sodium salt (sulfo-NHS); Triton X-100 and polyethylene glycol (PEG) with average mol wt 10,000 were purchased from Sigma-Aldrich. Hydrogen tetrachloroaurate (III) hydrate ($HAuCl_4 \times XH_2O$), 99.999%; L-(+)-ascorbic acid, 99+% and 1-(3-dimethylaminopropyl)-3-ethylcarbodiimide hydrochloride, 98+% (EDC) were purchased from Alfa Aesar. HEPES and hydrogen peroxide 30% were purchased from EMD Biosciences, Inc. Monoamino gold nanoparticles were obtained from Nanoprobes, Inc. Centricon separation devices and 0.6 μm polycarbonate membrane filters were purchased from Millipore. Ultrapure water from a NANOpure Diamond (Barnstead) source was used throughout all of the experiments.

General Methods

Transmission electron microscopy (TEM) images were taken on JEOL 2010 and JEOL 200CX instruments (acceleration voltage 200 KV) using 200-mesh carbon-coated copper grid (Electron Microscopy Sciences). All atomic force microscopy (AFM) imaging measurements were performed at room temperature by using a Multimode scanning probe microscope with a

Nanoscope 3A controller (Digital Instruments/Veeco Probes). AFM topographical images were taken on samples deposited on freshly cleaved grade v-4 mica surfaces (Structure Probe, Inc.) that were first passivated with a 5 mM $MgCl_2$ solution for 1 min followed by drop casting the solution of interest. Images were taken with Ultrasharp SiN AFM tips (MikroMasch) in tapping mode at their resonant frequency, and these images were analyzed with WsXM SPIP software (Nanotec).[1a] Confocal Raman microscopy was performed using a Horiba Jobin Yvon Raman confocal microscope (model LabRAM-HR) with a 784.4 nm (1.58 eV) laser as the excitation light source. A x50 objective was used for imaging with a pin hole size of 300 microns. All sonication procedures were conducted with an ultrasonic bath (Branson Ultrasonics Corporation, model 3510). SEM images were taken with a cold field-emission gun scanning electron microscope (FEG-SEM).

Shortening and Oxidation of SWCNT

Commercial HiPco SWCNTs were cut and etched according to a reported procedure[1b] with some modification, to give shortened SWCNTs bearing carboxylic groups at their ends (SWCNT-COOH) and also as defect sites on the sidewalls. Specifically, 50 mg pristine pure HiPco SWCNTs were place in oxidative reaction of 24 mL suspension contains a 3:1 H_2SO_4 (98%)/HNO_3 (70%) solution at 40 °C and under sonication at 42 kHz. Sonication during the cutting protocol was reduced to 35 min. The solution was filtered using a 0.6 μm polycarbonate membrane filter and then etched for 30 minutes with a 20 mL of a 4:1 H_2SO_4 (98%)/H_2O_2 30% solution to remove all carbon particles produced by the first reaction. The resulting diluted nanotube-acid mixture was then filtered using a 0.6 μm polycarbonate membrane filter leaving a

SWCNT filter cake. The nanotubes were then rinsed with water until a pH above 5 was obtained. Final rinsing was done using ethanol and the resulting filter cake dried in a vacuum desiccator.

Shielding SWCNT-COOH Sidewall Surface

Typically, 0.1% SWCNTs-COOH (wt/v) were place in water solution contains 0.25% Triton x-100 (v/v) and 0.25% PEG (10,000 M_r) (wt/v) in a final volume of 1 mL, and sonicated for 4 hrs at 42 kHz in ice bath, followed by centrifugation at 14,000 r.p.m for 1 hour. Next, the supernatant was collected; leaving a small residual amount of unwanted aggregated SWCNTs behind.

Tethering AU-NPs to the Termini of Shielded SWCNT-COOH

Generally, 0.02% SWCNT-COOH (wt/v) were placed in a HEPES buffer solution 0.1 M, pH 7.4 consisting of 0.05% Triton X-100 (v/v), 0.05% PEG (10,000 M_r) (wt/v), 0.6×10^{-9} mol 1.4 nm monoamino gold nanoparticles, 2 mM EDC and 5 mM sulfo-NHS in a final volume of 1 mL, and stirred gently overnight in the dark at room temperature. The reaction mix was then purified and separated from the excess Au-nanoparticles using a Centricon filtration device (100,000 cutoff), and concentrated to a final volume of 500 μL.

Synthesis of Gold Nanorods

Gold nanorods were synthesized by the three-step seeding protocol as described by Murphy et al.[3] Specifically, two 20 mL flasks and one 100 mL conical flask (labeled A, B, and C, respectively) were used. To these flasks were added 9 mL (in flasks A and B) and 45 mL (in flask C) of growth solution containing a mixture of 2.5×10^{-4} M $HAuCl_4$ and 0.1 M CTAB

solutions and kept at 27 °C. Then, 50 μL of 0.1 M freshly prepared ascorbic acid (flasks A and B) and 250 μL (flask C) were added and hand shaken, the solutions became colorless. Next, 200 μL of seed solution (Au-NP/SWCNT/Au-NP) was added to flask A (step 1) and gently mixed. Immediately after 15 seconds 1 mL of the resulting mixture was transferred quickly from flask A to flask B and gently mixed (step 2). This was followed by transferring 5 mL portion of flask B into flask C after 30 seconds and mixing gently by hand shaking (step 3). The color of the resulting solution slowly changed to purple. Flask C was then kept undisturbed for additional 16 h at 27 °C. High aspect ratio nanorods along with other shapes (triangles, hexagons, and small rods) precipitate from the solution and form a thin barely noticeable film at the bottom of the flask. The resulting supernatant, which contained mostly spherical nanoparticles, was carefully removed and the film on the bottom was carefully rinsed with a small portion of pure water to remove the residual amount of the supernatant. The same procedure was used for the SWCNTs.

Reference

1. (a) Lieber, C. M.; Hu, J. T.; Ouyang, M.; Yang, P. D., Controlled growth and electrical properties of heterojunctions of carbon nanotubes and silicon nanowires. *Nature* **1999,** *399* (6731), 48-51; (b) Zhang, Y.; Ichihashi, T.; Landree, E.; Nihey, F.; Iijima, S., Heterostructures of single-walled carbon nanotubes and carbide nanorods. *Science* **1999,** *285* (5434), 1719-1722; (c) Jana, N. R.; Gearheart, L.; Murphy, C. J., Wet chemical synthesis of high aspect ratio cylindrical gold nanorods. *J. Phys. Chem. B* **2001,** *105* (19), 4065-4067; (d) Zhu, J.; Luo, J.; Zhang, L.; Zhang, Y. J., Controlled growth of one-dimensional metal-semiconductor and metal-carbon nanotube heterojunctions. *Adv. Mater.* **2002,** *14* (19), 1413-1414; (e) Murphy, C. J.; Gole, A., Seed-mediated synthesis of gold nanorods: Role of the size and nature of the seed. *Chem. Mater.* **2004,** *16* (19), 3633-3640; (f) Zamborini, F. P.; Mieszawska, A. J.; Jalilian, R.; Sumanasekera, G. U., Synthesis of gold nanorod/single-wall carbon nanotube heterojunctions directly on surfaces. *J. Am. Chem. Soc.* **2005,** *127* (31), 10822-10823; (g) Asaka, K.; Nakahara, H.; Saito, Y., Nanowelding of a multiwalled carbon nanotube to metal surface and its electron field emission properties. *Appl. Phys. Lett.* **2008,** *92* (2) 2311-2314; (h) Star, A.; Kauffman, D. R., Carbon nanotube gas and vapor sensors. *Angew. Chem. Int. Ed.* **2008,** *47* (35), 6550-6570; (i) Swager, T. M.; Wang, F.; Gu, H. W., Carbon nanotube/polythiophene chemiresistive sensors for chemical warfare agents. *J. Am. Chem. Soc.* **2008,** *130* (16), 5392-5393; (j) Banhart, F.; Rodriguez-Manzo, J. A.; Terrones, M.; Terrones, H.; Grobert, N.; Ajayan, P. M.; Sumpter, B. G.; Meunier, V.; Wang, M.; Bando, Y.; Golberg, D., Heterojunctions between metals and carbon nanotubes as ultimate nanocontacts. *Proc. Nat. Acad. Sci. USA* **2009,** *106* (12), 4591-4595; (k) Swager, T. M.; Lobez, J. M., Radiation Detection: Resistivity Responses in Functional Poly(Olefin Sulfone)/Carbon Nanotube Composites. *Angew. Chem. In. Ed.* **2010,** *49* (1), 95-98.

2. (a) Tour, J. M.; Bahr, J. L., Covalent chemistry of single-wall carbon nanotubes. *J. Mater. Chem.* **2002,** *12* (7), 1952-1958; (b) Wong, S. S.; Banerjee, S.; Hemraj-Benny, T., Covalent surface chemistry of single-walled carbon nanotubes. *Adv. Mater.* **2005,** *17* (1), 17-29; (c) Swager, T. M.; Zhang, W., Functionalization of single-walled carbon nanotubes and fullerenes via a dimethyl acetylenedicarboxylate-4-dimethylaminopyridine zwitterion approach. *J. Am. Chem. Soc.* **2007,** *129* (25), 7714-7715; (d) Swager, T. M.; Zhang, W.; Sprafke, J. K.; Ma, M. L.; Tsui, E. Y.; Sydlik, S. A.; Rutledge, G. C., Modular Functionalization of Carbon Nanotubes and Fullerenes. *J. Am. Chem. Soc.* **2009,** *131* (24), 8446-8454.

3. Murphy, C. J.; Busbee, B. D.; Obare, S. O., An improved synthesis of high-aspect-ratio gold nanorods. *Adv. Mater.* **2003,** *15* (5), 414-415.

4. Smalley, R. E.; Liu, J.; Rinzler, A. G.; Dai, H. J.; Hafner, J. H.; Bradley, R. K.; Boul, P. J.; Lu, A.; Iverson, T.; Shelimov, K.; Huffman, C. B.; Rodriguez-Macias, F.; Shon, Y. S.; Lee, T. R.; Colbert, D. T., Fullerene pipes. *Science* **1998,** *280* (5367), 1253-1256.

5. (a) Dai, H. J.; Chen, R. J.; Bangsaruntip, S.; Drouvalakis, K. A.; Kam, N. W. S.; Shim, M.; Li, Y. M.; Kim, W.; Utz, P. J., Noncovalent functionalization of carbon nanotubes for highly specific electronic biosensors. *Proc. Nat. Acad. Sci. USA* **2003,** *100* (9), 4984-4989; (b) Rastogi, R.; Kaushal, R.; Tripathi, S. K.; Sharma, A. L.; Kaur, I.; Bharadwaj, L. M., Comparative study of carbon nanotube dispersion using surfactants. *J. Colloid Inter. Sci.* **2008,** *328* (2), 421-428.

6. (a) Zamborini, F. P.; Wei, Z. Q., Directly monitoring the growth of gold nanoparticle seeds into gold nanorods. *Langmuir* **2004,** *20* (26), 11301-11304; (b) Zamborini, F. P.; Wei, Z. Q.; Mieszawska, A. J., Synthesis and manipulation of high aspect ratio gold nanorods grown directly on surfaces. *Langmuir* **2004,** *20* (11), 4322-4326.

7. (a) Corio, P.; Santos, A. P.; Santos, P. S.; Temperini, M. L. A.; Brar, V. W.; Pimenta, M. A.; Dresselhaus, M. S., Characterization of single wall carbon nanotubes filled with silver and with chromium compounds. *Chem. Phys. Lett.* **2004,** *383* (5-6), 475-480; (b) Dresselhaus, M. S.; Dresselhaus, G.; Saito, R.; Jorio, A., Raman spectroscopy of carbon nanotubes. *Phys. Rep.* **2005,** *409* (2), 47-99; (c) Dresselhaus, G.; Dresselhaus, M. S.; Hofmann, M., The big picture of Raman scattering in carbon nanotubes. *Vib. Spectrosc.* **2007,** *45* (2), 71-81.

8. Liu, Z. F.; Wu, B.; Zhang, J.; Wei, Z.; Cai, S. M., Chemical alignment of oxidatively shortened single-walled carbon nanotubes on silver surface. *J. Phys. Chem. B* **2001,** *105* (22), 5075-5078.

Curriculum Vitae

Jeewoo Lim

EDUCATION

Ph.D. Chemistry: **Massachusetts Institute of Technology**, *Cambridge, MA.*
- Division: Organic Chemistry. Research Advisor: Timothy M. Swager. (9/2006-present)

A.B. Chemistry: **Princeton University**, *Princeton, NJ.* (6/2006)
- Undergraduate Research Advisor: Erik J. Sorensen.
- Graduated with High Honors.

RESEARCH EXPERIENCE

Massachusetts Institute of Technology (9/2006-Present)
Heavily Fluorinated Electronic Polymers
- Syntheses, characterization, and applications of novel fluorescent fluorous polymers.
- Fluorous biphase chemistry for polymer synthesis.
- Syntheses, characterization, and applications of novel conjugated polymers with perfluoroaryl moieties.

Metal Nanoparticle – Carbon Nanotube Hybrids
- Synthesis of end-functionalized CNT's and their hybridization with metal nanoparticles.
- Characterization of metal nanorod-CNT hybrid materials.
- Device fabrication from various metal nanoparticle – CNT – metal nanoparticle hybrids.

Princeton University (2/2004-6/2006)
Development of 1-hydrazino-1,3-dienes as Building Blocks for Organic Synthesis
- Syntheses and characterization of various 1-hydrazino-1,3-diene derivatives.
- Development of methodologies involving hetero Diels-Alder reactions of these dienes.

PAPERS

1. *Fluorous Biphase Synthesis of a Poly(p-phenyleneethynylene) and its Fluorescent Aqueous Fluorous Phase Emulsion.* **Jeewoo Lim** and Timothy M. Swager* - *Angew. Chem. Int. Ed.* **2010**, *49*, 7486-7488.

2. *Regiospecific Synthesis of Au-Nanorod/SWCNT/Au-Nanorod Heterojunctions.* Yossi Weizmann, **Jeewoo Lim**, David Chenoweth, Timothy M. Swager* *Nano Lett.*, **2010**, *10* (7), 2466–2469.

PRESENTATIONS

"Microparticle-Supported Fluorescent Polymers for Protease Detection"
Jeewoo Lim, Jessica H. Liao, Timothy M. Swager*
- Oct. 2007. Program for Excellence in Nanotechnology Meeting, Santa Barbara, CA.

"Fluorous Phase Soluble Electronic Polymers"
Jeewoo Lim, Timothy M. Swager*
- Aug 2009. 238th ACS National Meeting, Washington D.C.

"Heavily Fluorinated Electronic Polymers: Syntheses and Properties"

Jeewoo Lim, Timothy M. Swager*

- Aug 2009. 9th International Symposium on Fluorine Chemistry, Jackson Hole, WY.

AWARDS and HONORS

Everett S. Wallis Prize in Organic Chemistry (2006)

- Awarded to an undergraduate student in Princeton University department of chemistry with the highest overall achievements in the field of organic chemistry.

Pfizer Undergraduate Research Fellowship in Synthetic Organic Chemistry (2004)

- Awarded annually to 20 undergraduate students in the United States.

MIT Teaching Award (2007)

- Awarded to teaching assistants with highest ratings in student evaluations over two semesters.

Graduate Student Mentor for MIT Energy Initiative (MITei) Program (2009)

- Served as a mentor for undergraduate students in energy research.

Acknowledgements

First and foremost, I would like to express my gratitude to Tim, the Master Blaster, for his guidance, patience, and support throughout my time in graduate school. Tim was a constant source of inspiration not only through his creativity, intuition, and passion, but also through the warm and caring manner with which he guided his students. I would also like to thank Professor Gregory C. Fu, the chair of my thesis committee, for his care and advice on my research projects. Professor Erik J. Sorensen, my undergraduate advisor, encouraged me to pursue chemistry in graduate school and beyond. I owe him much thanks. My interest in chemistry was initially sparked by Dr. Bongsub Kim, my high school chemistry teacher, who has led many students like me to pursue degrees in chemistry.

I was very fortunate to be amongst the Swager Group members, who were always helpful and friendly and brought to the table knowledge from their backgrounds which ranged from physics to chemistry to biomedical engineering. I would like to thank, especially, Koushik Venkatesan, Yossi Weizmann, Dave Chenoweth, and Barney Walker, the post-docs in lab who I could always rely on for research and life advice. Some of them were also a part of the "Losers," which included Trisha Andrew, Kazunori Sugiyasu, Ryo Takita, Becca Parkhurst, Jose Lobez, and Joel Batson. Countless days discussing research and other important things at the Muddy with the Losers will definitely be some of my most cherished memories in graduate school. Shuang Liu, a great friend a co-worker, has been a part of the fluorous chemistry team for the past few years and has given me valuable new perspectives on my research. I would also like to thank Jolene Mork for taking over role as the safety officer and Caitlin for being an amazing lab manager. My acknowledgements will not be complete without mentioning "Swager Like Us," our summer volleyball team (Barney, Becca, Birgit, Joel, Jolene, Derek, Marco, Sam, and Tyler) whose amazing run went all the way to the finals.

My appreciation extends to the MIT Kendo Club, with whom I was able to continue to pursue a martial art which I love. I would also like to thank the team OTL (Hyomin Lee, Joonhwan Lee, and Jinyoung Baek). Music Director Francis Kwon of the Korean Catholic Community of Boston and the members of the choir, including Chul Young Lee and Jongsuk Lee, have also been a big part of my life in graduate school.

The Korean chemists at MIT were full of characters and formed a fun and caring community. Among them I would like to thank Woonju Song, Sunkyu Han, and Heesun Han, my fellow year-mates. I would also like to thank Hyangsoo Jeong. Junwon Choi, also a member of Dr. Bonsub Kim's squad from my high school, also deserves mention here. Donghyun Kim and Jeewoo Park of the physics department have been and will continue to be great friends. I hope our paths cross again in the near future.

My final and the biggest thank-you goes to my family. I wouldn't have been able to endure nearly ten years of life far away from home without them. I cannot thank them enough.